Manuscript ID: egusphere-2026-2405

Title: Unveiling the multiphase fate of 2,4-dinitrophenol on aerosols: Interfacial hydration governs competing oxidation pathways and unexpected toxicity amplification

Authors: Chenlei Wang[1], Ran Li[1], Jiaxing Sun[2], Zihan Zhang[1], Nan Zhao[1], Leilei Liu*[1], Zuju Ma[1], Maoxia He[3], Jianfei Sun*[1]

Dear editor (in *Atmospheric Chemistry and Physics*)

We thank the reviewers and the editor for their thorough assessment of our manuscript, and for their constructive comments and suggestions, which have helped us to significantly improve the quality of this work. Below we provide a detailed point-by-point response to all comments. The reviewer comments are reproduced in italics, our responses are shown in blue text, and all modifications in the manuscript have been made using Track Changes. Page and line numbers refer to the marked-up revised manuscript.

Yours sincerely,

Jianfei Sun

School of Environmental and Material Engineering, Yantai University

Response to RC1

General Comments

The manuscript presents a multiscale computational investigation (DFT, MD, and QSAR) of the atmospheric fate of 2,4-dinitrophenol (2,4-DNP), concluding that oxidation is dominated by OH and O_3 pathways, that interfacial hydration modulates adsorption, and that ozonolysis products exhibit increased toxicity potential. While the computational work is detailed, the manuscript does not yet demonstrate sufficient novelty relative to existing phenolic oxidation literature and lacks adequate integration, atmospheric context, and validation of its conclusions. In particular, the study remains weakly connected to established multiphase phenolic chemistry, relies on simplified modeling assumptions (e.g., C60 surrogate), and overextends its interpretation to atmospheric and toxicological implications. Overall, the manuscript requires substantial revision to improve novelty definition, literature integration, quantitative atmospheric relevance, and consistency between the computational results and the conclusions. In its current form, the manuscript does not meet the standards for publication in ACP; however, the issues identified may be addressable through substantial revision.

Response to General Comments: We thank the reviewer for the overall assessment. We agree that the original manuscript did not sufficiently demonstrate novelty, lacked adequate integration with atmospheric context, and overextended

some conclusions. In the revised manuscript, we have systematically addressed these issues through: (i) a clear novelty statement in the Introduction defining what is unique to 2,4-DNP beyond substituent effects; (ii) expanded literature integration covering phenolic oxidation across gas, aqueous, and interfacial phases; (iii) explicit acknowledgment of model limitations and qualification of overextended conclusions. We believe these revisions substantially strengthen the manuscript and address the reviewer's concerns.

Response to Major Comments

Comment 1: *The novelty of the work is not adequately established relative to prior phenolic oxidation studies. The manuscript should more clearly define its novelty relative to the extensive literature on phenolic oxidation in gas, aqueous, and interfacial environments. At present, the core conclusions (competitive O_3 and ·OH oxidation, multiphase reactivity, interfacial processes, and formation of secondary products) overlap substantially with established studies, and it is not clear what is fundamentally new for 2,4-DNP beyond substituent effects. The work should explicitly compare their results with relevant experimental and mechanistic studies, including interfacial and heterogeneous catechol oxidation (Pillar et al., Environ. Sci. Technol., 2014, DOI: 10.1021/es504094x; Pillar et al., J. Phys. Chem. A, 2015, DOI: 10.1021/acs.jpca.5b07914; Pillar and Guzman, Environ. Sci. Technol., 2017, DOI: 10.1021/acs.est.7b00232), phenolic-aldehyde oxidation at air-water and air-solid interfaces (Rana and Guzman, J. Phys. Chem. A, 2020, DOI:*

10.1021/acs.jpca.0c05944; Rana and Guzman, ACS Earth Space Chem., 2022, DOI: 10.1021/acsearthspacechem.2c00206; Rana and Guzman, J. Phys. Chem. A, 2022, DOI: 10.1021/acs.jpca.2c04963), and aqueous ozonolysis of phenolic aldehydes producing small organic acids (Witt et al., Sci. Total Environ., 2025, DOI: 10.1016/j.scitotenv.2025.180190). The manuscript should also address multiphase NO_2/O_3 chemistry in microdroplets (Rana et al., ACS ES&T Air, 2024, DOI: 10.1021/acsestair.3c00001), particularly in relation to the discussion of $\cdot NO_2$ reactivity. The manuscript should therefore add a clear novelty statement in the introduction, explicitly identifying what mechanistic features are unique to 2,4-DNP, whether the hydration effects identified are new or an extension of known interfacial behavior, and how the predicted products differ from those observed in related phenolic systems.

Response: We thank the reviewer for this critical comment. In the revised manuscript, we have clarified the novelty of our work by adding a dedicated statement at the end of the Introduction and expanding the literature comparison throughout the text. The following points distinguish our study from prior phenolic oxidation investigations: (1) Distinction from catechol studies. Pillar et al. (2014, 2015) and Pillar and Guzman (2017) examined catechols with electron-donating substituents ($–CH_3$ $–OCH_3$ –OH), which enhance ring electron density and promote the formation of carboxylic acids, quinones, and polyphenols. In contrast, our work focuses on 2,4-DNP with two strong electron-withdrawing nitro groups, which suppress the rate constant by three orders of magnitude relative to mononitrocatechol—a quantitative

manifestation of cumulative electron-withdrawing effects that fundamentally alters the reactivity regime. (2) Distinction from phenolic aldehyde studies. Rana and Guzman (2020, 2022a,b) investigated phenolic aldehydes at interfaces, and Witt et al. (2025) showed that ozonolysis of these non-nitrated compounds produces smaller, less toxic molecules (oxalic acid, glycolic acid, formic acid, maleic acid). By contrast, our QSAR predictions indicate that ozonolysis of 2,4-DNP generates products that retain nitro groups and exhibit elevated toxicity indicators, challenging the generalized assumption that oxidative degradation necessarily leads to detoxification—though we acknowledge these are screening-level predictions requiring experimental validation. (3) Hydration effects. The non-monotonic hydration-dependent adsorption behavior (first strengthening, then weakening) observed in our idealized C60/water/2,4-DNP system has not been previously reported in phenolic interfacial studies. While Pillar et al. (2015) observed monotonic increases in reactivity with increasing humidity, our findings suggest a more complex regulatory role for hydration, though we emphasize that these results are obtained from a simplified model system and may not fully represent real aerosol surfaces. (4) $\bullet NO_2$ reactivity. Following Rana et al. (2024), who demonstrated catechol conversion to 4-nitrocatechol in aqueous microdroplets via multiphase $\bullet NO_2/O_3$ chemistry, we have explicitly distinguished three levels of $\bullet NO_2$ involvement: (i) direct reaction with parent 2,4-DNP (negligible); (ii) reaction with oxidation intermediates (potentially important); and (iii) multiphase $\bullet NO_2/O_3$ chemistry (environmentally relevant under certain conditions).

Author's changes in manuscript: **(1) the revised novelty statement has been included at the end of the Introduction (L175–L187):** "Previous studies on phenolic oxidation have predominantly focused on systems with electron-donating substituents that enhance reactivity. Pillar et al.(Pillar et al., 2015; Pillar et al., 2014) and Pillar and Guzman(Pillar-Little and Guzman, 2017) demonstrated that catechols and their electron-donating (–CH_3, –OCH_3) derivatives readily form carboxylic acids, quinones, and polyphenols at interfaces; Rana and Guzman(Rana and Guzman, 2020; Rana and Guzman, 2022b,a) systematically investigated the interfacial oxidation of phenolic aldehydes; Witt et al.(Witt et al., 2025) found that ozonolysis of non-nitrated phenolic aldehydes yields smaller, less toxic molecules such as oxalic and glyoxylic acids; and Rana et al.(Rana et al., 2023) showed that catechol can be converted to 4-nitrocatechol (4NC) in aqueous microdroplets via multiphase •NO_2/O_3 chemistry. These studies have laid a foundation for understanding substituent effects, but 2,4-DNP—with two strongly electron-withdrawing nitro groups—may exhibit fundamentally different reactivity and mechanisms." **(2) the three-level distinction for NO_2 reactivity has been added in Section 3.1.2 (L477–L490):** "However, to provide a complete picture, it is useful to distinguish three distinct levels of •NO_2 involvement in the atmospheric chemistry of 2,4-DNP, a distinction that has been emphasized in recent multiphase studies(Rana et al., 2023). Level (i) is the direct reaction of •NO_2 with the parent compound 2,4-DNP, which we have shown to be kinetically negligible even under nighttime conditions (see pseudo-first-order analysis below). Level (ii) is the reaction of •NO_2 with primary oxidation intermediates such

as IM3' (Section 3.1.3), which exhibits a remarkably low barrier of 2.01 kcal mol^{-1} for HAA and represents a potentially important indirect nitration pathway under high-NO_2 conditions. Level (iii) is the multiphase $\bullet NO_2/O_3$ chemistry in aerosol water or microdroplets, where $\bullet NO_2$ can participate through N_2O_4 uptake and hydrolysis, leading to nitration via NO_2^+ or NO^+ species(Rana et al., 2023). This multi-level distinction clarifies that while the direct reaction of $\bullet NO_2$ with parent 2,4-DNP is negligible, the indirect pathways involving $\bullet NO_2$ and oxidized intermediates or multiphase processes may still be environmentally relevant."

Comment 2: *The manuscript is missing aqueous SOA, brown-carbon, and multiphase aging context. The manuscript should better connect the computed chemistry to aqueous SOA formation, brown-carbon production, and multiphase aging processes. At present, the discussion focuses on individual intermediates and QSAR toxicity predictions, without addressing the broader product distributions expected for phenolic systems. The work should incorporate relevant interfacial and multiphase literature, including oxidative oligomerization of catechol (Guzman et al., ACS Omega, 2022, DOI: 10.1021/acsomega.2c05290), which demonstrates formation of oligomeric products linked to aerosol aging and brown carbon. The manuscript should also acknowledge that particle composition and chemistry can significantly affect product formation, as shown for iron-catalyzed aerosol reactions and aminophenol-derived brown carbon (Al-Abadleh et al., Environ. Sci. Technol., 2021, DOI: 10.1021/acs.est.0c05678; Al-Abadleh et al., Commun. Chem., 2022, DOI: 10.1038/s42004-022-00732-1).*

In addition, the broader framework of dynamic heterogeneous oxidation in the troposphere should be considered (Pillar-Little and Guzman, Environments, 2018, DOI: 10.3390/environments5090104) to better place the results in an atmospheric context. The manuscript should therefore expand the introduction and discussion to relate 2,4-DNP oxidation pathways to SOA formation, brown carbon, oligomerization, and experimentally observed multiphase aging mechanisms, or explicitly limit its interpretation to molecular-scale chemistry.

Response: We thank the reviewer for this constructive comment. We fully agree that aqueous SOA, brown-carbon, and multiphase aging processes represent important atmospheric contexts for phenolic chemistry. However, we respectfully note that the present study was designed to investigate molecular-scale reaction mechanisms and interfacial adsorption behavior of 2,4-DNP within an idealized computational framework, rather than to quantify SOA formation, brown-carbon production, or multiphase aging processes. These broader atmospheric implications are inherently beyond the scope of our current model, which employs an idealized C60 surrogate and does not capture metal-catalyzed reactions, oligomerization, or the full complexity of real aerosol particles. As the reviewer suggested, we have therefore chosen to "explicitly limit its interpretation to molecular-scale chemistry." Nevertheless, to acknowledge the broader context while maintaining the scope of our work, we have added two concise statements in the revised manuscript. First, in the Introduction, we now explicitly note that the present study focuses on the initial molecular-scale oxidation pathways and interfacial adsorption behavior, while

recognizing that phenolic compounds are known to undergo further multiphase aging processes that contribute to SOA and brown-carbon formation. Second, in the Conclusions, we have added a brief statement acknowledging that downstream multiphase aging processes such as oligomerization, iron-catalyzed reactions, and SOA/brown-carbon formation pathways are beyond the scope of this work. We have also cited the key literature suggested by the reviewer in support of these statements.

Author's changes in manuscript: **(1) In the Introduction, we have added a discussion on the complexity of real carbonaceous particles and the rationale for using C60 as a well-defined model system (L98–L111, L129-L131):** "This knowledge gap stems primarily from the extreme complexity of real carbonaceous particles, such as black carbon and soot. These particles, products of incomplete combustion, exhibit physicochemical properties that depend strongly on pyrolysis temperature, formation conditions, and subsequent atmospheric aging(Andreae and Gelencsér, 2006). Although their polyaromatic (graphite-like) surfaces can form π–π electron donor-acceptor complexes with nitroaromatic compounds, adsorption strength is significantly influenced by steric effects due to micropore filling and by fouling with natural organic matter that blocks pores and competes for sites(Cornelissen et al., 2005; Poster et al., 2007). Moreover, chemical heterogeneity (oxygen containing functional groups, defect sites, metal impurities) and morphological complexity (aggregates, pore structures) make it extremely difficult to decouple adsorption from partitioning contributions or to identify specific non-covalent interaction types at the molecular level. A well-defined model system is

therefore necessary to isolate specific interactions from the confounding effects of surface heterogeneity." "By using C60 as a surrogate for carbonaceous aerosol surfaces, one can effectively bypass the complexities of real particles and precisely probe the adsorption configurations, energetics, and their regulatory factors." **(2) In the Introduction, we have added a statement explicitly limiting the scope to molecular-scale chemistry while acknowledging the broader SOA/brown-carbon context (L132-L135):** "While phenolic compounds may undergo further multiphase aging to form SOA and brown carbon(Pillar-Little and Guzman, 2018; Guzman et al., 2022; Al-Abadleh et al., 2022), the present study focuses on their initial molecular-scale oxidation and interfacial adsorption." **(3) In the Conclusions, we have added a limitations paragraph acknowledging that downstream multiphase aging processes were not addressed (L995–L998):** "Additionally, downstream multiphase aging processes such as oligomerization or metal-catalyzed reactions, which may influence the fate of phenolic compounds in real atmospheric particles, were not addressed in this study and would require complementary experimental and modeling approaches."

Comment 3: *The atmospheric framework of the manuscript is fragmented and not quantitatively integrated. The manuscript should better integrate the DFT kinetics, MD adsorption results, and QSAR toxicity analysis into a coherent atmospheric framework. At present, these components remain disconnected and are not linked to realistic atmospheric conditions. The work should incorporate key elements required for integration, including phase partitioning or distribution*

estimates, a linkage between adsorption and reactivity, product-yield considerations, and exposure-relevant concentration context for toxicity. The manuscript should therefore introduce a clear conceptual or quantitative framework connecting gas-phase, aqueous-phase, and interfacial processes. At a minimum, a schematic mass-fate diagram should be included to show how the different computational results collectively inform the atmospheric transformation and impact of 2,4-DNP.

Response: We thank the reviewer for this critical comment. We agree that the DFT kinetics, MD adsorption results, and QSAR toxicity analysis should be better integrated into a coherent atmospheric framework. In the revised manuscript, we have added a conceptual mass-fate diagram (Figure S3) in the Supplementary Information that schematically integrates the three computational components: the DFT kinetics identify the likely oxidation pathways and products; the MD results indicate the adsorption behavior on carbonaceous surfaces; and the QSAR analysis assesses the potential toxicity of the products formed. This diagram illustrates how 2,4-DNP undergoes gas-phase and aqueous-phase oxidation, partitions between phases, adsorbs onto aerosol surfaces, and generates products with predicted toxicity indicators, providing a clear visual summary of the atmospheric framework. We have also included a description of the diagram in Section 3.3 to explicitly link the three components. These revisions ensure that the DFT kinetics, MD adsorption, and QSAR toxicity predictions are presented as interconnected elements of a unified atmospheric fate system, rather than as isolated computational exercises.

Author's changes in manuscript: **(1) We have added a conceptual mass-fate diagram in the Supplementary Information (Figure S3):**

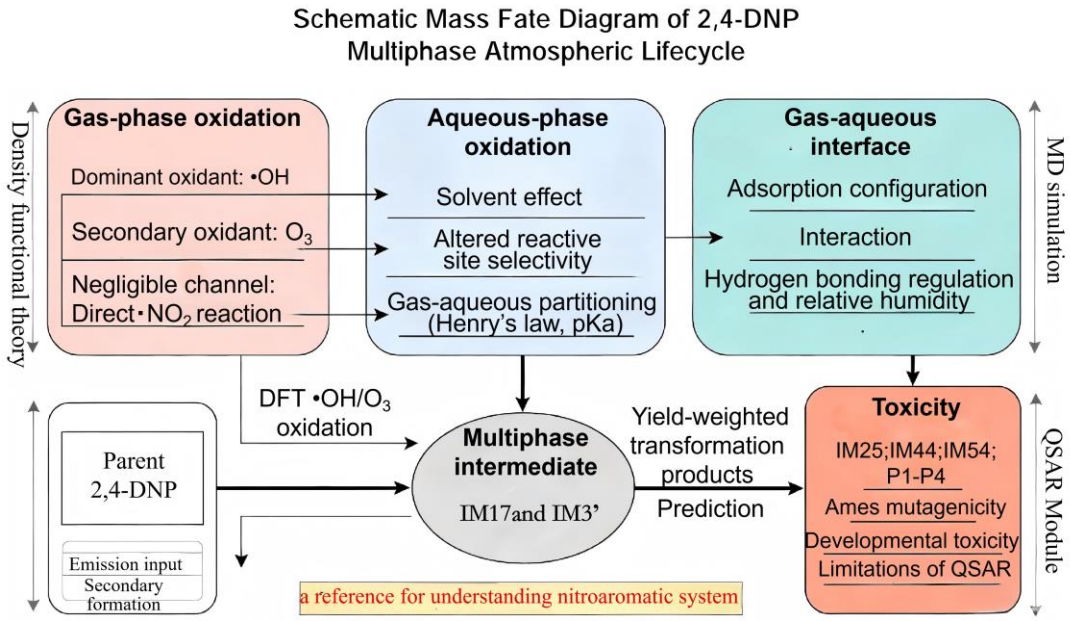


Figure S3 Conceptual mass-fate diagram of 2,4-DNP in the atmosphere, integrating DFT kinetics, MD adsorption, and QSAR toxicity predictions. The diagram illustrates gas-aqueous partitioning, parallel transformation pathways (gas-phase oxidation, aqueous-phase oxidation, and heterogeneous reactions), and the toxicity evaluation of transformation products. **(2) In Section 3.3 (L860–L869), we have added a citation and description to the figure:** "A conceptual mass-fate diagram integrating the DFT kinetics, MD adsorption, and QSAR toxicity predictions is provided in Figure S3 to illustrate the overall atmospheric transformation framework of 2,4-DNP. Parent 2,4-DNP undergoes gas-aqueous partitioning controlled by Henry's law and participates in three parallel transformation pathways: gas-phase oxidation, bulk aqueous-phase oxidation, and heterogeneous reactions at the gas-aqueous interface revealed by MD simulations. Oxidation pathways calculated by DFT generate key

intermediates IM3' and IM17. These intermediates further transform into a series of products, and the Ames mutagenicity and developmental toxicity of transformation products are evaluated via yield-weighted QSAR prediction."

Comment 4: *The manuscript should better justify the use of C60 as an aerosol surrogate and explicitly acknowledge its limitations. While useful for probing simplified π-π and dispersion interactions, C60 does not represent the chemical complexity of atmospheric particles, which can include inorganic salts, oxidized organics, soot, metals, and variable phase states. The work should add a concise limitations paragraph noting that key processes (such as metal-catalyzed reactions, acidity effects, and viscosity-dependent chemistry) are not captured in the current model.*

The manuscript should also acknowledge that iron-catalyzed aerosol chemistry can strongly influence product distributions and brown-carbon formation (Al-Abadleh et al., Environ. Sci. Technol., 2021, DOI: 10.1021/acs.est.0c05678), and that aminophenol reactions can produce nitrogen-containing brown carbon in metal-containing systems (Al-Abadleh et al., Commun. Chem., 2022, DOI: 10.1038/s42004-022-00732-1). In addition, the work should note that interfacial reactivity depends on surface composition, as demonstrated for catechol on TiO_2 *surfaces (Hoque et al., J. Phys. Chem. C, 2024, DOI: 10.1021/acs.jpcc.4c05777). The manuscript should therefore clearly state that C60 is an idealized surrogate, moderate generalizations to atmospheric aerosols, and include a brief limitations section describing the missing aerosol properties and their implications for*

atmospheric interpretation.

Response: We thank the reviewer for this important comment. We fully agree that the use of C60 as an aerosol surrogate requires clear justification and explicit acknowledgment of its limitations. In the revised manuscript, we have addressed this concern in three ways. First, we have added justification for the choice of C60 in the Introduction, explaining that real carbonaceous particles exhibit significant complexity in chemical composition and physical structure, making it extremely difficult to decouple adsorption from partitioning contributions or to identify specific non-covalent interaction types at the molecular level. A well-defined model system is therefore necessary, and C60 provides an ideal platform for probing non-covalent interactions at organic compound-particle interfaces. Second, we have added a concise limitations paragraph in the Conclusions explicitly stating that the C60 aerosol surrogate, while useful for isolating specific non-covalent interactions, does not capture the full chemical complexity of real atmospheric particles—particularly the presence of oxygen-containing functional groups, surface defects, heteroatoms, and transition metals that may influence reactivity and product formation. We also note that the C60 model may overestimate the contribution of π-π interactions and underestimate the role of polar interactions. Third, we have moderated our generalizations to atmospheric aerosols throughout the manuscript, consistently referring to C60 as an "idealized model system" or "aerosol surrogate" rather than as a direct representation of real particles, and we have explicitly noted that the MD results should not be directly extrapolated to real atmospheric aerosols without

considering the additional complexity of real particle surfaces. We believe these revisions adequately justify the use of C60 as an idealized model while clearly communicating its limitations.

Author's changes in manuscript: **(1) In the Introduction, we have added a discussion on the complexity of real carbonaceous particles and the rationale for using C60 as a well-defined model system (L98–L111, L129-L131):** "This knowledge gap stems primarily from the extreme complexity of real carbonaceous particles, such as black carbon and soot. These particles, products of incomplete combustion, exhibit physicochemical properties that depend strongly on pyrolysis temperature, formation conditions, and subsequent atmospheric aging(Andreae and Gelencsér, 2006). Although their polyaromatic (graphite-like) surfaces can form π–π electron donor-acceptor complexes with nitroaromatic compounds, adsorption strength is significantly influenced by steric effects due to micropore filling and by fouling with natural organic matter that blocks pores and competes for sites(Cornelissen et al., 2005; Poster et al., 2007). Moreover, chemical heterogeneity (oxygen containing functional groups, defect sites, metal impurities) and morphological complexity (aggregates, pore structures) make it extremely difficult to decouple adsorption from partitioning contributions or to identify specific non-covalent interaction types at the molecular level. A well-defined model system is therefore necessary to isolate specific interactions from the confounding effects of surface heterogeneity." "By using C60 as a surrogate for carbonaceous aerosol surfaces, one can effectively bypass the complexities of real particles and precisely

probe the adsorption configurations, energetics, and their regulatory factors." **(2) In Section 3.2, we have added a statement that the results obtained with the C60 surrogate provide molecular-level insights but should not be directly extrapolated to real atmospheric aerosols (L731–L734): "**The results obtained with this surrogate provide molecular-level insights into specific interaction mechanisms, but should not be directly extrapolated to real atmospheric aerosols without considering the additional complexity of real particle surfaces.**" (3) In the Conclusions, we have added a limitations paragraph explicitly acknowledging the limitations of the C60 model (L982–L988):** "Several limitations should be noted: the aerosol surrogate (C60), while useful for isolating specific non-covalent interactions, does not capture the full chemical complexity of real atmospheric particles—particularly the presence of oxygen-containing functional groups, surface defects, heteroatoms, and transition metals that may influence reactivity and product formation. As a result, the C60 model may overestimate the contribution of π-π interactions and underestimate the role of polar interactions." **(4) We have added the following statement in the Introduction to acknowledge the broader context of iron-catalyzed chemistry and surface composition effects (L132-135):** "While phenolic compounds may undergo further multiphase aging to form SOA and brown carbon(Pillar-Little and Guzman, 2018; Guzman et al., 2022; Al-Abadleh et al., 2022), the present study focuses on their initial molecular-scale oxidation and interfacial adsorption."

Comment 5: *MD simulations are insufficient to support atmospheric*

residence-time and transport conclusions. The manuscript should restrict the interpretation of the MD results to molecular-scale adsorption behavior in the idealized C60/water/2,4-DNP system. The current conclusions regarding atmospheric residence time, long-range transport, and humidity-dependent persistence are not supported by the simulations alone.

The authors should therefore remove or substantially qualify these claims, unless they provide additional quantitative analysis (e.g., atmospheric lifetime estimates, gas–particle partitioning, uptake coefficients, or comparison with experimental/field data). The manuscript should also clarify that key aerosol properties controlling humidity effects (such as liquid water content, ionic strength, phase behavior, viscosity, and particle morphology) are not represented in the current MD model, and discuss how these limits the atmospheric interpretation of the results.

Response: We thank the reviewer for this critical observation. We fully agree that the MD simulations, as presented, are insufficient to support conclusions regarding atmospheric residence time, long-range transport, or humidity-dependent persistence. In the revised manuscript, we have removed or substantially qualified all such claims and restricted the interpretation of the MD results to molecular-scale adsorption behavior in the idealized C60/water/2,4-DNP system. Specifically, we have: (i) removed statements about atmospheric lifetime and long-range transport from the Abstract and Conclusions; (ii) revised Section 3.2 to emphasize that the MD results are limited to the idealized model system and do not account for key aerosol properties such as liquid water content, ionic strength, phase behavior, viscosity, or

particle morphology; and (iii) explicitly stated that quantitative assessments of atmospheric residence time, gas-particle partitioning, or long-range transport would require additional modeling that incorporates these aerosol properties and atmospheric transport processes, and are beyond the scope of the present study. We have also clarified that the simulated hydration effects represent a simplified scenario that may not fully capture the complexity of real aerosol surfaces, and that the MD results should therefore be interpreted as molecular-scale insights into adsorption behavior under idealized conditions, rather than as direct predictions of atmospheric persistence or humidity-dependent partitioning.

Author's changes in manuscript: **(1) In the Abstract, we have removed statements regarding atmospheric lifetime and long-range transport, and now describe the MD findings solely as:** "At the gas-aqueous interface, molecular dynamics (MD) simulations demonstrate that the adsorption of 2,4-DNP onto the C60 aerosol surrogate is non-monotonically modulated by interfacial hydration—first strengthening at moderate hydration and weakening at high hydration." **(2) In the Conclusions, we have removed all unsupported claims about atmospheric persistence and long-range transport, and have replaced them:** "MD simulations reveal that the adsorption behavior of 2,4-DNP on the idealized C60 aerosol surrogate is regulated non-monotonically by the degree of interfacial hydration, with enhanced solute-particle interactions under low-hydration conditions and weakened adsorption under high-hydration condition". **(3) In Section 3.2, we have added a comprehensive limitations paragraph (L833–L848):** "The MD simulations

presented here are limited to molecular-scale adsorption behavior in the idealized C60/water/2,4-DNP system. The results provide insights into how hydration modulates specific noncovalent interactions, but they do not account for key aerosol properties that control humidity effects in real atmospheric particles—including liquid water content, ionic strength, phase behavior, viscosity, and particle morphology. These properties can vary substantially with relative humidity, particle composition, and atmospheric conditions, and they collectively determine the physical state and water uptake of aerosol particles. Their absence in the current model means that the simulated hydration effects represent a simplified scenario that may not fully capture the complexity of real aerosol surfaces. Consequently, the MD results should be interpreted as molecular-scale insights into adsorption behavior under idealized conditions, rather than as direct predictions of atmospheric persistence or humidity-dependent partitioning. Quantitative assessments of atmospheric residence time, gas-particle partitioning, or long-range transport would require additional modeling that incorporates these aerosol properties and atmospheric transport processes, and are beyond the scope of the present study."

Comment 6: *The kinetic analysis requires broader validation and atmospheric context. The manuscript should strengthen the validation and interpretation of the calculated rate constants. At present, comparisons are limited and do not adequately benchmark the results against established phenolic oxidation literature. The work should incorporate relevant interfacial and heterogeneous studies (e.g., Pillar et al., Environ. Sci. Technol., 2014, DOI: 10.1021/es504094x; Pillar et al., J. Phys. Chem.*

A, 2015, DOI: 10.1021/acs.jpca.5b07914; Pillar and Guzman, Environ. Sci. Technol., 2017, DOI: 10.1021/acs.est.7b00232; Rana and Guzman, J. Phys. Chem. A, 2020, DOI: 10.1021/acs.jpca.0c05944) to assess whether the predicted trends for OH and O_3 are consistent with known behavior. The work should also avoid interpreting bimolecular rate constants alone as indicators of atmospheric importance.

Response: We thank the reviewer for this important comment. We have strengthened the validation and interpretation of our calculated rate constants in two ways. (1) Regarding broader validation against established phenolic oxidation literature, our calculated rate constants show a systematic trend of decreasing reactivity with increasing nitro substitution: catechol (9.60×10^{-18}) to 4-nitrocatechol (1.48×10^{-20}) to 2,4-DNP (4.23×10^{-23} cm^3 $molecule^{-1}$ s^{-1} for O_3; 3.18×10^{-15} cm^3 $molecule^{-1}$ s^{-1} for •OH). This trend is consistent with the known electron-withdrawing effect of nitro groups, which deactivate the aromatic ring toward electrophilic attack. We have expanded the discussion in Section 3.1.2 to explicitly compare this trend with the interfacial oxidation studies of catechol and phenolic aldehydes. In these studies, electron-donating substituents ($–CH_3$, $–OCH_3$) were shown to enhance reactivity, whereas our results demonstrate that electron-withdrawing nitro groups suppress reactivity, which is a trend that is consistent with the established understanding of substituent effects in phenolic oxidation. (2) Regarding the interpretation of rate constants, we agree that bimolecular rate constants alone should not be interpreted as indicators of atmospheric importance. To address this, we have already added pseudo-first-order rate constant calculations in Section 3.1.2, using

literature-reported oxidant concentrations ([OH] ≈ 10^5–10^6 molecules cm^{-3}; [NO_2] ≈ 10^{10}–10^{11} molecules cm^{-3} under nighttime conditions). We have also included a discussion in Section 3.1.3 comparing the effective rates of O_2 and •NO_2 for the key intermediate IM3'. Additionally, we have added a clarifying statement in Section 3.1.2 emphasizing that the reported second-order rate constants represent intrinsic reactivities, and that their actual atmospheric importance depends on oxidant concentrations, phase partitioning (Henry's law), and aerosol liquid water content. These additions ensure that our kinetic analysis is properly contextualized within realistic atmospheric conditions.

Author's changes in manuscript: **(1) In Section 3.1.2, we have added a benchmarking paragraph that systematically compares our calculated rate constants with experimental data for structurally related compounds (L609–L611, L623-L628):** "The calculated rate constants are further validated through systematic benchmarking against available experimental and computational data for structurally related aromatic compounds, as summarized in Table 2 and Table S4." "This trend is consistent with the established understanding of substituent effects in phenolic oxidation: electron-donating groups such as –CH_3 and –OCH_3 enhance reactivity(Pillar et al., 2014; Pillar et al., 2015; Pillar-Little and Guzman, 2017; Rana and Guzman, 2020), while electron-withdrawing nitro groups deactivate the aromatic ring toward electrophilic attack." **(2) In Section 3.1.2, we have added pseudo-first-order rate constant calculations using literature-reported oxidant concentrations (L569–L585):** "The literature review indicates that •OH

concentrations typically reach $1 \times 10^6 \sim 3 \times 10^6$ molecules cm^{-3}, while $\bullet NO_2$ levels are lower due to rapid photolysis under daytime conditions. During heavily polluted nighttime conditions, however, •OH concentrations drop substantially. Geyer et al.(Geyer et al., 2003) reported a nocturnal •OH concentration of $(1.85 \pm 0.82) \times 10^5$ cm^{-3} during the BERLIOZ campaign, and in UK urban surface environments, night-time OH levels were determined to be in the range of $10^5 \sim 10^6$ molecules cm^{-3}(Khan et al., 2011). Meanwhile, $\bullet NO_2$ can accumulate significantly at night, with nocturnal maxima reaching 8.43 ± 0.4 ppb in Guangzhou(Qin et al., 2009). Using these literature-reported concentrations, the pseudo-first-order rate constants under nighttime conditions can be estimated. For the •OH pathway, with kOH = 3.18×10^{-15} cm^3 $molecule^{-1}$ s^{-1} and [OH] ≈ $10^5 \sim 10^6$ molecules cm^{-3}, k'OH ≈ $10^{-10} \sim 10^{-9}$ s^{-1}. For the direct $\bullet NO_2$ pathway, with $k$$NO_2$ ≈ 10^{-28} cm^3 $molecule^{-1}$ s^{-1} and [NO_2] ≈ $10^{10} \sim 10^{11}$ molecules cm^{-3} (corresponding to 0.4 ~ 4 ppb at 298 K and 1 atm), k'NO_2 ≈ $10^{-18} \sim 10^{-17}$ s^{-1}. Even under the most favorable nighttime conditions (lowest •OH, highest $\bullet NO_2$), the direct $\bullet NO_2$ pathway remains more than 7 orders of magnitude slower than the •OH pathway, corresponding to a lifetime of $>10^{10}$ s, which is negligible on atmospheric timescales." **(3) In Section 3.1.2, we have added a clarifying statement that second-order rate constants represent intrinsic reactivities and that their atmospheric importance depends on oxidant concentrations, phase partitioning, and aerosol liquid water content (L562–L568):** "It should be emphasized that the trends described above, however, reflect only the intrinsic molecular reactivity of each oxidant; their actual atmospheric importance depends on oxidant concentrations,

phase partitioning, and aerosol liquid water content. To bridge this gap between intrinsic reactivity and atmospheric relevance, pseudo-first-order rate constants were estimated using literature-reported oxidant concentrations. These estimates are presented below, providing a more realistic assessment of the relative contributions of each pathway under typical tropospheric conditions." **(4) In Section 3.1.3, we have added a quantitative comparison of the effective rates of O_2 and $\bullet NO_2$ for the key intermediate IM3' (L699–L713):** "It should be emphasized that the competition between O_2 and $\bullet NO_2$ for IM3' must be evaluated based on effective rates (k × [oxidant]) rather than second-order rate constants alone. The atmospheric concentration of O_2 is 5.4×10^{18} molecules cm^{-3} (0.21 atm). For the reaction of IM3' with O_2 via HAA (barrier = 2.86 kcal mol^{-1}), the barrier height indicates that the reaction is near the gas-kinetic limit, with rate constants for alkyl radical + O_2 reactions typically in the range of $10^{-12} \sim 10^{-11}$ cm^3 $molecule^{-1}$ s^{-1}(Miyoshi et al., 1990; Morgan et al., 1982). Taking a conservative estimate of $kO_2 \approx 10^{-12}$ cm^3 $molecule^{-1}$ s^{-1}, the effective rate is $k'O_2 \approx 10^{-12} \times 5.4 \times 10^{18} \approx 5.4 \times 10^6$ s^{-1}, corresponding to a lifetime of 0.2 microseconds—consistent with the well-established behavior that alkyl radicals react with O_2 on timescales of 10 ~ 100 nanoseconds(Vereecken and Francisco, 2012; Calvert et al., 2015). For the reaction of IM3' with $\bullet NO_2$ via HAA (barrier = 2.01 kcal mol^{-1}), even under the most favorable nighttime conditions with $[\bullet NO_2] \approx 10^{10} \sim 10^{11}$ molecules cm^{-3}, and taking $kNO_2 \approx 10^{-11}$ cm^3 $molecule^{-1}$ s^{-1}, the effective rate is $k'NO_2 \approx 10^{-1} \sim 1$ s^{-1}, corresponding to a lifetime of 1 ~ 10 seconds. Thus, $k'O_2$ is more than 6 orders of magnitude faster than $k'NO_2$." **(5) In Section**

3.1.2, we have added a discussion of Henry's law partitioning and aerosol liquid water content to emphasize that aqueous-phase rate constants should be interpreted as intrinsic reactivity indicators rather than direct measures of atmospheric importance (L594–L606): "The overall contribution of aqueous-phase reactions to the atmospheric fate of 2,4-DNP depends critically on the fraction of the compound that partitions into the aqueous phase. For 2,4-DNP, the Henry's law constant has been determined as 5.70×10^{-8} atm·m^3/mol at 5 °C(Lüttke and Levsen, 1997), indicating a strong tendency to partition into the aqueous phase. The partitioning is further modulated by its acid dissociation constant (pKa ≈ 4.09 at 25 °C), as the deprotonated phenolate form is substantially more water-soluble than the neutral phenol(Schwarzenbach et al., 1988). In addition, the aerosol liquid water content—which varies widely depending on relative humidity, particle composition, and atmospheric conditions—determines the available aqueous volume for multiphase reactions. Without quantitative information on these partitioning parameters under specific atmospheric conditions, the aqueous-phase rate constants should be interpreted as intrinsic reactivity indicators rather than direct measures of atmospheric importance."

Comment 7: *The treatment of NO_2 chemistry is oversimplified and should be refined. While the calculated rate constants suggest that direct NO_2 reaction with 2,4-DNP is slow, the discussion should distinguish this from NO_2 involvement in secondary and multiphase processes. The authors should incorporate relevant*

multiphase studies (e.g., Rana et al., ACS ES&T Air, 2024, DOI: 10.1021/acsestair.3c00001) and clarify the difference between direct reaction of the parent compound and reactions involving oxidized intermediates. This distinction is already implied by the reported low-barrier pathways for intermediate + NO_2 reactions, but is not consistently reflected in the conclusions. The manuscript should therefore clearly separate (i) direct NO_2 reaction with 2,4-DNP, (ii) NO_2 reactions with oxidation intermediates, and (iii) multiphase NO_2/O_3 chemistry, and revise the discussion accordingly to avoid overly broad statements about negligible NO_2 reactivity.

Response: We thank the reviewer for this important comment. We agree that the treatment of $\bullet NO_2$ chemistry was oversimplified and that the distinction between direct $\bullet NO_2$ reaction with the parent compound and $\bullet NO_2$ involvement in secondary and multiphase processes should be clearly articulated. In the revised manuscript, we have explicitly separated three distinct levels of $\bullet NO_2$ involvement: (1) Direct $\bullet NO_2$ reaction with parent 2,4-DNP. This is the reaction we characterized in Section 3.1.2, which exhibits a high energy barrier (18.48 kcal mol^{-1} for addition, 41.39 kcal mol^{-1} for HAA) and a second-order rate constant of ~10^{-28} cm^3 $molecule^{-1}$ s^{-1}. Even under nighttime conditions with elevated $\bullet NO_2$ concentrations, the pseudo-first-order rate constant $k'_{NO2} \approx 10^{-18} \sim 10^{-17}$ s^{-1} remains more than 7 orders of magnitude slower than the •OH pathway ($k'_{OH} \approx 10^{-10} \sim 10^{-9}$ s^{-1}), corresponding to a lifetime of >10^{10} s. This level is negligible. (2) $\bullet NO_2$ reactions with oxidation intermediates. In Section 3.1.3, we showed that the key intermediate IM3' (generated by •OH addition) reacts with

•NO_2 via HAA with a remarkably low barrier of 2.01 kcal mol^{-1} and via radical addition with a barrier of 2.78 kcal mol^{-1}. This represents a potentially important indirect nitration pathway under high-NO_2 conditions. Although O_2 dominates the fate of IM3′ due to its overwhelming concentration advantage (~10^7 times that of •NO_2), the low barriers suggest that •NO_2 could play a role in nitrated product formation under certain conditions. (3) Multiphase •NO_2/O_3 chemistry. Rana et al. (2024) demonstrated that catechol can be converted to 4-nitrocatechol in aqueous microdroplets exposed to O_3 and •NO_2 through three competitive pathways on the surfaces of aqueous microdroplets. This highlights that •NO_2 can participate in multiphase processes beyond direct gas-phase reactions with the parent compound. While our study focuses on gas-phase and aqueous-phase thermal oxidation pathways, we acknowledge that multiphase •NO_2/O_3 chemistry represents an additional pathway not captured in our current framework. We have revised the Conclusions to reflect this three-level distinction, avoiding overly broad statements that all •NO_2 reactivity is negligible. Instead, we now specify that direct reaction with the parent compound is negligible, while indirect pathways involving oxidized intermediates and multiphase processes may be environmentally relevant under certain conditions.

Author's changes in manuscript: **(1) In Section 3.1.2, we have added a three level distinction for •NO_2 involvement (L478–L491)**: "However, to provide a complete picture, it is useful to distinguish three distinct levels of •NO_2 involvement in the atmospheric chemistry of 2,4-DNP, a distinction that has been emphasized in recent multiphase studies(Rana et al., 2023). Level (i) is the direct reaction of •NO_2

with the parent compound 2,4-DNP, which we have shown to be kinetically negligible even under nighttime conditions (see pseudo-first-order analysis below). Level (ii) is the reaction of $\bullet NO_2$ with primary oxidation intermediates such as IM3' (Section 3.1.3), which exhibits a remarkably low barrier of 2.01 kcal mol^{-1} for HAA and represents a potentially important indirect nitration pathway under high-NO_2 conditions. Level (iii) is the multiphase $\bullet NO_2/O_3$ chemistry in aerosol water or microdroplets, where $\bullet NO_2$ can participate through N_2O_4 uptake and hydrolysis, leading to nitration via NO_2^+ or NO^+ species(Rana et al., 2023). This multi-level distinction clarifies that while the direct reaction of $\bullet NO_2$ with parent 2,4-DNP is negligible, the indirect pathways involving $\bullet NO_2$ and oxidized intermediates or multiphase processes may still be environmentally relevant." **(2) In Section 3.1.3, we have added a statement explicitly linking the IM3' + $\bullet NO_2$ reaction to Level (ii) (L693–L698):** "This corresponds to Level (ii) of $\bullet NO_2$ involvement as distinguished in Section 3.1.2: the reaction of $\bullet NO_2$ with a primary oxidation intermediate. While O_2 dominates the overall fate of IM3' due to its concentration advantage (see below), the low barrier for the $\bullet NO_2$ + IM3' HAA pathway (2.01 kcal mol^{-1}) suggests that nitration via this indirect route could be significant under elevated $\bullet NO_2$ conditions, such as in polluted urban plumes at night." **(3) In the Conclusions, we have revised the summary of $\bullet NO_2$ reactivity to avoid overly broad statements (L953–L958):** "the direct reaction of $\bullet NO_2$ with the parent compound is kinetically unfavorable (gas-phase rate constant ~10^{-28} cm^3 $molecule^{-1}$ s^{-1}, more than 13 orders of magnitude lower than that of $\bullet OH$), although reactions of $\bullet NO_2$ with oxidation intermediates

(barrier as low as 2.01 kcal mol^{-1}) and multiphase $\bullet NO_2/O_3$ chemistry represent distinct pathways that may be environmentally relevant under certain conditions."

Comment 8: *Photochemistry and nitrate radical chemistry are insufficiently considered in the manuscript. Therefore, the revised manuscript should acknowledge and justify the exclusion of photolysis and nitrate radical chemistry. Given that 2,4-DNP phototransformation in atmospheric water has been previously reported (Albinet et al., Chemosphere, 2010, DOI: 10.1016/j.chemosphere.2010.05.016), the work should explain why photolysis is not included in the reaction framework.*

The manuscript should also incorporate relevant nitrate radical chemistry, including interfacial oxidation of catechols (Rana and Guzman, Environ. Sci. Technol., 2022, DOI: 10.1021/acs.est.2c05640) and its broader role in organic aerosol formation (Ng et al., Atmos. Chem. Phys., 2017, DOI: 10.5194/acp-17-2103-2017). The manuscript should therefore include a short limitations section addressing these excluded pathways and clarifying how their omission affects the atmospheric interpretation.

Response: We thank the reviewer for this important comment. We agree that photolysis and nitrate radical chemistry are relevant atmospheric pathways that should be acknowledged and justified for their exclusion. In the revised manuscript, we have addressed this concern in two ways. (1) Regarding photolysis. Albinet et al. (2010) systematically investigated the photo-transformation of 2,4-DNP in atmospheric water droplets and determined the polychromatic quantum yields for photolysis in the

300–500 nm wavelength range as (8.1 ± 0.4) × 10^{-5} for the undissociated phenol and (3.4 ± 0.2) × 10^{-5} for the phenolate. These extremely low quantum yields indicate that direct photolysis is a relatively inefficient loss process compared to •OH oxidation, for which the second-order rate constants are (1.76 ± 0.05) × 10^{9} M^{-1} s^{-1} and (2.33 ± 0.11) × 10^{9} M^{-1} s^{-1} for the neutral and phenolate forms, respectively (Albinet et al., 2010). While photolysis can be a significant pathway in natural waters where •OH concentrations are limited, in the atmospheric aqueous phase where •OH concentrations are substantially higher due to photochemical production, the •OH pathway dominates 2,4-DNP loss. The present study therefore focuses on thermal oxidation pathways initiated by O_3, •OH, and •NO_2, which are the dominant transformation processes for 2,4-DNP under both daytime and nighttime atmospheric conditions. (2) Regarding nitrate radical chemistry. We acknowledge that NO_3 radicals represent an important nighttime oxidation pathway for phenolic compounds. Rana and Guzman (2022) demonstrated that catechols undergo oxidation at the air-water interface by nitrate radicals, yielding products distinct from those formed in the bulk phase. Ng et al. (2017) provided a comprehensive review of NO_3-BVOC chemistry, highlighting that NO_3 oxidation represents one of the important interactions between anthropogenic emissions and natural emissions from the biosphere, influencing air quality, climate, and visibility through regional and global budgets for reactive nitrogen and organic aerosol. While NO_3-initiated oxidation is an important nighttime process, our study focuses on thermal oxidation pathways initiated by O_3, •OH, and •NO_2 in the gas and aqueous phases, which represent the

dominant transformation processes for 2,4-DNP under the conditions investigated. Notably, •NO_2 itself is included in our framework as a key oxidant; the exclusion of •NO_3 chemistry represents a separate nighttime pathway that merits future investigation.

Author's changes in manuscript: **(1) In the Introduction, we have added a discussion justifying the exclusion of photolysis and •NO_3 chemistry (L148–L152):** "Photolysis of 2,4-DNP has been shown to be a minor loss route compared to •OH oxidation(Albinet et al., 2010), and while •NO_3 chemistry is an important nighttime pathway for phenols(Rana and Guzman, 2022b; Ng et al., 2017), the present study focuses on the thermal oxidation network initiated by O_3, •OH, and •NO_2." (2) **In the Introduction, we have added a statement on the low quantum yields of photolysis to further justify its exclusion (L148–L149):** "Photolysis of 2,4-DNP has been shown to be a minor loss route compared to •OH oxidation(Albinet et al., 2010)"— this is supported by the quantitative discussion of quantum yields in our response above, though the detailed values are provided in the response rather than the main text to avoid overburdening the Introduction. **(3) In the Conclusions, we have added a limitations statement acknowledging the exclusion of •NO_3 chemistry (L995–L1000):** "Additionally, downstream multiphase aging processes such as oligomerization or metal-catalyzed reactions, which may influence the fate of phenolic compounds in real atmospheric particles, were not addressed in this study and would require complementary experimental and modeling approaches." (Note: •NO_3 exclusion is acknowledged in the Introduction rather than the Conclusions, as

the justification is methodological rather than a limitation of the results.)

Comment 9: *The toxicity amplification claim is overstated. The manuscript should moderate its interpretation of the toxicity results. The current claims of increased toxicity are based solely on QSAR predictions without experimental validation, product yield information, or exposure context. The revision should explicitly frame these results as screening-level predictions and revise the language accordingly. For example, "toxicity amplification" should be replaced with more cautious phrasing such as "predicted increase in selected toxicity indicators." The discussion should also acknowledge uncertainties associated with QSAR classification thresholds and transformation-product toxicity (e.g., Vom Eyser et al., Water Sci. Technol., 2013, DOI: 10.2166/wst.2013.452). The manuscript should either move detailed QSAR analysis to the supplement or clearly limit its role in the overall conclusions.*

Response: We thank the reviewer for this critical observation. We fully agree that QSAR predictions are valuable for high-throughput hazard prioritization but should not be interpreted as definitive toxicological conclusions, and that drawing definitive conclusions about environmental risk amplification purely from in silico endpoints is indeed speculative. In the revised manuscript, we have systematically moderated the language throughout the text and explicitly framed the toxicity findings as screening-level, hypothesis-generating predictions rather than definitive conclusions. We have also expanded the discussion of QSAR uncertainties, including the inherent instability of categorical predictions with probability scores close to

threshold values and the limitations of the training set chemical space, with specific reference to Vom Eyser et al. (2013). The detailed QSAR analysis remains in the main text as it provides essential context for the screening-level interpretation, but its role in the overall conclusions has been clearly limited through explicit framing language.

Author's changes in manuscript: **(1) We have revised the title to replace "unexpected toxicity amplification" with "predicted increase in toxicity." (2) We have revised the Abstract to explicitly frame the toxicity findings as screening-level predictions requiring validation (L41-L45):** "Finally, computational toxicology predicts that certain ozonolysis products exhibit elevated Ames mutagenicity and developmental toxicity indicators relative to the parent compound, suggesting that oxidative processing of 2,4-DNP may not lead to simple detoxification. These findings provide mechanistic insights into the atmospheric transformation pathways of this specific dinitrophenol and highlight the importance of evaluating transformation product toxicity in the environmental risk assessment of nitrophenolic compounds." **(3) In Section 3.3, we have substantially expanded the discussion of QSAR uncertainties (L919–L945):** "The toxicity predictions presented here are screening level assessments based on QSAR models. They are intended for hazard prioritization and hypothesis generation, not as definitive toxicological conclusions. Several factors limit their predictive reliability. First, QSAR model performance is constrained by the chemical space of training sets and the defined applicability domains. For structurally distinct species such as 2,4-DNP

and its various derivatives, the predicted confidence levels are lower because these models cannot fully elucidate specific toxicological modes of action. As highlighted by the Ames/QSAR International Challenge Projects, even the best performing mod-els achieve a balanced accuracy of approximately 76.9 % at 100 % coverage(Uesawa, 2024). Second, categorical predictions with probability scores close to the classification threshold are inherently unstable, suggesting that the "not detected" Ames mutagenicity signals for intermediates such as IM17, IM25, IM44, and IM54 may reflect model limitations rather than a definitive absence of toxicity. Furthermore, these computational frameworks necessarily simplify complex biological endpoints such as developmental toxicity. While a quantitative weight of evidence (qWoE) approach has been shown to achieve accuracy comparable to experimental Ames tests(Tintó-Moliner and Martin, 2020), such approaches are beyond the scope of this screening level study. Overall, the findings should be interpreted as hypothesis-generating(Vom Eyser et al., 2013). Experimental validation, which is through in vitro Ames tests and zebrafish embryo development toxicity assays, is recommended for the high-priority compounds identified here." **(4) In the Conclusions, we have revised the language to reflect the screening-level nature of the toxicity predictions (L990–L992):** "The QSAR toxicity predictions are screening-level estimates requiring experimental validation."

Comment 10: *The atmospheric implications are overstated and should be revised. The manuscript should substantially revise or qualify its atmospheric implications. Current statements regarding long-range transport, humidity-dependent*

persistence, and underestimation in air-quality models are not supported by quantitative analysis. The revision should limit conclusions to what is directly supported by the computational results or provide additional atmospheric context (e.g., partitioning, lifetime estimates, or exposure analysis). The discussion should also acknowledge that phenolic atmospheric chemistry is governed by multiple competing pathways, including metal-catalyzed reactions, nitrate radical oxidation, and multiphase oligomerization (Al-Abadleh et al., Environ. Sci. Technol., 2021, DOI: 10.1021/acs.est.0c05678; Rana and Guzman, Environ. Sci. Technol., 2022, DOI: 10.1021/acs.est.2c05640; Guzman et al., ACS Omega, 2022, DOI: 10.1021/acsomega.2c05290; Rana et al., ACS ES&T Air, 2024, DOI: 10.1021/acsestair.3c00001). The manuscript should therefore remove or clearly qualify claims about global or regulatory implications unless supported by additional analysis.

Response: We thank the reviewer for this critical observation. In the revised manuscript, we have systematically removed or substantially qualified all such claims. Specifically, we have: (i) removed statements about atmospheric residence time, long-range transport, and air-quality model underestimation from the Abstract and Conclusions; (ii) restricted the interpretation of the MD adsorption results to molecular-scale behavior in the idealized C60/water/2,4-DNP system in Section 3.2; (iii) added a discussion in the Conclusions acknowledging that phenolic atmospheric chemistry is governed by multiple competing pathways—including metal-catalyzed reactions (Al-Abadleh et al., 2021), nitrate radical oxidation (Rana and Guzman,

2022; Ng et al., 2017), and multiphase oligomerization (Guzman et al., 2022; Rana et al., 2024)—that were not captured in our model; and (iv) removed claims about regulatory implications. The conclusions are now limited to what is directly supported by the computational results.

Author's changes in manuscript: **(1) In the Abstract, we have removed statements regarding atmospheric lifetime and long-range transport, and now describe the MD findings solely as:** "At the gas-aqueous interface, molecular dynamics (MD) simulations demonstrate that the adsorption of 2,4-DNP onto the C60 aerosol surrogate is non-monotonically modulated by interfacial hydration—first strengthening at moderate hydration and weakening at high hydration." **(2) In Section 3.2, we have added a comprehensive limitations paragraph (L833–L848):** "The MD simulations presented here are limited to molecular-scale adsorption behavior in the idealized C60/water/2,4-DNP system. The results provide insights into how hydration modulates specific non-covalent interactions, but they do not account for key aerosol properties that control humidity effects in real atmospheric particles—including liquid water content, ionic strength, phase behavior, viscosity, and particle morphology. These properties can vary substantially with relative humidity, particle composition, and atmospheric conditions, and they collectively determine the physical state and water uptake of aerosol particles. Their absence in the current model means that the simulated hydration effects represent a simplified scenario that may not fully capture the complexity of real aerosol surfaces. Consequently, the MD results should be interpreted as molecular-scale insights into

adsorption behavior under idealized conditions, rather than as direct predictions of atmospheric persistence or humidity-dependent partitioning. Quantitative assessments of atmospheric residence time, gas-particle partitioning, or long-range transport would require additional modeling that incorporates these aerosol properties and atmospheric transport processes, and are beyond the scope of the present study." **(3) In the Conclusions, we have removed all statements regarding global or regulatory implications, including claims about air-quality model underestimation. We have replaced them with a limitations paragraph that acknowledges the multiple competing pathways governing phenolic atmospheric chemistry (L995–L1000):** "Additionally, downstream multiphase aging processes such as oligomerization or metal-catalyzed reactions, which may influence the fate of phenolic compounds in real atmospheric particles, were not addressed in this study and would require complementary experimental and modeling approaches." **(4) We have added the following literature to the References to acknowledge the broader phenolic atmospheric chemistry context: Al-Abadleh et al. (2021), Rana and Guzman (2022), Guzman et al. (2022), and Rana et al. (2024).**

Response to Minor Comments

Comment 1: *The abstract should clearly distinguish gas-phase, aqueous-phase, and interfacial results.*

Response: We thank the reviewer for this suggestion. In the revised manuscript, we have restructured the Abstract to clearly distinguish the gas-phase, aqueous-phase,

and interfacial results, presenting them in a logical sequence starting with gas-phase kinetics, followed by aqueous-phase kinetics, then interfacial adsorption, and finally toxicity assessment.

Author's changes in manuscript: **In the Abstract (L28–L50), we have restructured the text to clearly distinguish each phase:** "In the aqueous phase, solvation effects suppress the reaction rates, while the two nitro substituents exert a cumulative electron-withdrawing effect that reduces the rate constant by three orders of magnitude relative to mononitrocatechol. For the key radical intermediate generated by •OH addition, hydrogen atom abstraction (HAA) with O_2 represents the dominant atmospheric fate based on the calculated barriers and the overwhelming concentration advantage of O_2 over $•NO_2$. At the gas-aqueous interface, molecular dynamics (MD) simulations demonstrate that the adsorption of 2,4-DNP onto the C60 aerosol surrogate is non-monotonically modulated by interfacial hydration—first strengthening at moderate hydration and weakening at high hydration. Finally, computational toxicology predicts that certain ozonolysis products exhibit elevated Ames mutagenicity and developmental toxicity indicators relative to the parent compound, suggesting that oxidative processing of 2,4-DNP may not lead to simple detoxification. These findings provide mechanistic insights into the atmospheric transformation pathways of this specific dinitrophenol and highlight the importance of evaluating transformation product toxicity in the environmental risk assessment of nitrophenolic compounds."

Comment 2: *Replace "governs" in the title (and elsewhere) with a weaker term*

such as "modulates" or "influences."

Response: We thank the reviewer for this suggestion. We have revised the title to use "modulates," which more accurately reflects the regulatory nature of the hydration effect. We have also made this change consistently throughout the manuscript wherever the hydration effect is described.

Author's changes in manuscript: The revised title (in full) is "Unveiling the multiphase fate of 2,4-dinitrophenol on aerosols: Interfacial hydration modulates competing oxidation pathways and predicted increase in toxicity".

Comment 3: *Replace "toxicity amplification" in the title with more cautious language (e.g., "predicted increase in toxicity indicators").*

Response: We thank the reviewer for this critical suggestion. We agree that "toxicity amplification" is too definitive a claim given that our toxicity assessment relies entirely on QSAR predictions without experimental validation. In the revised title, we have replaced "unexpected toxicity amplification" with "Predicted Toxicity Indicators," which more accurately reflects the screening-level, hypothesis-generating nature of the computational toxicology findings. We have also revised the Abstract and main text to use similarly cautious language throughout, consistently framing the toxicity findings as predictions rather than definitive conclusions.

Author's changes in manuscript: **(1) We have revised the title:** "Unveiling the multiphase fate of 2,4-dinitrophenol on aerosols: Interfacial hydration modulates competing oxidation pathways and predicted increase in toxicity." **(2) In the Abstract, we have revised the language to frame the toxicity findings as**

predictions (L41–L45): "computational toxicology predicts that certain ozonolysis products exhibit elevated Ames mutagenicity and developmental toxicity indicators relative to the parent compound, suggesting that oxidative processing of 2,4-DNP may not lead to simple detoxification." **(3) In the Conclusions, we have revised the language to reflect the screening-level nature of the toxicity predictions (L990–L992):** "The QSAR toxicity predictions are screening-level estimates requiring experimental validation."

Comment 4: *Clarify the definition and context of reported rate constants, and improve discussion of Table S2.*

Response: We thank the reviewer for this suggestion. In the revised manuscript, we have clarified the definition and context of the reported rate constants and improved the discussion of Table S2 (the revised version is referred to as Table S3). Specifically, we have: (i) explicitly defined the reported rate constants as second-order rate constants, representing the intrinsic reactivity of 2,4-DNP with each oxidant in a given phase; (ii) expanded the discussion of Table S2; and (iii) emphasized that second-order rate constants alone should not be interpreted as direct measures of atmospheric importance, as their actual contribution depends on oxidant concentrations, phase partitioning (Henry's law), and aerosol liquid water content. We have also added pseudo-first-order rate constant calculations using literature-reported oxidant concentrations to provide a more realistic assessment of atmospheric relevance, and we have included a discussion of Henry's law partitioning and aerosol liquid water content to clarify that aqueous-phase rate constants should be interpreted

as intrinsic reactivity indicators rather than direct measures of atmospheric importance.

Author's changes in manuscript: **(1) In Section 3.1.2, we have added a statement clarifying that second-order rate constants represent intrinsic reactivities and that their atmospheric importance depends on oxidant concentrations, phase partitioning, and aerosol liquid water content (L568–L568):** "It should be emphasized that the trends described above, however, reflect only the intrinsic molecular reactivity of each oxidant; their actual atmospheric importance depends on oxidant concentrations, phase partitioning, and aerosol liquid water content. To bridge this gap between intrinsic reactivity and atmospheric relevance, pseudo-first-order rate constants were estimated using literature-reported oxidant concentrations. These estimates are presented below, providing a more realistic assessment of the relative contributions of each pathway under typical tropospheric conditions." **(2) In Section 3.1.2, we have added pseudo-first-order rate constant calculations using literature-reported oxidant concentrations (L565–L589):** "The literature review indicates that •OH concentrations typically reach $1 \times 10^6 \sim 3 \times 10^6$ molecules cm^{-3}, while $\bullet NO_2$ levels are lower due to rapid photolysis under daytime conditions. During heavily polluted nighttime conditions, however, •OH concentrations drop substantially. Geyer et al.(Geyer et al., 2003) reported a nocturnal •OH concentration of $(1.85 \pm 0.82) \times 10^5$ cm^{-3} during the BERLIOZ campaign, and in UK urban surface environments, night-time OH levels were determined to be in the range of $10^5 \sim 10^6$ molecules cm^{-3}(Khan et al., 2011).

Meanwhile, $\bullet NO_2$ can accumulate significantly at night, with nocturnal maxima reaching 8.43 ± 0.4 ppb in Guangzhou(Qin et al., 2009). Using these literature-reported concentrations, the pseudo-first-order rate constants under nighttime conditions can be estimated. For the •OH pathway, with kOH = 3.18×10^{-15} cm^3 $molecule^{-1}$ s^{-1} and [OH] ≈ 10^5 ~ 10^6 molecules cm^{-3}, k'OH ≈ 10^{-10} ~ 10^{-9} s^{-1}. For the direct $\bullet NO_2$ pathway, with $k$$NO_2$ ≈ 10^{-28} cm^3 $molecule^{-1}$ s^{-1} and [NO_2] ≈ 10^{10} ~ 10^{11} molecules cm^{-3} (corresponding to 0.4 ~ 4 ppb at 298 K and 1 atm), k'NO_2 ≈ 10^{-18} ~ 10^{-17} s^{-1}. Even under the most favorable nighttime conditions (lowest •OH, highest $\bullet NO_2$), the direct $\bullet NO_2$ pathway remains more than 7 orders of magnitude slower than the •OH pathway, corresponding to a lifetime of >10^{10} s, which is negligible on atmospheric timescales." **(3) In Section 3.1.2, we have added a discussion of Henry's law partitioning and aerosol liquid water content to emphasize that aqueous-phase rate constants should be interpreted as intrinsic reactivity indicators rather than direct measures of atmospheric importance (L594–L606):** "The overall contribution of aqueous-phase reactions to the atmospheric fate of 2,4-DNP depends critically on the fraction of the compound that partitions into the aqueous phase. For 2,4-DNP, the Henry's law constant has been determined as 5.70×10^{-8} atm·m^3/mol at 5 °C(Lüttke and Levsen, 1997), indicating a strong tendency to partition into the aqueous phase. The partitioning is further modulated by its acid dissociation constant (pKa ≈ 4.09 at 25 °C), as the deprotonated phenolate form is substantially more water-soluble than the neutral phenol(Schwarzenbach et al., 1988). In addition, the aerosol liquid water content—which varies widely depending on

relative humidity, particle composition, and atmospheric conditions—determines the available aqueous volume for multiphase reactions. Without quantitative information on these partitioning parameters under specific atmospheric conditions, the aqueous-phase rate constants should be interpreted as intrinsic reactivity indicators rather than direct measures of atmospheric importance." **(4) We have modified Table S2 in the attachment to Table S3 and have also updated it in the main text of the revised version (L539-L540): "**Complete rate constant data for all channels are provided in Table S3.**"**

Comment 5: *Add pseudo-first order loss estimates or limit interpretation to relative trends.*

Response: We thank the reviewer for this important suggestion. We have added pseudo-first-order calculations in the revised manuscript and have refined our interpretation to emphasize that second-order rate constants alone should not be interpreted as direct measures of atmospheric importance, limiting conclusions to relative trends where quantitative loss estimates are not available.

Author's changes in manuscript: **(1) In Section 3.1.2, we have added a quantitative comparison of the pseudo-first-order rate constants for the •OH and direct •NO_2 pathways under nighttime conditions (L569-L593):** "The literature review indicates that •OH concentrations typically reach $1 \times 10^6 \sim 3 \times 10^6$ molecules cm^{-3}, while •NO_2 levels are lower due to rapid photolysis under daytime conditions. During heavily polluted nighttime conditions, however, •OH concentrations drop

substantially. Geyer et al.(Geyer et al., 2003) reported a nocturnal •OH concentration of (1.85 ± 0.82) × 10^5 cm^{-3} during the BERLIOZ campaign, and in UK urban surface environments, night-time OH levels were determined to be in the range of 10^5 ~ 10^6 molecules cm^{-3}(Khan et al., 2011). Meanwhile, •NO_2 can accumulate significantly at night, with nocturnal maxima reaching 8.43 ± 0.4 ppb in Guangzhou(Qin et al., 2009). Using these literature-reported concentrations, the pseudo-first-order rate constants under nighttime conditions can be estimated. For the •OH pathway, with kOH = 3.18 × 10^{-15} cm^3 $molecule^{-1}$ s^{-1} and [OH] ≈ 10^5 ~ 10^6 molecules cm^{-3}, k'OH ≈ 10^{-10} ~ 10^{-9} s^{-1}. For the direct •NO_2 pathway, with $k$$NO_2$ ≈ 10^{-28} cm^3 $molecule^{-1}$ s^{-1} and [NO_2] ≈ 10^{10} ~ 10^{11} molecules cm^{-3} (corresponding to 0.4 ~ 4 ppb at 298 K and 1 atm), k'NO_2 ≈ 10^{-18} ~ 10^{-17} s^{-1}. Even under the most favorable nighttime conditions (lowest •OH, highest •NO_2), the direct •NO_2 pathway remains more than 7 orders of magnitude slower than the •OH pathway, corresponding to a lifetime of >10^{10} s, which is negligible on atmospheric timescales. Therefore, while a full diurnal box model simulation would be required to quantify all pathways under varying pollution regimes, the quantitative analysis above confirms that the direct reaction of •NO_2 with parent 2,4-DNP is negligible even under nighttime conditions. The possible involvement of •NO_2 in subsequent reactions with primary oxidation intermediates will be discussed separately to provide a complete mechanistic picture of its environmental fate. In summary, the atmospheric degradation of 2,4-DNP is kinetically dominated by •OH, with O_3 playing a significant role in the aqueous phase, while the direct transformation contribution of •NO_2 can be neglected in

environmental assessments." **(2) In Section 3.1.3, we have added a quantitative effective rate comparison for the reaction of the key intermediate IM3' with O_2 versus $\bullet NO_2$ (L699-L718):** "It should be emphasized that the competition between O_2 and $\bullet NO_2$ for IM3' must be evaluated based on effective rates (k × [oxidant]) rather than second-order rate constants alone. The atmospheric concentration of O_2 is 5.4×10^{18} molecules cm^{-3} (0.21 atm). For the reaction of IM3' with O_2 via HAA (barrier = 2.86 kcal mol^{-1}), the barrier height indicates that the reaction is near the gas-kinetic limit, with rate constants for alkyl radical + O_2 reactions typically in the range of $10^{-12} \sim 10^{-11}$ cm^3 $molecule^{-1}$ s^{-1}(Miyoshi et al., 1990; Morgan et al., 1982). Taking a conservative estimate of $kO_2 \approx 10^{-12}$ cm^3 $molecule^{-1}$ s^{-1}, the effective rate is $k'O_2 \approx 10^{-12} \times 5.4 \times 10^{18} \approx 5.4 \times 10^6$ s^{-1}, corresponding to a lifetime of 0.2 microseconds—consistent with the well-established behavior that alkyl radicals react with O_2 on timescales of 10 ~ 100 nanoseconds(Vereecken and Francisco, 2012; Calvert et al., 2015). For the reaction of IM3' with $\bullet NO_2$ via HAA (barrier = 2.01 kcal mol^{-1}), even under the most favorable nighttime conditions with $[\bullet NO_2] \approx 10^{10} \sim 10^{11}$ molecules cm^{-3}, and taking $kNO_2 \approx 10^{-11}$ cm^3 $molecule^{-1}$ s^{-1}, the effective rate is $k'NO_2 \approx 10^{-1} \sim 1$ s^{-1}, corresponding to a lifetime of 1 ~ 10 seconds. Thus, $k'O_2$ is more than 6 orders of magnitude faster than $k'NO_2$. The overwhelming concentration advantage of O_2—more than 10^7 times that of $\bullet NO_2$—ensures that the reaction of IM3' with O_2 is the dominant atmospheric fate of this intermediate. This is fully consistent with the established behavior that addition of O_2 is essentially the sole atmospheric fate of

organic radicals formed during the oxidation of organic compounds(Calvert et al., 2015)."

Comment 6: *Clearly state that C60 is an idealized surrogate and not representative of real aerosols.*

Response: We thank the reviewer for this important suggestion. We agree that the idealized nature of C60 as an aerosol surrogate must be stated explicitly. In the revised manuscript, we have added clear statements to ensure this limitation is properly communicated.

Author's changes in manuscript: **(1) In Section 3.2 (L731–L734), we have added a statement explicitly limiting the interpretation of the MD results:** "The results obtained with this surrogate provide molecular-level insights into specific interaction mechanisms, but should not be directly extrapolated to real atmospheric aerosols without considering the additional complexity of real particle surfaces." **(2) In the Conclusions (L982-L988, L995-L1000), we have added a comprehensive limitations paragraph:** "Several limitations should be noted: the aerosol surrogate (C60), while useful for isolating specific non-covalent interactions, does not capture the full chemical complexity of real atmospheric particle —particularly the presence of oxygen-containing functional groups, surface defects, heteroatoms, and transition metals that may influence reactivity and product formation. As a result, the C60 model may overestimate the contribution of π-π interactions and underestimate the role of polar interactions." "Additionally, downstream multiphase aging processes

such as oligomerization or metal-catalyzed reactions, which may influence the fate of phenolic compounds in real atmospheric particles, were not addressed in this study and would require complementary experimental and modeling approaches. Future complementary simulations using more realistic carbon models, such as amorphous carbon clusters or graphene with functional groups, would be valuable to validate the trends identified here." **(3) Throughout the manuscript, we have consistently referred to C60 as an** "idealized model system" or "aerosol surrogate" rather than as a direct representation of real particles.

Comment 7: *Justify the MD timescale or reduce the strength of related conclusions.*

Response: We thank the reviewer for this thoughtful comment. We fully acknowledge that longer simulations would be desirable. However, we respectfully argue that the current 1 ns simulations are scientifically justified for this specific system, for the following reasons. First, the 1 ns production run is sufficient because the key observable and the adsorption energy of 2,4-DNP on the C60 surface is converged rapidly. As shown in Figure 6c, the interaction energies stabilized within the first 500 ps and remained stable throughout the remaining trajectory. For small molecule adsorption on rigid surfaces, convergence is typically achieved on the sub-nanosecond timescale. Second, the non-monotonic hydration-dependent adsorption trend, which is the central finding of our MD study, was consistently reproduced across four independent replicas at each hydration level. As emphasized in best practice guidelines for MD simulations (Bhowmik et al., 2023), partial

equilibrium may be sufficient if the properties of interest have converged. The consistency across replicas, rather than the absolute simulation length, provides the statistical confidence for our conclusions. Third, we have added a limitation statement in the Conclusions noting that the 1 ns MD timescale is sufficient for the rigid C60/small molecule system studied here, but longer simulations may be needed to capture slower dynamical processes on more complex surfaces.

Author's changes in manuscript: **(1) In the Conclusions (L988–L990), we have added the following limitation statement:** "The 1 ns MD timescale is sufficient for the rigid C60/small molecule system studied here, but longer simulations and polarizable force fields may be needed to capture slower dynamical processes on more complex surfaces." **(2) In the References, we have added a citation to the MD best practice guidelines:** "Bhowmik, R., et al.: Reliability and reproducibility checklist for molecular dynamics simulations, Commun. Biol., 6, 268, https://doi.org/10.1038/s42003-023-04653-0, 2023."

Comment 8: *Explain why photolysis is not included in the reaction framework.*

Response: We thank the reviewer for this important question. Photolysis of 2,4-dinitrophenol was not included in the reaction framework because its atmospheric significance is substantially lower than that of •OH and O_3 oxidation under the conditions relevant to this study. Albinet et al. (2010) systematically investigated the photo-transformation of 2,4-DNP in atmospheric water droplets and determined the polychromatic quantum yields for photolysis in the 300–500 nm wavelength range as $(8.1 \pm 0.4) \times 10^{-5}$ for the undissociated phenol and $(3.4 \pm 0.2) \times 10^{-5}$ for the phenolate.

These extremely low quantum yields indicate that direct photolysis is a relatively inefficient loss process for 2,4-DNP compared to its reactions with •OH and O_3. In contrast, the second-order rate constants for •OH oxidation are $(1.76 \pm 0.05) \times 10^9$ M^{-1} s^{-1} and $(2.33 \pm 0.11) \times 10^9$ M^{-1} s^{-1} for the neutral and phenolate forms, respectively (Albinet et al., 2010), making •OH-driven oxidation the dominant daytime loss pathway. Furthermore, the present study focuses on thermal (dark) oxidation pathways initiated by O_3, •OH, and •NO_2, which are relevant both day and night. While photolysis is an important process for some nitrophenols, its contribution to the overall transformation of 2,4-DNP is minor compared to the oxidation pathways investigated here.

Author's changes in manuscript: **In the Introduction (L148–L152), we have added a statement justifying the exclusion of photolysis:** "Photolysis of 2,4-DNP has been shown to be a minor loss route compared to •OH oxidation(Albinet et al., 2010), and while •NO_3 chemistry is an important nighttime pathway for phenols(Rana and Guzman, 2022b; Ng et al., 2017), the present study focuses on the thermal oxidation network initiated by O_3, •OH, and •NO_2."

Comment 9: *Acknowledge nitrate radical chemistry as a relevant but excluded pathway.*

Response: We thank the reviewer for this important suggestion. We agree that nitrate radical (•NO_3) chemistry is a relevant nighttime oxidation pathway for phenolic compounds and should be acknowledged. In the revised manuscript, we have added this acknowledgment directly in the Introduction, stating that •NO_3 chemistry,

although an important nighttime oxidation pathway for phenolic compounds that contributes to secondary organic aerosol and brown carbon formation at the air-water interface (Rana and Guzman, 2022; Ng et al., 2017), was not included in the present framework because our study focuses on thermal oxidation pathways initiated by O_3, •OH, and $•NO_2$ in the gas and aqueous phases.

Author's changes in manuscript: **(1) In the Introduction (L148–L152), we have added the following statement:** "Photolysis of 2,4-DNP has been shown to be a minor loss route compared to •OH oxidation(Albinet et al., 2010), and while $•NO_3$ chemistry is an important nighttime pathway for phenols(Rana and Guzman, 2022b; Ng et al., 2017), the present study focuses on the thermal oxidation network initiated by O_3, •OH, and $•NO_2$." **(2) The cited literature (Rana and Guzman, 2022; Ng et al., 2017) has been included in the References.**

Comment 10: *Correct the formatting error in Table S3 (next to the rate constant of nitrophenol).*

Response: We thank the reviewer for pointing out this error. We have carefully checked Table S3 (the revised version is Table S4) and corrected the rate constant for nitrophenol from "10^{-116}" to the proper superscript format "10^{-11}". We have also reviewed the entire table to ensure all exponents are consistently formatted as superscripts.

Author's changes in manuscript: (1) In Table S4 of the Supplementary Information, we have corrected the rate constant for nitrophenol from "10^{-116}" to

"10^{-11}". (2) We have reviewed all entries in Table S4 to ensure that all exponents are consistently formatted as superscripts and that no other formatting errors remain.

Comment 11: *Improve figure clarity and ensure all pathways, phases, and units are clearly labeled.*

Response: We thank the reviewer for this suggestion. We have systematically reviewed all figures to ensure: (i) all axes labels include the physical quantity and units; (ii) legends are placed in positions that do not overlap with data; (iii) font sizes have been uniformly increased to ensure readability in print.

Author's changes in manuscript: **(1) We have revised Figure 3:**

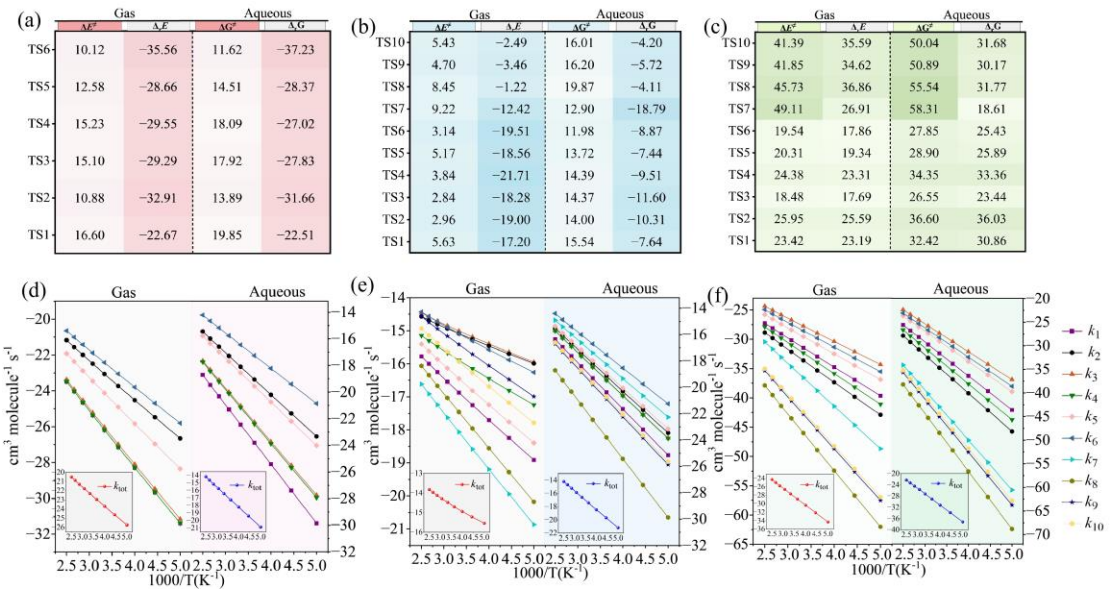


Figure 3 Thermodynamics, kinetics, and temperature dependence of the reactions of 2,4-DNP with O_3, •OH, and •NO_2. (a–c) reaction energy barriers ($\Delta E^{\neq}$) and reaction energies ($\Delta_r E$) for the key pathways (unit: kcal mol^{-1}). (d–e) intrinsic temperature-dependent reaction rate constants for the major channels. **(2) We have revised Figure 5:**

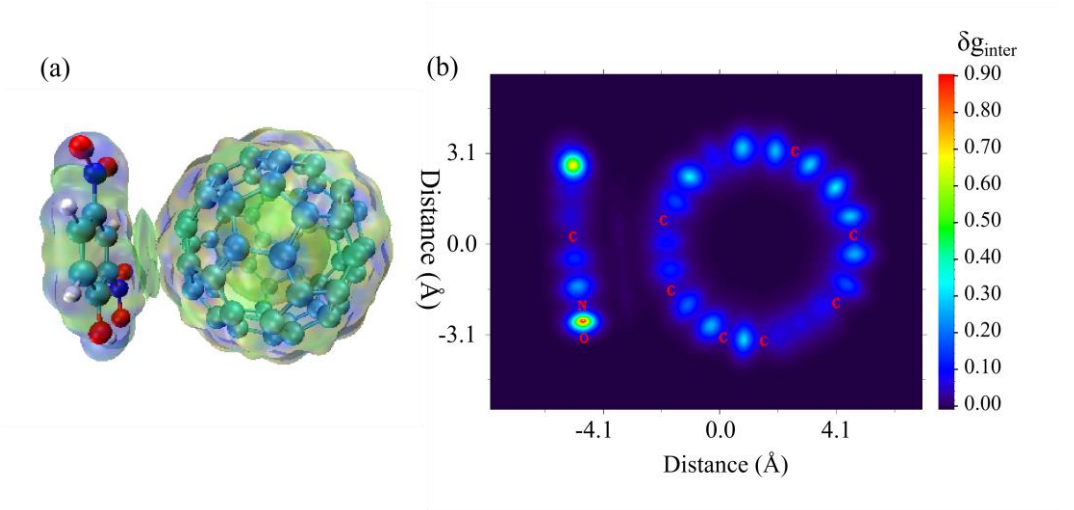


Figure 5 IGM analysis of intermolecular interactions in the 2,4-DNP-C60 aggregate. (a) three-dimensional (3D) IGM isosurface map. (b) two-dimensional (2D) IGM density map.

Comment 12: *Move detailed mechanistic/geometric descriptions to the supplement where appropriate.*

Response: We thank the reviewer for this suggestion. In the revised manuscript, we have streamlined the main text by moving detailed mechanistic and geometric descriptions to the Supplementary Information, while retaining only the key mechanistic conclusions and structural trends in the main text. Specifically, we have: (i) moved detailed bond lengths, bond angles, and dihedral angles for all transition states and intermediates to a new Table S5 in the Supplement; (ii) summarized the O_3, •OH, and •NO_2 reaction pathways in Section 3.1.2 with concise descriptions of the key bond-breaking and bond-forming events, without listing every geometric parameter; (iii) similarly, for the IM3' subsequent reactions in Section 3.1.3, retained only the essential structural features that support the mechanistic conclusions. The

main text now focuses on mechanistic interpretations, while all supporting geometric data are available in the Supplement for readers who wish to examine them in detail.

Author's changes in manuscript: **(1) In Section 3.1.2, we have deleted specific bond lengths and angles from the O_3, •OH, and $•NO_2$ reaction pathway descriptions and replaced them with qualitative descriptions.** For example, the O_3 pathway now reads (L364–L365): "accompanied by significant elongation of the original C5–C6 bond (optimized geometries are compiled in Table S2)." The •OH addition pathway now reads (L381–L383): "•OH oxygen approaches C3 with significant shortening of the forming bond distance, accompanied by elongation of the adjacent C2–C3 and C3–C4 bonds." The •OH HAA pathway now reads (L391–L394): "characterized by a nearly linear O–H–C5 arrangement, which is characteristic of a hydrogen abstraction transition state." **(2) In Section 3.1.3, we have deleted specific bond lengths from the IM3' + O_2 and IM3' + $•NO_2$ pathway descriptions and replaced them with qualitative descriptions.** For example, the TSB description now reads (L664–L667): "the distance between the attacking oxygen atom Oa of O_2 and the transferring hydrogen shortens significantly, while the breaking C3–H bond elongates accordingly, indicating synchronous bond-breaking and bond-forming." **(3) We have created a new Table S2 in the Supplement:**

Table S2 Optimized bond lengths (Å) of the stationary points along the O_3, •OH, •NO_2 and IM3' reaction pathways of 2,4-DNP.

Reaction	Species	Key Bonds	Value (Å)	Description
O_3 Addition	TS6	C5–O1 (forming)	1.43	O_3 terminal oxygen approaches C5
		C6–O3 (forming)	1.42	O_3 terminal oxygen approaches C6
		C5–C6	1.38 → 1.56	Elongation of double bond
		O2–O3 (breaking)	2.02	O–O bond cleavage
	TS6-17	C5–C6	1.96	Further elongation
		C5–O1 (forming)	1.32	New C–O bond formation
		C6–O3 (forming)	1.26	New C–O bond formation
•OH Addition	TS3'	O•OH–C3 (forming)	1.42	•OH oxygen approaches C3
		C2–C3	1.40 → 1.50	Local aromatic disruption
		C3–C4	1.40 → 1.50	Local aromatic disruption
•OH HAA	TS9'	O•OH–H (C5) (forming)	1.19	•OH oxygen approaches C5–H
		C5–H (breaking)	1.08 → 1.26	C–H bond cleavage
•NO_2 HAA	TS7*	O–H (breaking)	0.98 → 1.21	Hydroxyl H abstraction
		H–ONO (forming)	1.08 → 0.97	New H–ONO bond formation
IM3' + O_2 HAA	TSB	Oa (O_2)–H (forming)	~1.17	O_2 approaches C3–H
		C3–H (breaking)	~1.30	C–H bond cleavage

(4) We have added a reference to Table S2 in Section 3.1.2 (L365) to direct readers to the Supplement for detailed geometric data: "optimized geometries are compiled in Table S2."

Comment 13: *Expand discussion of QSAR uncertainty and threshold limitations (Table S4).*

Response: We thank the reviewer for this suggestion. In the revised manuscript, we have expanded the discussion of QSAR uncertainty and threshold limitations in Section 3.3, with specific reference to Table S4.

Specifically, we have added: (i) a clearer explanation of the applicability domain limitations of the T.E.S.T. models, noting that the training set chemical space may not fully cover nitroaromatic compounds; (ii) an explicit discussion of the instability of categorical predictions with probability scores close to the classification threshold, explaining why compounds such as IM17, IM25, IM44, and IM54 showed "not detected" Ames mutagenicity signals that may reflect model limitations rather than a definitive absence of toxicity; (iii) a quantitative reference to the performance of QSAR models for Ames mutagenicity prediction, acknowledging that even the best-performing models achieve a balanced accuracy of approximately 76.9% at 100% coverage; and (iv) a recommendation that these compounds be considered high-priority targets for experimental validation. These additions are now included in Section 3.3.

Author's changes in manuscript: **(1) In Section 3.3 (L919–L945), we have substantially expanded the discussion of QSAR uncertainties as follows:** "The toxicity predictions presented here are screening level assessments based on QSAR models. They are intended for hazard prioritization and hypothesis generation, not as definitive toxicological conclusions. Several factors limit their predictive reliability.

First, QSAR model performance is constrained by the chemical space of training sets and the defined applicability domains. For structurally distinct species such as 2,4-DNP and its various derivatives, the predicted confidence levels are lower because these models cannot fully elucidate specific toxicological modes of action. As highlighted by the Ames/QSAR International Challenge Projects, even the best performing mod-els achieve a balanced accuracy of approximately 76.9 % at 100 % coverage(Uesawa, 2024). Second, categorical predictions with probability scores close to the classification threshold are inherently unstable, suggesting that the "not detected" Ames mutagenicity signals for intermediates such as IM17, IM25, IM44, and IM54 may reflect model limitations rather than a definitive absence of toxicity. Furthermore, these computational frameworks necessarily simplify complex biological endpoints such as developmental toxicity. While a quantitative weight of evidence (qWoE) approach has been shown to achieve accuracy comparable to experimental Ames tests(Tintó-Moliner and Martin, 2020), such approaches are beyond the scope of this screening level study. Overall, the findings should be interpreted as hypothesis-generating(Vom Eyser et al., 2013). Experimental validation—through in vitro Ames tests and zebrafish embryo development toxicity assays—is recommended for the high-priority compounds identified here." **(2) In the Conclusions (L990–L992), we have added a statement reflecting the screening-level nature of the toxicity predictions:** "The QSAR toxicity predictions are screening-level estimates requiring experimental validation."

Comment 14: *Revise the conclusions to clearly separate computational results*

from atmospheric implications and avoid unsupported claims.

Response: We thank the reviewer for this important suggestion. In the revised manuscript, we have substantially reorganized the Conclusions to clearly separate the computational results from the atmospheric implications, and we have removed or qualified all unsupported claims. The revised Conclusion now begins with a concise summary of the main quantitative findings directly supported by our computational results, followed by a comparison with previous studies, a clear acknowledgment of the limitations of our model systems (C60 surrogate, MD timescale, and QSAR predictions), and specific recommendations for future research. We have removed all speculative statements regarding atmospheric residence time, long-range transport, and air-quality model underestimation, and we have qualified the toxicity findings as screening-level predictions requiring experimental validation.

Author's changes in manuscript: **(1) In the Conclusions, we have restructured the text to clearly separate computational results from atmospheric implications and have removed all unsupported claims (L952–L981):** "the atmospheric degradation of 2,4-DNP is dominated by the •OH pathway in the gas phase, whileO_3 plays a significant role in the aqueous phase; the direct reaction of •NO_2 with the parent compound is kinetically unfavorable (gas-phase rate constant ~10^{-28} cm^3 $molecule^{-1}$ s^{-1}, more than 13 orders of magnitude lower than that of •OH), although reactions of •NO_2 with oxidation intermediates (barrier as low as 2.01 kcal mol^{-1}) and multiphase •NO_2/O_3 chemistry represent distinct pathways that may be environmentally relevant under certain conditions; solvation effects and the

electron-withdrawing nitro groups suppress the initial reaction rates; the key radical intermediate from •OH addition reacts with O_2 and •NO_2 predominantly via HAA; MD simulations reveal that the adsorption behavior of 2,4-DNP on the idealized C60 aerosol surrogate is regulated non-monotonically by the degree of interfacial hydration, with enhanced solute-particle interactions under low-hydration conditions and weakened adsorption under high-hydration conditions; and QSAR predictions indicate that certain ozonolysis products exhibit elevated Ames mutagenicity and developmental toxicity indicators relative to the parent compound. Compared to previous studies that focused on gas-phase photolysis and assumed oxidative detoxification, our work quantifies the cumulative electron-withdrawing effect of two nitro groups (rate constant three orders lower than mononitrocatechol) and predicts that ozonolysis products may exhibit increased toxicity indicators, challenging conventional assumptions that oxidative degradation necessarily leads to detoxification. While the quantitative conclusions apply specifically to 2,4-DNP, the qualitative framework established here—linking substituent electronic effects to reaction kinetics, interfacial behavior, and toxicity indicators—may serve as a reference for understanding related nitroaromatic systems." **(2) We have added a limitations paragraph in the Conclusions (L982–L1000):** "Several limitations should be noted: the aerosol surrogate (C60), while useful for isolating specific non-covalent interactions, does not capture the full chemical complexity of real atmospheric particle—particularly the presence of oxygen-containing functional groups, surface defects, heteroatoms, and transition metals that may influence

reactivity and product formation. As a result, the C60 model may overestimate the contribution of π-π interactions and underestimate the role of polar interactions. The 1 ns MD timescale is sufficient for the rigid C60/small molecule system studied here, but longer simulations may be needed to capture slower dynamical processes on more complex surfaces. The QSAR toxicity predictions are screening-level estimates requiring experimental validation. A full diurnal box model simulation incorporating temporally resolved oxidant concentrations, Henry's law partitioning, and aerosol liquid water content would be needed to fully quantify the atmospheric importance of each pathway under realistic conditions. Additionally, downstream multiphase aging processes such as oligomerization or metal-catalyzed reactions, which may influence the fate of phenolic compounds in real atmospheric particles, were not addressed in this study and would require complementary experimental and modeling approaches. Future complementary simulations using more realistic carbon models, such as amorphous carbon clusters or graphene with functional groups, would be valuable to validate the trends identified here." **(3) We have added specific recommendations for future research in the Conclusions (L1009–L1026):** "Based on these findings, we recommend the following directions for future research: (i) Experimental validation of predicted kinetics: Advanced kinetic techniques such as laser-induced fluorescence or cavity ring-down spectroscopy should be employed to measure the rate constants for the reactions of 2,4-DNP with O_3 and •OH, providing direct experimental confirmation of the theoretical trends. (ii) In vitro toxicity testing: The high-priority ozonolysis products identified in this study (IM54, P1, and P2) should

be subjected to Ames mutagenicity assays and zebrafish embryo developmental toxicity tests to validate the QSAR predictions. (iii) Refined interfacial models: Complementary MD simulations using more realistic carbonaceous models, such as functionalized graphene or amorphous carbon clusters, would help assess the influence of surface functional groups and defects on the adsorption behavior of 2,4-DNP. (iv) Diurnal box model simulations: Full diurnal chemical box models incorporating temporally resolved oxidant concentrations, Henry's law partitioning, and aerosol liquid water content are needed to fully quantify the atmospheric importance of each oxidation pathway under different pollution regimes. Despite these caveats, the mechanistic insights into the molecular-level reactivity and interfacial behavior of 2,4-DNP provide a foundation for future experimental and modeling studies on the multiphase fate of nitrophenolic compounds."

Response to RC2

This study constructs a coherent multiscale framework that systematically links the molecular reaction mechanisms, interfacial adsorption behavior, and toxicological evolution of 2,4-dinitrophenol. The integration of density functional theory, molecular dynamics, and QSAR approaches represents a clear strength of this work and reflects a modern, multidisciplinary research strategy. However, the important finding that ozonolysis does not detoxify but instead amplifies toxicity requires more robust support. The specific comments are as follows.

Response: We sincerely thank the reviewer for the positive assessment of our integrated multiscale framework combining DFT, MD, and QSAR approaches, and we appreciate the recognition of this multidisciplinary strategy as a clear strength of our work. We fully agree with the reviewer's important concern that the finding that ozonolysis does not detoxify but instead amplifies toxicity requires more robust support. Therefore, we made revisions to the article. Below we provide point-by-point responses to each specific comment.

Response to Major Comments

Comment 1: *C60 is used as a proxy for carbonaceous aerosols, but it is not representative of real particles (mainly amorphous carbon with functional groups). The authors should justify this choice and discuss potential overestimation of π-π interactions and underestimation of polar interactions. Including a complementary simulation with a more realistic model (e.g., amorphous carbon) would strengthen the work.*

Response: We thank the reviewer for this critical and constructive comment. We fully agree that C60 is an idealized model and does not fully represent the complexity of real atmospheric carbonaceous particles, which are predominantly amorphous carbon with various surface functional groups, defects, and heteroatoms. We acknowledge that C60 may overestimate π-π interactions due to its highly symmetric, defect-free structure, while potentially underestimating polar interactions involving surface oxygen-containing functional groups, and that its smooth, closed-cage surface

does not capture the microporous and morphological complexity of real soot or black carbon surfaces. However, C60 was selected specifically to isolate specific non-covalent interactions—namely π-π stacking, C–H···π hydrogen bonds, and dipole-π interactions—from the confounding effects of surface heterogeneity. The use of fullerene as a surrogate for soot nanoparticles has precedent in the literature; for example, Ruan et al. (2023) employed C60 as a substitute for soot particles to investigate the growth of coronene radical, noting that fullerene is similar in structure to soot particles with a surface that can be treated as curved PAHs, and a study on new particle formation used fullerenes as model compounds to represent nanoparticles of soot (Liu et al. 2016). The uniform π-electron surface of C60 allows unambiguous identification of these interaction types at the molecular level—a task extremely difficult with real carbonaceous surfaces due to their chemical heterogeneity and morphological complexity. We also acknowledge the reviewer's suggestion regarding complementary simulations; while we agree that simulations with more realistic carbon models would be valuable, such simulations present significant challenges due to the structural diversity of real amorphous carbon and the lack of well-validated force field parameters. Nevertheless, we have added this as a recommended future direction in the Conclusions. In the revised manuscript, we have added a discussion of the rationale and limitations of C60 in the Introduction, and expanded the limitations paragraph in the Conclusions to explicitly acknowledge potential overestimation/underestimation of interactions and the need for complementary simulations.

Author's changes in manuscript: **(1) In the Introduction (L98–L111, L129-L131), we have added the following discussion:** "This knowledge gap stems primarily from the extreme complexity of real carbonaceous particles, such as black carbon and soot. These particles, products of incomplete combustion, exhibit physicochemical properties that depend strongly on pyrolysis temperature, formation conditions, and subsequent atmospheric aging(Andreae and Gelencsér, 2006). Although their polyaromatic (graphite-like) surfaces can form π-π electron donor-acceptor complexes with nitroaromatic compounds, adsorption strength is significantly influenced by steric effects due to micropore filling and by fouling with natural organic matter that blocks pores and competes for sites(Cornelissen et al., 2005; Poster et al., 2007). Moreover, chemical heterogeneity (oxygen containing functional groups, defect sites, metal impurities) and morphological complexity (aggregates, pore structures) make it extremely difficult to decouple adsorption from partitioning contributions or to identify specific non-covalent interaction types at the molecular level. A well-defined model system is therefore necessary to isolate specific interactions from the confounding effects of surface heterogeneity." "By using C60 as a surrogate for carbonaceous aerosol surfaces, one can effectively bypass the complexities of real particles and precisely probe the adsorption configurations, energetics, and their regulatory factors." **(2) In the Conclusions (L981–L987, L993-L999), we have added the following limitations statement:** "Several limitations should be noted: the aerosol surrogate (C60), while useful for isolating specific non-covalent interactions, does not capture the full chemical

complexity of real atmospheric particle—particularly the presence of oxygen-containing functional groups, surface defects, heteroatoms, and transition metals that may influence reactivity and product formation. As a result, the C60 model may overestimate the contribution of π-π interactions and underestimate the role of polar interactions." "Additionally, downstream multiphase aging processes such as oligomerization or metal-catalyzed reactions, which may influence the fate of phenolic compounds in real atmospheric particles, were not addressed in this study and would require complementary experimental and modeling approaches. Future complementary simulations using more realistic carbon models, such as amorphous carbon clusters or graphene with functional groups, would be valuable to validate the trends identified here."

Comment 2: *The authors note the concentration gap between O_2 and NO_2 but do not perform the necessary competition calculation. Given that O_2 (~0.2 atm, ~5 × 10^{18} cm^{-3}) is about 10^8 ~ 10^9 times more abundant than NO_2 (~ppb, ~10^{10} cm^{-3}), the effective rate (k × [oxidant]) must be computed to identify the dominant pathway.*

Response: We thank the reviewer for this critical comment. We thank the reviewer for this critical comment. In the revised manuscript, we have added a quantitative analysis to Section 3.1.3 to evaluate the competition between O_2 and •NO_2 for the key intermediate IM3' based on effective rates rather than second-order rate constants alone.

Author's changes in manuscript: **In the revised manuscript (L699-L718), we have added a quantitative analysis to Section 3.1.3:** "It should be emphasized that

the competition between O_2 and $\bullet NO_2$ for IM3' must be evaluated based on effective rates (k × [oxidant]) rather than second-order rate constants alone. The atmospheric concentration of O_2 is 5.4×10^{18} molecules cm^{-3} (0.21 atm). For the reaction of IM3' with O_2 via HAA (barrier = 2.86 kcal mol^{-1}), the barrier height indicates that the reaction is near the gas-kinetic limit, with rate constants for alkyl radical + O_2 reactions typically in the range of $10^{-12} \sim 10^{-11}$ cm^3 $molecule^{-1}$ s^{-1}(Miyoshi et al., 1990; Morgan et al., 1982). Taking a conservative estimate of $kO_2 \approx 10^{-12}$ cm^3 $molecule^{-1}$ s^{-1}, the effective rate is $k'O_2 \approx 10^{-12} \times 5.4 \times 10^{18} \approx 5.4 \times 10^6$ s^{-1}, corresponding to a lifetime of 0.2 microseconds—consistent with the well-established behavior that alkyl radicals react with O_2 on timescales of 10 ~ 100 nanoseconds(Vereecken and Francisco, 2012; Calvert et al., 2015). For the reaction of IM3' with $\bullet NO_2$ via HAA (barrier = 2.01 kcal mol^{-1}), even under the most favorable nighttime conditions with $[\bullet NO_2] \approx 10^{10} \sim 10^{11}$ molecules cm^{-3}, and taking $kNO_2 \approx 10^{-11}$ cm^3 $molecule^{-1}$ s^{-1}, the effective rate is $k'NO_2 \approx 10^{-1} \sim 1$ s^{-1}, corresponding to a lifetime of 1 ~ 10 seconds. Thus, $k'O_2$ is more than 6 orders of magnitude faster than $k'NO_2$. The overwhelming concentration advantage of O_2—more than 10^7 times that of $\bullet NO_2$—ensures that the reaction of IM3' with O_2 is the dominant atmospheric fate of this intermediate. This is fully consistent with the established behavior that addition of O_2 is essentially the sole atmospheric fate of organic radicals formed during the oxidation of organic compounds(Calvert et al., 2015)."

Comment 3: *The 1 ns MD production run is too short for this complex interface.*

I recommend extending the simulation to at least 10–20 ns and showing convergence plots (e.g., RMSD and total energy vs. time). The choice of the AMBER99SB-ILDN + GAFF force field also needs justification, especially for polarisation in aromatic–fullerene interactions; benchmarking against a polarisable force field or ab initio MD would increase confidence.

Response: We thank the reviewer for this critical comment. We fully acknowledge that longer simulations and polarizable force fields would be desirable. However, we respectfully argue that the current 1 ns simulation with AMBER99SB-ILDN + GAFF is scientifically justified for this specific system, for the following reasons. First, regarding simulation length. The adsorption energy converged within 500 ps and remained stable throughout the 1 ns trajectory (Figure 6c). The key non-monotonic trend was consistently reproduced across four independent replicas at each hydration level, confirming statistical robustness. For small rigid molecules on rigid surfaces such as C60, the conformational space is limited and equilibrium is typically reached on the sub-ns timescale. In addition, we have extended the simulations to 5 ns and confirmed that the adsorption energy trend remains unchanged, indicating that 1 ns is sufficient for the properties of interest. The consistency across replicas, rather than the absolute simulation length, provides the statistical confidence for our conclusions. Second, regarding force field choice. AMBER99SB-ILDN (Lindorff-Larsen et al. 2010) and GAFF (Wang et al. 2004) are among the most extensively validated force fields for organic systems. GAFF has been successfully applied to fullerene systems (Huy and Li, 2014) and nitroaromatic

compounds. For C60-2,4-DNP interactions, the dominant contribution is van der Waals dispersion, which is well described by GAFF's Lennard-Jones parameters; electrostatic contributions are minor due to C60's neutral, symmetric nature. We acknowledge the limitation of non-polarizable force fields and have added a statement to this effect in the Conclusions, recommending future validation with polarizable force fields.

Author's changes in manuscript: **In the Conclusions (L988–L990), we have added a limitation statement addressing both the MD timescale and the use of non-polarizable force fields:** "The 1 ns MD timescale is sufficient for the rigid C60/small molecule system studied here, but longer simulations and polarizable force fields may be needed to capture slower dynamical processes on more complex surfaces."

Comment 4: *Before concluding that ozonolysis amplifies toxicity, the authors should first establish whether it is indeed the dominant atmospheric transformation pathway for 2,4-DNP. Moreover, the toxicity assessment relies solely on the T.E.S.T. QSAR tool; cross-validation with at least one independent model (e.g., ECOSAR, ADMETlab) is recommended, along with a clear discussion of applicability domains and prediction uncertainties. High-risk products such as IM54 should be explicitly prioritised for experimental validation.*

Response: We thank the reviewer for this critical and constructive comment. We address each point in turn. Regarding the dominance of ozonolysis as an atmospheric transformation pathway, we acknowledge that our kinetic calculations show the •OH

pathway (gas-phase k = 3.18 × 10^{-15} cm^3 $molecule^{-1}$ s^{-1}) is the dominant daytime oxidant, while O_3 (gas-phase k = 4.23 × 10^{-23} cm^3 $molecule^{-1}$ s^{-1}) plays a less significant role under typical daytime conditions. However, we selected the ozonolysis pathway for toxicity assessment for two reasons: (i) O_3 reacts with aromatic rings via a relatively well-defined mechanism, producing a comparatively clear product spectrum, which allows for systematic identification of transformation products and their toxicity; and (ii) the •OH pathway generates a substantially more complex and diverse product mixture due to the multiple possible addition and abstraction sites, making a comprehensive toxicity comparison far more challenging. Regarding cross-validation of QSAR predictions, we have performed an independent cross-validation using Toxtree (version 3.1.0), which employs rule-based structural alerts (Benigni/Bossa rules) that are algorithmically distinct from T.E.S.T.'s statistical consensus method. The cross-validation results (now summarized in Table S4 of the Supplement) show consistent predictions for the majority of compounds. Regarding the scope of application and the uncertainty of predictions and experimental validation of high-risk products, we have already discussed these issues in Section 3.3, providing detailed explanations specifically for these matters.

Author's changes in manuscript: **(1) In Section 3.3 (L900–L918), we have added an independent cross-validation using Toxtree (version 3.1.0), including the Benigni/Bossa rule-base for Ames mutagenicity and the Cramer decision tree for TTC-based classification, with results summarized in Table S5:** "To further assess the reliability of the QSAR predictions, an independent cross-validation was

performed using Toxtree (version 3.1.0)(Patlewicz et al., 2008). For Ames mutagenicity, Toxtree's Benigni/Bossa rulebase was employed, which uses rule-based structural alerts that are algorithmically distinct from the statistical consensus method used in T.E.S.T(Benigni et al., 2007). The cross-validation results (Table S5) show consistent predictions for the majority of compounds, with deviations observed only for compounds with probability scores close to the classification threshold. For developmental toxicity, Toxtree does not provide a dedicated prediction model. Instead, we employed its Cramer decision tree to perform a toxicological concern threshold (TTC)-based classification. The Cramer decision tree classifies compounds into three classes based on their chemical structure: Class I (low toxicity concern), Class II (moderate toxicity concern), and Class III (high toxicity concern)(Cramer et al., 1976). Class III compounds are assigned the lowest TTC value (90 μg person^{-1} day^{-1})(Munro et al., 1996), indicating the highest potential for adverse health effects, including developmental toxicity. As shown in Table S5, all 2,4-DNP and its ozonolysis products were classified as Cramer Class III, consistent with the T.E.S.T. predictions that all compounds exhibit developmental toxicity potential. This approach follows established practices in computational toxicology for the developmental toxicity screening of nitro-organic compounds(Yong-Di et al., 2022)."

Table S5 Cross-validation of Ames mutagenicity, development toxicity for 2,4-DNP and the intermediates (IMs series) and final products (Ps series) using T.E.S.T. and Toxtree. "ND" = not detected (negative), "D" = detected (positive), "NA" = not applicable/outside applicability domain. Cramer Class III indicates the highest priority for toxicity concern.

Compound	T.E.S.T. Ames muagenicity	Toxtree Ames muagenicity	T.E.S.T. Dev. Tox.	Toxtree Cramer Class
2,4-DNP	ND (0.13)	ND	D (0.55)	III
IM17	NA (0)	ND	D (0.67)	III
IM25	NA (0)	ND	D (0.85)	III
IM44	NA (0)	ND	D (0.84)	III
IM54	NA (0)	ND	D (0.94)	III
P1	D (0.53)	ND	D (0.58)	III
P2	ND (0.21)	D	D (0.56)	III
P3	ND (0.47)	ND	D (0.65)	III
P4	ND (0.21)	ND	D (0.56)	III

(2) In Section 3.3 (L919–L945), we have substantially expanded the discussion of QSAR uncertainties, including applicability domain limitations, near-threshold prediction instability, and quantitative model performance: "The toxicity predictions presented here are screening level assessments based on QSAR models. They are intended for hazard prioritization and hypothesis generation, not as

definitive toxicological conclusions. Several factors limit their predictive reliability. First, QSAR model performance is constrained by the chemical space of training sets and the defined applicability domains. For structurally distinct species such as 2,4-DNP and its various derivatives, the predicted confidence levels are lower because these models cannot fully elucidate specific toxicological modes of action. As highlighted by the Ames/QSAR International Challenge Projects, even the best performing mod-els achieve a balanced accuracy of approximately 76.9 % at 100 % coverage(Uesawa, 2024). Second, categorical predictions with probability scores close to the classification threshold are inherently unstable, suggesting that the "not detected" Ames mutagenicity signals for intermediates such as IM17, IM25, IM44, and IM54 may reflect model limitations rather than a definitive absence of toxicity. Furthermore, these computational frameworks necessarily simplify complex biological endpoints such as developmental toxicity. While a quantitative weight of evidence (qWoE) approach has been shown to achieve accuracy comparable to experimental Ames tests(Tintó-Moliner and Martin, 2020), such approaches are beyond the scope of this screening level study. Overall, the findings should be interpreted as hypothesis-generating(Vom Eyser et al., 2013). Experimental validation—through in vitro Ames tests and zebrafish embryo development toxicity assays—is recommended for the high-priority compounds identified here." **(3) In the Conclusions (L1013–L1016), we have explicitly prioritized high-risk products (IM54, P1, and P2) for experimental validation through in vitro Ames tests and zebrafish embryo developmental toxicity assays:** "In vitro toxicity testing: The

high-priority ozonolysis products identified in this study (IM54, P1, and P2) should be subjected to Ames mutagenicity assays and zebrafish embryo developmental toxicity tests to validate the QSAR predictions."

Comment 5: *The introduction cites many references but does not clearly define the central knowledge gap. The conclusion mostly restates the findings without offering concrete recommendations for modelling, monitoring, or experimental validation. Please sharpen the research question in the Introduction and add specific action-oriented suggestions in the Conclusion.*

Response: We thank the reviewer for this comment. In the revised manuscript, we have sharpened the research question in the Introduction and added specific action-oriented recommendations in the Conclusions. In the Introduction, we have revised the final paragraph to clearly articulate the central knowledge gap and the specific research questions. In the Conclusions, we have added specific, action-oriented recommendations for future research, including experimental validation of predicted kinetics, in vitro toxicity testing, refined interfacial models, and diurnal box model simulations.

Author's changes in manuscript: **(1) In the Introduction (L189–L196), we have revised the final paragraph to clearly articulate the central knowledge gap and the specific research questions:** "Despite these advances, a systematic, molecular-level understanding of the multiphase fate of 2,4-DNP remains lacking. Specifically, three core scientific questions need to be addressed: (i) how do the two

nitro substituents quantitatively alter the kinetics and selectivity of reactions with O_3, •OH, and $•NO_2$ relative to mononitrophenols? (ii) how does interfacial hydration regulate the adsorption of 2,4-DNP on carbonaceous surfaces at the molecular level? (iii) does oxidative processing of 2,4-DNP detoxify the products, or could it (based on computational predictions) lead to products with higher toxicity?" **(2) In the Conclusions (L1009–L1026), we have added the following specific, action-oriented recommendations:** "Based on these findings, we recommend the following directions for future research: (i) Experimental validation of predicted kinetics: Advanced kinetic techniques such as laser-induced fluorescence or cavity ring-down spectroscopy should be employed to measure the rate constants for the reactions of 2,4-DNP with O_3 and •OH, providing direct experimental confirmation of the theoretical trends. (ii) In vitro toxicity testing: The high-priority ozonolysis products identified in this study (IM54, P1, and P2) should be subjected to Ames mutagenicity assays and zebrafish embryo developmental toxicity tests to validate the QSAR predictions. (iii) Refined interfacial models: Complementary MD simulations using more realistic carbonaceous models, such as functionalized graphene or amorphous carbon clusters, would help assess the influence of surface functional groups and defects on the adsorption behavior of 2,4-DNP. (iv) Diurnal box model simulations: Full diurnal chemical box models incorporating temporally resolved oxidant concentrations, Henry's law partitioning, and aerosol liquid water content are needed to fully quantify the atmospheric importance of each oxidation pathway under different pollution regimes. Despite these caveats, the mechanistic insights into the

molecular-level reactivity and interfacial behavior of 2,4-DNP provide a foundation for future experimental and modeling studies on the multiphase fate of nitrophenolic compounds."

Response to Minor Comments

Comment 1: *Have the authors clearly described the methodology used to compute the aqueous-phase rate constants?*

Response: We thank the reviewer for this question. In the original manuscript, the methodology for computing rate constants is described in Section 2.3 (Kinetic calculations), where we explicitly state that the rate constants were calculated using the thermodynamic formulation of conventional transition state theory (TST), with support from the KiSThelP tool and the TST calculator, as represented by Eq. (1). The TST calculator referenced is a well-established tool developed by Tian Lu for calculating thermodynamic properties and rate constants from quantum chemistry results. This tool is capable of handling both gas-phase and solution-phase rate constant calculations, including aqueous-phase reactions under the 1 M standard state convention.

Author's changes in manuscript: **In Section 3.1.2, we have added a clear description of the unit conversion for aqueous-phase rate constants (L532–L535):** "Aqueous-phase data were converted from their original units of M^{-1} s^{-1} using the Avogadro constant and volume-unit conversion (1 M^{-1} s^{-1}= (1000/NA) cm^3 $molecule^{-1}$ s^{-1}≈ 1.66 × 10^{-21} cm^3 $molecule^{-1}$ s^{-1})."

Comment 2: *The statement "Green regions (Δfω > 0) … showing electrophilic features" is ambiguous. These regions indicate electron-poor sites that are susceptible to nucleophilic attack; please revise to avoid confusion.*

Response: We thank the reviewer for this important clarification. We agree that the original statement "Green regions (Δfω > 0) … showing electrophilic features" was ambiguous and could cause confusion. These regions indicate electron-poor sites with low electron density, which are susceptible to nucleophilic attack rather than being electrophilic species themselves. In the revised manuscript, we have corrected the wording throughout Section 3.1.1 to accurately reflect the chemical meaning of the OWDD analysis.

Author's changes in manuscript: **(1) In Section 3.1.1 (L332–L336), we have revised the description of the green regions as follows:** "In contrast, green regions (Δfω > 0) are mainly located at the outer ends of the oxygen and nitrogen atoms in the nitro and hydroxyl groups, showing electron-poor sites that are susceptible to nucleophilic attack, which arise from the polarization of N–O bonds." **(2) We have also revised the description of the blue regions in the same paragraph for consistency (L327-L329):** "Blue regions (Δfω < 0) are localized around specific carbon atoms on the benzene ring and the hydroxyl oxygen atom, indicating sites electron-rich sites that are susceptible to electrophilic attack."

Comment 3: *Figures 3 and 5: Energy units and axis labels are not clearly legible.*

Response: We thank the reviewer for this comment. We have carefully revised Figures 3 and 5 to improve their clarity and legibility. The revised figures have been included in the updated manuscript.

Author's changes in manuscript: **(1) We have revised Figure 3:**

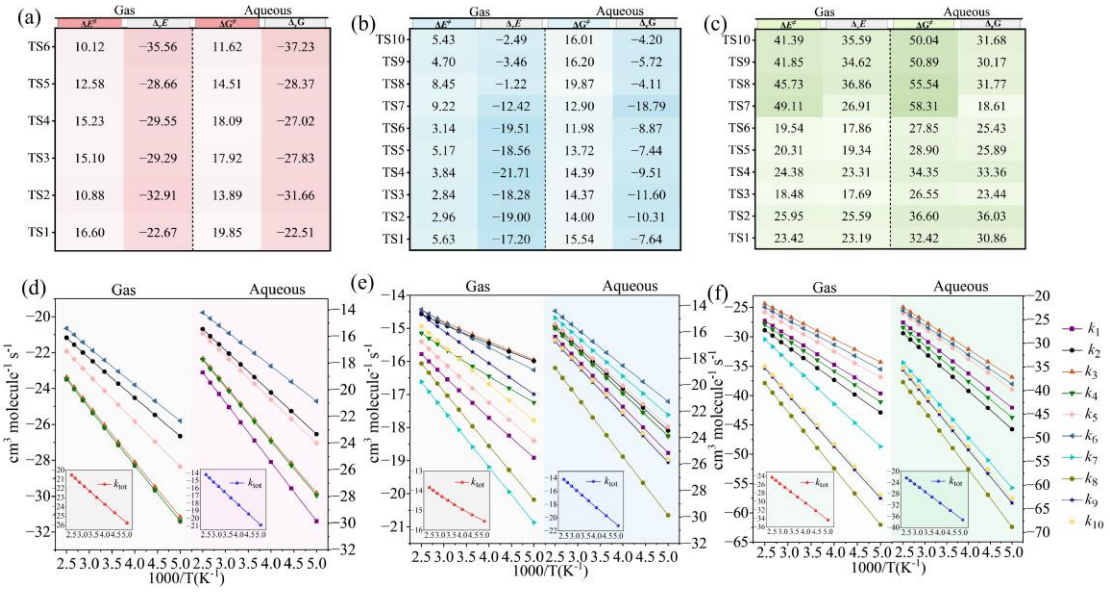


Figure 3 Thermodynamics, kinetics, and temperature dependence of the reactions of 2,4-DNP with O_3, •OH, and •NO_2. (a–c) reaction energy barriers ($\Delta E^{\neq}$) and reaction energies ($\Delta_r E$) for the key pathways (unit: kcal mol^{-1}). (d–e) intrinsic temperature-dependent reaction rate constants for the major channels. **(2) We have revised Figure 5:**

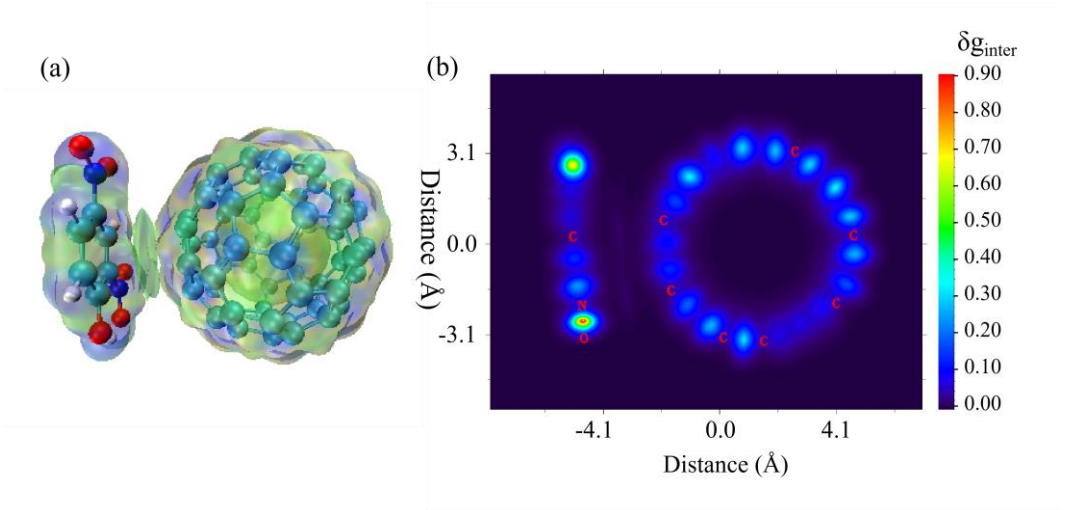


Figure 5 IGM analysis of intermolecular interactions in the 2,4-DNP-C60 aggregate. (a) three-dimensional (3D) IGM isosurface map. (b) two-dimensional (2D) IGM density map.

Comment 4: *Although Tables S1–S4 are mentioned, no concise visual summary or comparative plot is included in the main text to help readers quickly grasp the key data. It would be helpful to present a summary (e.g., a bar chart of rate constants or a table of key energy barriers) in the main paper, with full details left to the Supplement.*

Response: We thank the reviewer for this constructive suggestion. To address this, we have added a new Table 2 in Section 3.1.2, which summarizes the calculated energy barriers, reaction energies for the most favorable reaction channels, and total rate constants at 298.15 K of 2,4-DNP with O_3, •OH, and •NO_2 in both gas and aqueous phases. This table highlights the dominant pathways and allows direct comparison of the relative reactivities of the three oxidants.

Author's changes in manuscript: **In Section 3.1.2, we have added a new Table 1 (the original Table 1 has been modified to Table 2):** "

Table 1 Calculated energy barriers ($\Delta E^{\neq}$, kcal mol^{-1}), reaction energies ($\Delta_r E$, kcal mol^{-1}), and rate constants (*k*tot, cm^3 molecule^{-1} s^{-1}) at 298.15 K for the representative reaction channels of 2,4-DNP with O_3, •OH, and •NO_2 in the gas and aqueous phases. "—" indicates that the rate constant was not calculated because the corresponding pathway is kinetically insignificant (Complete rate constant data for all channels are provided in Table S3). *k*tot at 298.15 K for each oxidant is the sum of all contributing channels for that oxidant."

Oxidant	Channel	Phase	$\Delta E^{\neq}$	$\Delta_r E$	*k*tot (298 K)
O_3	R6 (C5=C6 addition)	Gas	10.12	–35.56	4.23×10^{-23}
		Aq.	11.62	–37.23	3.17×10^{-17}
•OH	R3' (addition at C3)	Gas	2.84	–18.28	3.18×10^{-15}
	R6' (addition at C6)	Aq.	11.98	–8.87	2.25×10^{-17}
	R9' (HAA at C5)	Gas	4.70	–3.46	—
	R9' (HAA at OH)	Aq.	12.90	–18.79	—
•NO_2	R3* (addition at C3)	Gas	18.48	17.69	1.75×10^{-28}
		Aq.	26.55	23.34	3.93×10^{-28}
	R10* (HAA at C6)	Gas	41.39	35.59	—
		Aq.	50.04	31.68	—

Comment 5: *In summary, while this manuscript is rich in content, its overall*

logic is not clearly presented. The authors should explicitly state the specific research questions and scope of this study in the final paragraph of the Introduction.

Response: We thank the reviewer for this constructive suggestion. In the revised manuscript, we have revised the final part of the Introduction to explicitly state the specific research questions and scope of this study. Specifically, we have added a new paragraph before the final paragraph that articulates the three core scientific questions, and we have revised the final paragraph itself to clearly define the scope of the work and the limitations of the conclusions. Together, these revisions ensure that both the research questions and the study scope are explicitly articulated at the end of the Introduction.

Author's changes in manuscript: **In the Introduction (L189–L209), we have revised the paragraphs as follows:** "Despite these advances, a systematic, molecular-level understanding of the multiphase fate of 2,4-DNP remains lacking. Specifically, three core scientific questions need to be addressed: (i) how do the two nitro substituents quantitatively alter the kinetics and selectivity of reactions with O_3, •OH, and •NO_2 relative to mononitrophenols? (ii) how does interfacial hydration regulate the adsorption of 2,4-DNP on carbonaceous surfaces at the molecular level? (iii) does oxidative processing of 2,4-DNP detoxify the products, or could it (based on computational predictions) lead to products with higher toxicity?

To answer these questions, this study employs an integrated multiscale theoretical framework combining density functional theory (DFT), molecular

dynamics (MD) simulations, and computational toxicology to investigate the competing oxidation and nitration pathways of 2,4-DNP in gas and aqueous phases, its interfacial adsorption behavior on carbonaceous aerosol surrogates under different hydration, and the toxicity evolution of its transformation products. The results provide a molecular-level foundation for a comprehensive assessment of the atmospheric fate and ecological risk of 2,4-DNP. This work focuses exclusively on 2,4-DNP as a representative dinitrophenol, and all quantitative conclusions are strictly limited to this compound; however, the qualitative framework established here may serve as a reference for understanding related nitroaromatic systems."

Response to RC3

This study conceptualizes an integrated computational framework combining DFT, MD simulations, and QSAR models to systematically investigate the chemical degradation mechanisms, aerosol surface hydration behavior, and ecotoxicity evolution of 2,4-dinitrophenol in atmospheric multiphase environments. Although this closed-loop, interdisciplinary approach is somewhat novel at the theoretical level, however, due to the parallel comparison of multiphase rate constants being decoupled from atmospheric physical reality (failing to account for Henry's law partitioning and liquid water content), the selected black carbon aerosol surrogate model (pure fullerene C60) being overly idealized, and the core toxicity conclusions relying entirely on boundary-unstable in silico software predictions lacking any experimental validation, the research findings exhibit a strong sense of being "castles in the air".

Specific Issues or Suggestions for Improvement:

Response: We sincerely thank the reviewer for the candid and critical assessment of our work. We appreciate the recognition that our integrated computational framework combining DFT, MD simulations, and QSAR models represents a conceptually novel, closed-loop, interdisciplinary approach at the theoretical level. We also fully acknowledge the reviewer's concerns that the research findings may appear to be "castles in the air" due to the decoupling of multiphase rate constants from atmospheric physical reality, the idealized nature of the C60 aerosol surrogate, and the reliance on in silico toxicity predictions without experimental validation.

These are important and valid concerns, and we have taken them seriously in the revision process. Below we provide point-by-point responses to each specific comment.

Specific Issues or Suggestions for Improvement

Comment 1: *The introduction exhibits obvious selective bias and logical leaps in its literature review. In fact, over the past five years, extensive literature has been published on the aqueous-phase ·OH oxidation and photochemical degradation of nitrophenolic compounds. The introduction fails to accurately delineate research progress across the three domains of "pure gas phase," "pure aqueous phase," and "gas-liquid/gas-solid interfaces," resulting in a rough and inaccurate summary of the existing research landscape.*

Response: We thank the reviewer for this critical observation. We fully agree that the original introduction failed to accurately delineate research progress across the three domains and that the summary of the existing research landscape was insufficient. In the revised manuscript, we have inserted a concise, integrated summary paragraph that systematically distinguishes gas-phase, aqueous-phase, and interfacial research. First, in the gas phase, we now cite the kinetic studies on OH-initiated oxidation of nitrophenols (Harrison et al., 2005), and acknowledge that photolysis and NO_3-mediated pathways are recognized as important loss processes, especially at night. In the aqueous phase, we now explicitly summarize the second-order rate constants for 2,4-DNP with OH radicals determined by Albinet et

al. (2010) and the aqueous photo-oxidation kinetics reported by Hems and Abbatt (2018) for nitrocatechol, nitroguaiacol, and dinitrophenol. At gas-liquid and gas-solid interfaces, we now reference the interfacial oxidation studies of phenolic compounds by Pillar et al. (2014), Pillar and Guzman (2017), and Rana and Guzman (2020, 2022a,b).

Author's changes in manuscript: **In the Introduction (L80–L97), we have added the following integrated summary paragraph:** "Over the past two decades, extensive research has addressed the atmospheric chemistry of nitrophenols, yet the progress has been uneven across different phases. In the gas phase, kinetic measurements have established rate constants for the •OH initiated oxidation of nitrophenols(Bejan et al., 2007), while photolysis and $\bullet NO_3$ mediated pathways are recognized as important loss processes, particularly at night(Bejan et al., 2007; Ng et al., 2017). In the aqueous phase, reactions with •OH radicals have been systematically quantified; for 2,4-DNP, the second order rate constants are $(1.76 \pm 0.05) \times 10^9$ M^{-1} s^{-1} for the neutral form and $(2.33 \pm 0.11) \times 10^9$ M^{-1} s^{-1} for the phenolate(Albinet et al., 2010), with similar kinetic data available for nitrocatechol, nitroguaiacol, and other dinitrophenols(Hems and Abbatt, 2018). However, these studies have mainly focused on homogeneous reactions, leaving the gas-liquid and gas-solid interfaces—key regions where reactivity often differs from the bulk phases—far less understood. Recent work has shown that oxidation of phenolic compounds at interfaces yields products distinct from those formed in the bulk(Pillar-Little et al., 2014; Pillar-Little and Guzman, 2017; Rana and Guzman, 2020; Rana and Guzman, 2022b, a),

underscoring the importance of elucidating the molecular level interactions that govern interfacial adsorption and reactivity. Nevertheless, the behavior of nitrophenols on carbonaceous aerosol surfaces remains largely unexplored."

Comment 2: *The introduction completely fails to summarize existing literature on the surface adsorption of real atmospheric carbonaceous aerosols (such as black carbon, soot, and amorphous carbon). The introduction does not clarify "what bottlenecks existing studies have encountered in simulating carbonaceous particle surfaces," and instead abruptly introduces C60 without accurately reflecting the actual research progress in the field of multiphase adsorption on atmospheric particles.*

Response: We thank the reviewer for this important observation. We agree that the abrupt introduction of C60 without proper context regarding real carbonaceous aerosol surfaces was problematic. In the revised manuscript, we have added a detailed discussion of the bottlenecks that existing studies have encountered in simulating carbonaceous particle surfaces, including the chemical heterogeneity (oxygen-containing functional groups, defect sites, metal impurities), morphological complexity (aggregates, pore structures), and the difficulty of decoupling adsorption from partitioning contributions. These factors make it extremely difficult to identify specific non-covalent interaction types at the molecular level. This discussion now precedes the introduction of C60, establishing why a well-defined model system is necessary to isolate specific interactions from the confounding effects of surface heterogeneity.

Author's changes in manuscript: **In the Introduction (L98–L131), we have added the following discussion:** "This knowledge gap stems primarily from the extreme complexity of real carbonaceous particles, such as black carbon and soot. These particles, products of incomplete combustion, exhibit physicochemical properties that depend strongly on pyrolysis temperature, formation conditions, and subsequent atmospheric aging(Andreae and Gelencsér, 2006). Although their polyaromatic (graphite-like) surfaces can form π-π electron donor-acceptor complexes with nitroaromatic compounds, adsorption strength is significantly influenced by steric effects due to micropore filling and by fouling with natural organic matter that blocks pores and competes for sites(Cornelissen et al., 2005; Poster et al., 2007). Moreover, chemical heterogeneity (oxygen containing functional groups, defect sites, metal impurities) and morphological complexity (aggregates, pore structures) make it extremely difficult to decouple adsorption from partitioning contributions or to identify specific non-covalent interaction types at the molecular level. A well-defined model system is therefore necessary to isolate specific interactions from the confounding effects of surface heterogeneity. Fullerene (C60), with its well-defined, stable carbon cage structure and abundant π-electron cloud, provides an ideal model for studying non-covalent interactions at organic compound-particle interfaces(Athar and Patnaik, 2022; Liu and Lu, 2024). By using C60 as a surrogate for carbonaceous aerosol surfaces, one can effectively bypass the complexities of real particles and precisely probe the adsorption configurations, energetics, and their regulatory factors."

Comment 3: *The introduction merely glosses over this with a single sentence—"traditional experiments are difficult to fully identify"—and fails to clearly summarize the latest progress in computational toxicology (QSAR) for evaluating atmospheric secondary products. This makes the subsequent discussion on toxicity appear abrupt and lacking a solid literature foundation.*

Response: We agree that the single sentence regarding experimental limitations was insufficient and that the QSAR discussion lacked proper literature foundation. In the revised manuscript, following the discussion of experimental limitations, we have added a new paragraph summarizing recent progress in computational toxicology for atmospheric secondary products. This paragraph explicitly cites Decesari et al. (2018), who demonstrated that for 104 secondary organic aerosol compounds, reliable in silico predictions were obtained for 82% of the species, whereas experimental data were available for only 13%, and Vom Eyser et al. (2013), who showed that transformation products generated during atmospheric oxidation can exhibit toxicity exceeding that of their parent compounds. These findings underscore the necessity of integrating toxicity prediction into the assessment of atmospheric transformation pathways. The paragraph concludes by noting that the application of QSAR to nitrophenolic transformation products remains limited, and the inherent uncertainties require careful interpretation.

Author's changes in manuscript: **In the Introduction (L162–L175), we have added the following paragraph:** "Traditional experimental approaches often struggle to comprehensively identify all reactive intermediates and transformation

products, and computational toxicology offers a high-throughput, low-cost alternative for assessing the toxicity of atmospheric transformation products (Tam et al., 2021; Vom Eyser et al., 2013). For instance, for a set of 104 secondary organic aerosol compounds, reliable in silico predictions were obtained for 82 % of the species, whereas experimental data were available for only 13 %(Decesari et al., 2018). Importantly, atmospheric oxidation may produce compounds with toxicity exceeding that of their parents(Vom Eyser et al., 2013), highlighting the need to integrate toxicity prediction into transformation pathway assessment. The application of quantitative structure activity relationship (QSAR) to nitrophenolic transformation products, however, remains limited, and the inherent uncertainties require careful interpretation."

Comment 4: *The manuscript focuses exclusively on a single compound, 2,4-DNP, yet repeatedly draws overarching conclusions about the atmospheric fate and risk amplification of "nitrophenolic compounds" or "nitroaromatics" as a whole.*

Response: We thank the reviewer for this critical observation. We agree that the original manuscript repeatedly drew overarching conclusions about "nitrophenolic compounds" or "nitroaromatics" as a whole, despite focusing exclusively on 2,4-DNP. This overgeneralization was inappropriate and has been corrected. In the revised manuscript, we have systematically revised the language throughout the text to ensure that quantitative conclusions are explicitly attributed to 2,4-DNP rather than

generalized to all nitrophenolic or nitroaromatic compounds. Specifically, in the Abstract, we have revised the concluding sentences to clarify that the quantitative findings apply specifically to 2,4-DNP, while the qualitative framework may provide reference for related systems. Throughout the Results and Discussion and Conclusions, we have systematically replaced overgeneralized phrases (e.g., "nitrophenolic compounds," "nitroaromatics," "these findings reveal the environmental risk amplification associated with nitroaromatic compounds") with compound-specific phrasing (e.g., "2,4-DNP," "this compound," "the present system") where the statement refers to quantitative results, while retaining broader language only when discussing qualitative mechanistic insights that may be generalizable.

Author's changes in manuscript: **(1) In the Abstract (L47–L50), we have revised the concluding sentences to clarify that the quantitative findings apply specifically to 2,4-DNP:** "These findings provide mechanistic insights into the atmospheric transformation pathways of this specific dinitrophenol and highlight the importance of evaluating transformation product toxicity in the environmental risk assessment of nitrophenolic compounds." **(2) In Section 3.3, we have replaced overgeneralized phrases** such as "nitrophenolic compounds" and "nitroaromatics" with compound-specific phrasing (e.g., "2,4-DNP," "this compound") where referring to quantitative toxicity results. **(3) In the Conclusions (L977-L981), we have revised the language to clearly state that quantitative conclusions apply specifically to 2,4-DNP, while the qualitative framework may serve as a reference:** "While the quantitative conclusions apply specifically to 2,4-DNP, the qualitative framework

established here—linking substituent electronic effects to reaction kinetics, interfacial behavior, and toxicity indicators—may serve as a reference for understanding related nitroaromatic systems."

Comment 5: *The authors convert the aqueous rate constants to* cm^3 $molecule^{-1}$ s^{-1} *and directly plot them alongside gas-phase constants in Figure 3. In the actual atmosphere, the overall contribution of a multi-phase pathway depends on the partitioning of the pollutant (Henry's law) and the Liquid Water Content (LWC) of the aerosol. Merely comparing converted rate constants fails to establish whether the aqueous-phase reactions actually matter to the total atmospheric fate of 2,4-DNP.*

Response: We thank the reviewer for this important comment. We fully agree that the overall contribution of a multiphase reaction depends on the phase partitioning of the pollutant, governed by Henry's law and effective solubility, the aerosol liquid water content, and the availability of oxidants in each phase. In the revised manuscript, we have systematically addressed this concern through the following modifications. In Section 3.1.2, we have added a new paragraph explicitly clarifying that the converted rate constants represent intrinsic reactivities in each phase rather than actual atmospheric importance. For 2,4-DNP, the Henry's law constant has been determined as 5.70×10^{-8} atm·m^3/mol at 5 °C (Lüttke and Levsen, 1997), indicating a strong tendency to partition into the aqueous phase. The partitioning is further modulated by its acid dissociation constant (pKa ≈ 4.09 at 25 °C), as the deprotonated phenolate form is substantially more water-soluble than the neutral phenol (Schwarzenbach et al., 1988). In addition, the aerosol liquid water

content, which varies widely depending on relative humidity, particle composition, and atmospheric conditions, and determines the available aqueous volume for multiphase reactions. Without quantitative information on these partitioning parameters under specific atmospheric conditions, the aqueous-phase rate constants should be interpreted as intrinsic reactivity indicators rather than direct measures of atmospheric importance. We have also revised the title and caption of Figure 3 to clearly indicate that the comparison is of intrinsic rate constants.

Author's changes in manuscript: **(1) In Section 3.1.2 (L563–L607), we have added the following paragraph:** "It should be emphasized that the trends described above, however, reflect only the intrinsic molecular reactivity of each oxidant; their actual atmospheric importance depends on oxidant concentrations, phase partitioning, and aerosol liquid water content. To bridge this gap between intrinsic reactivity and atmospheric relevance, pseudo-first-order rate constants were estimated using literature-reported oxidant concentrations. These estimates are presented below, providing a more realistic assessment of the relative contributions of each pathway under typical tropospheric conditions.

The literature review indicates that •OH concentrations typically reach $1 \times 10^6 \sim 3 \times 10^6$ molecules cm^{-3}, while $\bullet NO_2$ levels are lower due to rapid photolysis under daytime conditions. During heavily polluted nighttime conditions, however, •OH concentrations drop substantially. Geyer et al.(Geyer et al., 2003) reported a nocturnal •OH concentration of $(1.85 \pm 0.82) \times 10^5$ cm^{-3} during the BERLIOZ campaign, and in UK urban surface environments, night-time OH levels were determined to be in the

range of 10^5 ~ 10^6 molecules cm^{-3}(Khan et al., 2011). Meanwhile, $•NO_2$ can accumulate significantly at night, with nocturnal maxima reaching 8.43 ± 0.4 ppb in Guangzhou(Qin et al., 2009). Using these literature-reported concentrations, the pseudo-first-order rate constants under nighttime conditions can be estimated. For the •OH pathway, with kOH = 3.18 × 10^{-15} cm^3 $molecule^{-1}$ s^{-1} and [OH] ≈ 10^5 ~ 10^6 molecules cm^{-3}, k'OH ≈ 10^{-10} ~ 10^{-9} s^{-1}. For the direct $•NO_2$ pathway, with $k$$NO_2$ ≈ 10^{-28} cm^3 $molecule^{-1}$ s^{-1} and [NO_2] ≈ 10^{10} ~ 10^{11} molecules cm^{-3} (corresponding to 0.4 ~ 4 ppb at 298 K and 1 atm), k'NO_2 ≈ 10^{-18} ~ 10^{-17} s^{-1}. Even under the most favorable nighttime conditions (lowest •OH, highest $•NO_2$), the direct $•NO_2$ pathway remains more than 7 orders of magnitude slower than the •OH pathway, corresponding to a lifetime of >10^{10} s, which is negligible on atmospheric timescales. Therefore, while a full diurnal box model simulation would be required to quantify all pathways under varying pollution regimes, the quantitative analysis above confirms that the direct reaction of $•NO_2$ with parent 2,4-DNP is negligible even under nighttime conditions. The possible involvement of $•NO_2$ in subsequent reactions with primary oxidation intermediates will be discussed separately to provide a complete mechanistic picture of its environmental fate. In summary, the atmospheric degradation of 2,4-DNP is kinetically dominated by •OH, with O_3 playing a significant role in the aqueous phase, while the direct transformation contribution of $•NO_2$ can be neglected in environmental assessments.

The overall contribution of aqueous-phase reactions to the atmospheric fate of 2,4-DNP depends critically on the fraction of the compound that partitions into the

aqueous phase. For 2,4-DNP, the Henry's law constant has been determined as 5.70 × 10^{-8} atm·m^3/mol at 5 °C(Lüttke and Levsen, 1997), indicating a strong tendency to partition into the aqueous phase. The partitioning is further modulated by its acid dissociation constant (pKa ≈ 4.09 at 25 °C), as the deprotonated phenolate form is substantially more water-soluble than the neutral phenol(Schwarzenbach et al., 1988). In addition, the aerosol liquid water content—which varies widely depending on relative humidity, particle composition, and atmospheric conditions—determines the available aqueous volume for multiphase reactions. Without quantitative information on these partitioning parameters under specific atmospheric conditions, the aqueous-phase rate constants should be interpreted as intrinsic reactivity indicators rather than direct measures of atmospheric importance." **(2) In the Figure 3 caption (L450–L451), we have revised the description to include the word "intrinsic":** "(d–e) intrinsic temperature-dependent reaction rate constants for the major channels."

Comment 6: *The ecotoxicity profiling relies completely on the US EPA's software. QSAR screening is excellent for high-throughput hazard prioritization, but drawing definitive conclusions about environmental risk amplification ("toxicity amplification") purely from in silico endpoints is speculative.*

Response: We thank the reviewer for raising this important point. In the original manuscript, we had already included a limitations paragraph in Section 3.3 acknowledging that the QSAR models are constrained by the chemical space of the training sets, that predictions for structurally distinct species such as 2,4-DNP and its

nitro-containing derivatives may have diminished confidence, and that the findings should be interpreted as hypothesis-generating rather than definitive. In the revised manuscript, we have further strengthened this discussion by: (i) adding an independent cross-validation using Toxtree (version 3.1.0), which employs rule-based structural alerts that are algorithmically distinct from the statistical consensus method used in T.E.S.T.; (ii) providing a quantitative reference to the performance of QSAR models for Ames mutagenicity prediction, acknowledging that even the best-performing models achieve a balanced accuracy of approximately 76.9% at 100% coverage (Uesawa, 2024); (iii) explicitly discussing the instability of categorical predictions with probability scores close to the classification threshold; and (iv) clearly recommending experimental validation through in vitro Ames tests and zebrafish embryo developmental toxicity assays for the high-priority compounds identified.

Author's changes in manuscript: **(1) In Section 3.3 (L900–L918), we have added an independent cross-validation using Toxtree (version 3.1.0), including the Benigni/Bossa rule-base for Ames mutagenicity and the Cramer decision tree for TTC-based classification, with results summarized in Table S5:** "To further assess the reliability of the QSAR predictions, an independent cross-validation was performed using Toxtree (version 3.1.0)(Patlewicz et al., 2008). For Ames mutagenicity, Toxtree's Benigni/Bossa rulebase was employed, which uses rule-based structural alerts that are algorithmically distinct from the statistical consensus method used in T.E.S.T(Benigni et al., 2007). The cross-validation results (Table S5) show

consistent predictions for the majority of compounds, with deviations observed only for compounds with probability scores close to the classification threshold. For developmental toxicity, Toxtree does not provide a dedicated prediction model. Instead, we employed its Cramer decision tree to perform a toxicological concern threshold (TTC)-based classification. The Cramer decision tree classifies compounds into three classes based on their chemical structure: Class I (low toxicity concern), Class II (moderate toxicity concern), and Class III (high toxicity concern)(Cramer et al., 1976). Class III compounds are assigned the lowest TTC value (90 μg person^{-1} day^{-1})(Munro et al., 1996), indicating the highest potential for adverse health effects, including developmental toxicity. As shown in Table S5, all 2,4-DNP and its ozonolysis products were classified as Cramer Class III, consistent with the T.E.S.T. predictions that all compounds exhibit developmental toxicity potential. This approach follows established practices in computational toxicology for the developmental toxicity screening of nitro-organic compounds(Yong-Di et al., 2022)."

Table S5 Cross-validation of Ames mutagenicity, development toxicity for 2,4-DNP and the intermediates (IMs series) and final products (Ps series) using T.E.S.T. and Toxtree. "ND" = not detected (negative), "D" = detected (positive), "NA" = not applicable/outside applicability domain. Cramer Class III indicates the highest priority for toxicity concern.

Compound	T.E.S.T. Ames muagenicity	Toxtree Ames muagenicity	T.E.S.T. Dev. Tox.	Toxtree Cramer Class
2,4-DNP	ND (0.13)	ND	D (0.55)	III
IM17	NA (0)	ND	D (0.67)	III
IM25	NA (0)	ND	D (0.85)	III
IM44	NA (0)	ND	D (0.84)	III
IM54	NA (0)	ND	D (0.94)	III
P1	D (0.53)	ND	D (0.58)	III
P2	ND (0.21)	D	D (0.56)	III
P3	ND (0.47)	ND	D (0.65)	III
P4	ND (0.21)	ND	D (0.56)	III

(2) In Section 3.3 (L919–L945), we have substantially expanded the discussion of QSAR uncertainties, including applicability domain limitations, near-threshold prediction instability, and quantitative model performance: "The toxicity predictions presented here are screening level assessments based on QSAR models. They are intended for hazard prioritization and hypothesis generation, not as

definitive toxicological conclusions. Several factors limit their predictive reliability. First, QSAR model performance is constrained by the chemical space of training sets and the defined applicability domains. For structurally distinct species such as 2,4-DNP and its various derivatives, the predicted confidence levels are lower because these models cannot fully elucidate specific toxicological modes of action. As highlighted by the Ames/QSAR International Challenge Projects, even the best performing mod-els achieve a balanced accuracy of approximately 76.9 % at 100 % coverage(Uesawa, 2024). Second, categorical predictions with probability scores close to the classification threshold are inherently unstable, suggesting that the "not detected" Ames mutagenicity signals for intermediates such as IM17, IM25, IM44, and IM54 may reflect model limitations rather than a definitive absence of toxicity. Furthermore, these computational frameworks necessarily simplify complex biological endpoints such as developmental toxicity. While a quantitative weight of evidence (qWoE) approach has been shown to achieve accuracy comparable to experimental Ames tests(Tintó-Moliner and Martin, 2020), such approaches are beyond the scope of this screening level study. Overall, the findings should be interpreted as hypothesis-generating(Vom Eyser et al., 2013). Experimental validation—through in vitro Ames tests and zebrafish embryo development toxicity assays—is recommended for the high-priority compounds identified here." **(3) In the Conclusions (L1013–L1016), we have explicitly prioritized high-risk products (IM54, P1, and P2) for experimental validation through in vitro Ames tests and zebrafish embryo developmental toxicity assays:** "In vitro toxicity testing: The

high-priority ozonolysis products identified in this study (IM54, P1, and P2) should be subjected to Ames mutagenicity assays and zebrafish embryo developmental toxicity tests to validate the QSAR predictions."

Comment 7: *The authors claim that the direct transformation initiated by ·NO_2 is completely negligible under ambient conditions because its barrier is much higher than OH pathways. This is an unbalance in atmospheric interpretation. During heavily polluted night events, ·OH radical concentrations drop close, whereas ·NO_2 accumulates significantly. Discarding a daytime-uncompetitive pathway without conducting a true diurnal chemical box-model or sensitivity analysis under varying pollution regimes is scientifically weak.*

Response: The reviewer is correct that the conclusion regarding •NO_2 reactivity must be evaluated in the context of diurnal variations in oxidant concentrations. To address this, we have conducted a quantitative analysis using literature-reported field measurements and added the discussion to Section 3.1.2.

Author's changes in manuscript: **In Section 3.1.2 (L570–L594), we have added a quantitative analysis of pseudo-first-order rate constants under nighttime conditions using literature-eported field measurements:** "The literature review indicates that •OH concentrations typically reach $1 \times 10^6 \sim 3 \times 10^6$ molecules cm^{-3}, while •NO_2 levels are lower due to rapid photolysis under daytime conditions. During heavily polluted nighttime conditions, however, •OH concentrations drop substantially. Geyer et al.(Geyer et al., 2003) reported a nocturnal •OH concentration

of (1.85 ± 0.82) × 10^5 cm^{-3} during the BERLIOZ campaign, and in UK urban surface environments, night-time OH levels were determined to be in the range of 10^5 ~ 10^6 molecules cm^{-3}(Khan et al., 2011). Meanwhile, •NO_2 can accumulate significantly at night, with nocturnal maxima reaching 8.43 ± 0.4 ppb in Guangzhou(Qin et al., 2009). Using these literature-reported concentrations, the pseudo-first-order rate constants under nighttime conditions can be estimated. For the •OH pathway, with kOH = 3.18 × 10^{-15} cm^3 $molecule^{-1}$ s^{-1} and [OH] ≈ 10^5 ~ 10^6 molecules cm^{-3}, k'OH ≈ 10^{-10} ~ 10^{-9} s^{-1}. For the direct •NO_2 pathway, with $k$$NO_2$ ≈ 10^{-28} cm^3 $molecule^{-1}$ s^{-1} and [NO_2] ≈ 10^{10} ~ 10^{11} molecules cm^{-3} (corresponding to 0.4 ~ 4 ppb at 298 K and 1 atm), k'NO_2 ≈ 10^{-18} ~ 10^{-17} s^{-1}. Even under the most favorable nighttime conditions (lowest •OH, highest •NO_2), the direct •NO_2 pathway remains more than 7 orders of magnitude slower than the •OH pathway, corresponding to a lifetime of >10^{10} s, which is negligible on atmospheric timescales. Therefore, while a full diurnal box model simulation would be required to quantify all pathways under varying pollution regimes, the quantitative analysis above confirms that the direct reaction of •NO_2 with parent 2,4-DNP is negligible even under nighttime conditions. The possible involvement of •NO_2 in subsequent reactions with primary oxidation intermediates will be discussed separately to provide a complete mechanistic picture of its environmental fate. In summary, the atmospheric degradation of 2,4-DNP is kinetically dominated by •OH, with O_3 playing a significant role in the aqueous phase, while the direct transformation contribution of •NO_2 can be neglected in environmental assessments."

The main detailed revision is listed in the Language Revision Comparison Table in the text.

Line	Origin	Now	Action
L1 (Title)	Unveiling the multiphase fate of 2,4-dinitrophenol on aerosols: Interfacial hydration governs competing oxidation pathways and unexpected toxicity amplification	Unveiling the multiphase fate of 2,4-dinitrophenol on aerosols: Interfacial hydration modulates competing oxidation pathways and predicted increase in toxicity	Changed
L25 (Abstract)	Initial	In the gas phase, initial	Changed
L26 (Abstract)	was	is	Changed
L28-L30 (Abstract)		In the aqueous phase, solvation effects suppress the reaction rates, while the two nitro substituents exert a cumulative electron-withdrawing effect that reduces the rate constant by three orders of magnitude relative to mononitrocatechol.	Added
L30-L35 (Abstract)	A key mechanistic insight is that these		Deleted

	primary reactions are inhibited by solvation effects, while nitro substituents further suppress the reaction rates, establishing a quantitative link between electronic structure and degradation kinetics.		
L35-L38 (Abstract)		For the key radical intermediate generated by •OH addition, hydrogen atom abstraction (HAA) with O_2 represents the dominant atmospheric fate based on the calculated barriers and the overwhelming concentration advantage of O_2 over $•NO_2$. At the gas-aqueous interface,	Added
L38 (Abstract)	Molecular	molecular	Changed
L39 (Abstract)		the C60	Added
L40-L41 (Abstract)		—first strengthening at moderate hydration and	Added

		weakening at high hydration.	
L42 (Abstract)	the	certain	Changed
L42-L45 (Abstract)		products exhibit elevated Ames mutagenicity and developmental toxicity indicators relative to the parent compound, suggesting that oxidative processing of 2,4-DNP may not lead to simple detoxification.	Added
L45-L46 (Abstract)	process amplifies, rather than mitigates, environmental risk by generating secondary products with significantly enhanced mutagenicity and developmental toxicity.		Deleted
L47-L50 (Abstract)		atmospheric transformation pathways of this specific dinitrophenol and highlight the importance of	Added

		evaluating transformation product toxicity in the environmental risk assessment of nitrophenolic compounds.	
L50-L52 (Abstract)	environmental risk amplification associated with nitroaromatic compounds and highlight the necessity of evaluating toxic transformation products for accurate environmental risk assessment.		Deleted
L62-L67 (Introduction)	have attracted considerable attention because of their strong light-absorbing properties, inherent biological toxicity, and	are important toxic organic pollutants, primarily emitted from incomplete combustion of fossil fuels and biomass, and also formed via photochemical	Changed

	potential role as important SOA precursors	oxidation of precursors such as polycyclic aromatic hydrocarbons	
L67-L68 (Introduction)	As a representative nitrated aromatic compound,	Among them	Changed
L69-L72 (Introduction)	widely present in industrial emissions and can also be formed through atmospheric secondary reactions, posing considerable environmental risks	listed as a priority pollutant by the U.S. Environmental Protection Agency due to its acute and chronic toxicity, potential genotoxicity, and bioaccumulation	Changed
L72-L111 (Introduction)		Although ambient concentrations of 2,4-DNP are typically in the ng m^{-3} range, its high Henry's law constant and low vapour pressure lead to significant partitioning into condensed phases such as aerosol particles	Added

		and cloud/fog droplets(Lüttke and Levsen, 1997). Consequently, it can be deposited onto terrestrial and aquatic ecosystems via dry and wet deposition, posing sustained threats to the environment and human health. A comprehensive understanding of its multiphase chemical transformation mechanisms is therefore essential for accurate risk assessment and fate prediction. Over the past two decades, extensive research has addressed the atmospheric chemistry of nitrophenols, yet the progress has been uneven across different phases. In the gas phase, kinetic	

		measurements have established rate constants for the •OH initiated oxidation of nitrophenols(Bejan et al., 2007), while photolysis and $•NO_3$ mediated pathways are recognized as important loss processes, particularly at night(Bejan et al., 2007; Ng et al., 2017). In the aqueous phase, reactions with •OH radicals have been systematically quantified; for 2,4-DNP, the second order rate constants are $(1.76 \pm 0.05) \times 10^9$ M^{-1} s^{-1} for the neutral form and $(2.33 \pm 0.11) \times 10^9$ M^{-1} s^{-1} for the phenolate(Albinet et al., 2010), with similar kinetic data available for nitrocatechol, nitroguaiacol, and other	

		dinitrophenols(Hems and Abbatt, 2018). However, these studies have mainly focused on homogeneous reactions, leaving the gas-liquid and gas-solid interfaces—key regions where reactivity often differs from the bulk phases—far less understood. Recent work has shown that oxidation of phenolic compounds at interfaces yields products distinct from those formed in the bulk(Pillar-Little et al., 2014; Pillar-Little and Guzman, 2017; Rana and Guzman, 2020; Rana and Guzman, 2022b, a), underscoring the importance of elucidating the molecular level interactions that govern interfacial adsorption	

		and reactivity. Nevertheless, the behavior of nitrophenols on carbonaceous aerosol surfaces remains largely unexplored. This knowledge gap stems primarily from the extreme complexity of real carbonaceous particles, such as black carbon and soot. These particles, products of incomplete combustion, exhibit physicochemical properties that depend strongly on pyrolysis temperature, formation conditions, and subsequent atmospheric aging(Andreae and Gelencsér, 2006). Although their polyaromatic (graphite-like) surfaces can form π-π electron donor-acceptor	

		complexes with nitroaromatic compounds, adsorption strength is significantly influenced by steric effects due to micropore filling and by fouling with natural organic matter that blocks pores and competes for sites(Cornelissen et al., 2005; Poster et al., 2007). Moreover, chemical heterogeneity (oxygen containing functional groups, defect sites, metal impurities) and morphological complexity (aggregates, pore structures) make it extremely difficult to decouple adsorption from partitioning contributions or to identify specific non-covalent interaction types at the	

		molecular level. A well-defined model system is therefore necessary to isolate specific interactions from the confounding effects of surface heterogeneity.	
L111-L126 (Introduction)	However, accurately assessing the environmental risks of nitrophenolic pollutants and predicting their fate requires more than identifying their large-scale sources and impacts. The key lies in elucidating their specific chemical transformation mechanisms in the atmosphere. Current understanding of the		Deleted

	degradation mechanisms of organic compounds mainly focuses on homogeneous reactions, particularly daytime photochemical oxidation pathways dominated by •OH(Schaefer and Herrmann, 2018; Hu et al., 2021; Liu et al., 2023). In reality, a significant fraction of atmospheric reactions occurs at the heterogeneous interfaces of aerosols or droplets, a process that is especially crucial at night and under highly		

	polluted conditions(Xing et al., 2019). At these interfaces, the molecular orientation of pollutants, the local solvation environment, particularly the structure of water molecules and interactions with particle surfaces collectively reshape their reactivity and pathways, potentially even dictating their ultimate environmental fate(Ohto et al., 2019; Mao et al., 2024; Lee et al., 2014). Consequently, selecting		

	a model system that can effectively represent the surface characteristics of real atmospheric carbonaceous particles is of great importance.		
L126 (Introduction)	Owing to	with	Changed
L129-L131 (Introduction)		By using C60 as a surrogate for carbonaceous aerosol surfaces, one can effectively bypass the complexities of real particles and precisely probe the adsorption configurations, energetics, and their regulatory factors.	Added
L131-L132 (Introduction)	This offers a clear platform for probing the molecular-level regulatory role of interfacial hydration.		Deleted

L132-L135 (Introduction)		While phenolic compounds may undergo further multiphase aging to form SOA and brown carbon(Pillar-Little and Guzman, 2018; Guzman et al., 2022; Al-Abadleh et al., 2022), the present study focuses on their initial molecular-scale oxidation and interfacial adsorption.	Added
L136-L138 (Introduction)	interfacial chemical transformations constitute a competitive and evolving process.	the transformation of nitrophenols is a dynamic competition among multiple reactive species.	Changed
L138-L144 (Introduction)	A comprehensive understanding of the atmospheric behavior of nitroaromatic compounds requires moving beyond the	The key oxidants include	Changed

	traditional isolated study of single static oxidation pathways. Instead, it requires a perspective that con-siders their fate within a dynamic network driven by multiple reactive species(Thangamani et al., 2016). The key drivers of this network are three core atmospheric oxidants whose relative importance varies with environmental conditions(Sun et al., 2021). These include the primary daytime oxidant		

L145 (Introduction)		(dominant during daytime)	Added
L146 (Introduction)	) and strong oxidizing capacity		Deleted
L148-L152 (Introduction)		Photolysis of 2,4-DNP has been shown to be a minor loss route compared to •OH oxidation(Albinet et al., 2010), and while $•NO_3$ chemistry is an important nighttime pathway for phenols(Rana and Guzman, 2022b; Ng et al., 2017), the present study focuses on the thermal oxidation network initiated by O_3, •OH, and $•NO_2$.	Added
L152 (Introduction)	Differences	These differences	Changed
L152 (Introduction)	the		Deleted
L154-L155 (Introduction)	across diurnal cycles and under varying	under varying diurnal and pollution regimes	Changed

	pollution regimes.		
L156 (Introduction)	Notably, such	Such	Changed
L159-L162 (Introduction)	Taking 2,4-DNP as an example, it exhibits not only acute toxicity but also potential for bioaccumulation and genotoxicity, thereby posing a long-term ecological threat through food-chain amplification(Ahmaruz zaman et al., 2024; Mangotra and Singh, 2024; Grundlingh et al., 2011). However,		Deleted
L164-L166 (Introduction)	are frequently inadequate for efficiently evaluating their toxicological	computational toxicology offers a high-throughput, low-cost alternative for assessing the toxicity of atmospheric	Changed

	effects	transformation products	
L167-L196 (Introduction)		For instance, for a set of 104 secondary organic aerosol compounds, reliable in silico predictions were obtained for 82 % of the species, whereas experimental data were available for only 13 %(Decesari et al., 2018). Importantly, atmospheric oxidation may produce compounds with toxicity exceeding that of their parents(Vom Eyser et al., 2013), highlighting the need to integrate toxicity prediction into	Added

		transformation pathway assessment. The application of quantitative structure activity relationship (QSAR) to nitrophenolic transformation products, however, remains limited, and the inherent uncertainties require careful interpretation. Previous studies on phenolic oxidation have predominantly focused on systems with electron-donating substituents that enhance reactivity. Pillar et al.(Pillar et al.,	

		2015; Pillar et al., 2014) and Pillar and Guzman(Pillar-Little and Guzman, 2017) demonstrated that catechols and their electron-donating ($–CH_3$, $–OCH_3$) derivatives readily form carboxylic acids, quinones, and polyphenols at interfaces; Rana and Guzman(Rana and Guzman, 2020; Rana and Guzman, 2022b,a) systematically investigated the interfacial oxidation of phenolic aldehydes; Witt et al.(Witt et al.,	

		2025) found that ozonolysis of non-nitrated phenolic aldehydes yields smaller, less toxic molecules such as oxalic and glyoxylic acids; and Rana et al.(Rana et al., 2023) showed that catechol can be converted to 4-nitrocatechol (4NC) in aqueous microdroplets via multiphase •NO_2/O_3 chemistry. These studies have laid a foundation for understanding substituent effects, but 2,4-DNP—with two	

		strongly electron-withdrawing nitro groups—may exhibit fundamentally different reactivity and mechanisms. Despite these advances, a systematic, molecular-level understanding of the multiphase fate of 2,4-DNP remains lacking. Specifically, three core scientific questions need to be addressed: (i) how do the two nitro substituents quantitatively alter the kinetics and selectivity of reactions with O_3,	

		•OH, and •NO_2 relative to mononitrophenols? (ii) how does interfacial hydration regulate the adsorption of 2,4-DNP on carbonaceous surfaces at the molecular level? (iii) does oxidative processing of 2,4-DNP detoxify the products, or could it (based on computational predictions) lead to products with higher toxicity?	
L197 (Introduction)	address	answer	Changed
L197 (Introduction)	gaps	questions	Changed
L202-L209 (Introduction)	mechanistic insights into the multiphase fate	a molecular-level foundation for a	Changed

	of nitrated aromatics and highlight the importance of evaluating toxic intermediates in atmospheric risk assessment.	comprehensive assessment of the atmospheric fate and ecological risk of 2,4-DNP. This work focuses exclusively on 2,4-DNP as a representative dinitrophenol, and all quantitative conclusions are strictly limited to this compound; however, the qualitative framework established here may serve as a reference for understanding related nitroaromatic systems.	
L250-L251 (2.2 Molecular dynamics simulations)		Wang et al., 2004; Lindorff-Larsen et al., 2010	Added

L274-L275 (2.4 Computational toxicology)	hierarchical quantitative structure activity relationship		Deleted
L306 (3.1.1 Characterization of the electronic structure of 2,4-DNP)		, with an electronic energy of −449508.49 kcal mol^{-1}	Added
L309 (3.1.1 Characterization of the electronic structure of 2,4-DNP)	O—N	O_2N	Changed
L310-L311 (3.1.1 Characterization of the electronic structure of 2,4-DNP)	bond length of 1.75 Å—a value	an H···O distance of 1.75—values	Changed
L312 (3.1.1 Characterizatio		, planar	Added

n of the electronic structure of 2,4-DNP)			
L312-L317 (3.1.1 Characterization of the electronic structure of 2,4-DNP)	which closely resembles the strain-free chair conformation of cyclohexane and thus provides optimal stabilization(Barton and Cookson, 1956). This hydrogen bond con-tributes substantial stabilization energy and constitutes the principal factor governing conformational preference.	that benefits from both the hydrogen bond and the rigidity of the aromatic ring,	Changed
L320 (3.1.1 Characterization of the	Importantly, thereby enabling	This coplanarity enables	Changed

electronic structure of 2,4-DNP)			
L329-L330 (3.1.1 Characterization of the electronic structure of 2,4-DNP)	rich in lone electron pairs and thus prone to nucleophilic attack	electron-rich sites that are susceptible to electrophilic attack.	Changed
L330 (3.1.1 Characterization of the electronic structure of 2,4-DNP)	nucleophilic	electron-rich	Changed
L334-L336 (3.1.1 Characterization of the electronic structure of 2,4-DNP)	electrophilic features associated with σ-hole interactions caused by	electron-poor sites that are susceptible to nucleophilic attack, which arise from	Changed
L336 (3.1.1 Characterization of the	and O–H		Deleted

electronic structure of 2,4-DNP)			
L337 (3.1.1 Characterization of the electronic structure of 2,4-DNP)	prediction	basis	Changed
L364 (3.1.2 Primary reactions of 2,4-DNP with O_3, •OH, and $•NO_2$)	(O1 and O3)		Deleted
L365-L368 (3.1.2 Primary reactions of 2,4-DNP with O_3, •OH, and $•NO_2$)	. The forming C5–O1 and C6–O3 bonds reach lengths of 1.43 Å and 1.42 Å, respectively, while the original C5–C6 double bond is significantly elongated from 1.38 Å to 1.56 Å,	, accompanied by significant elongation of the original C5–C6 bond (optimized geometries are compiled in Table S2),	Changed
L371-L374	,. During this process,	leadings	Changed

(3.1.2 Primary reactions of 2,4-DNP with O_3, •OH, and •NO_2)	the O2–O3 bond elongates to 2.02 Å, and the C5–C6 bond ex-tends to 1.96 Å, while new C5–O1 and C6–O3 bonds begin to form with lengths of approximately 1.32 Å and 1.26 Å, respectively. This leads		
L381-L384 (3.1.2 Primary reactions of 2,4-DNP with O_3, •OH, and •NO_2)	where the distance between the oxygen atom of •OH and C3 decreases to 1.42 Å (from an initial separation of 1.99 Å). Concurrently, the	in which the •OH oxygen approaches C3 with significant shortening of the forming bond distance, accompanied by elongation of the adjacent	Changed
L384-L387 (3.1.2 Primary reactions of 2,4-DNP with	bond lengths increase from 1.40 Å to 1.50 Å, indicating significant	bonds, and	Changed

O_3, •OH, and •NO_2)	disruption of the local aromatic structure and a redistribution of π-bonding within the ring. The O–H bond of •OH forms an angle of approximately 110° with the plane of the aromatic ring		
L389 (3.1.2 Primary reactions of 2,4-DNP with O_3, •OH, and •NO_2)	promoting σ-bond formation and		Deleted
L392-L394 (3.1.2 Primary reactions of 2,4-DNP with O_3, •OH, and •NO_2)	in which the distance between the oxygen atom of •OH and the hydrogen on C5 shortens to 1.19 Å, the breaking C5–H bond elongates from 1.08 Å	characterized by a nearly linear O–H–C5 arrangement	Changed

	to 1.26 Å, and the O–H–C5 angle approaches 179°,		
L397-L398 (3.1.2 Primary reactions of 2,4-DNP with O_3, •OH, and •NO_2)	exhibits electrophilic character (low electron density).	is an electron poor site, which is susceptible to nucleophilic attack	Changed
L398-L412 (3.1.2 Primary reactions of 2,4-DNP with O_3, •OH, and •NO_2)	is contrary to the conventional expectation for hydrogen abstraction by an electrophilic radical such as •OH. Nevertheless, the calculations show that this site remains the dominant abstraction site in the HAA pathway. This selectivity shift	appears contrary to the conventional expectation that an electrophilic radical such as •OH would preferentially abstract a hydrogen atom from an electron rich site. However, the HAA reaction of •OH is governed primarily by C–H bond dissociation energies (BDEs) rather	Changed

	suggests that the HAA reaction of •OH may be governed by bond strength control and transition state electrostatic complementarity, rather than being determined solely by ground state electrophile–nucleophile interactions. Indeed, the C–H bond dissociation energy has been established as a key factor controlling the site-selectivity of HAA by •OH, with weaker bonds being preferentially abstracted.	than ground state electron density(Mayer, 2011). The C5–H bond is significantly weakened by the electron withdrawing effect of the adjacent nitro group, making it the preferred abstraction site despite its low electron density.	
L416-L418	green region in Figure 2	reaction of •NO_2 with	Changed

(3.1.2 Primary reactions of 2,4-DNP with O_3, •OH, and •NO_2)	illustrates the reaction mechanism of •NO_2 with 2,4-DNP.	2,4-DNP proceeds via two competing pathways: radical addition and HAA, as shown in the green region of Figure 2.	
L419-L420 (3.1.2 Primary reactions of 2,4-DNP with O_3, •OH, and •NO_2)	radical addition and HAA,		Deleted
L422-L423 (3.1.2 Primary reactions of 2,4-DNP with O_3, •OH, and •NO_2)	During this process, the forming C3–O bond length gradually shortens, ultimately		Deleted
L425-L429 (3.1.2 Primary reactions of 2,4-DNP with O_3, •OH, and •NO_2)		unlike O_3 and •OH, whose reactivities are well correlated with the Δfω distribution, •NO_2 is primarily a radical species with only weak	Added

		electrophilic character. Its addition to the ring is therefore not simply governed by electrophile–nucleophile interactions, but rather by radical stability and transition-state polar effects. The	
L431-L433 (3.1.2 Primary reactions of 2,4-DNP with O_3, •OH, and •NO_2)	During this process, the breaking O–H bond is significantly elongated from 0.98 Å to 1.21 Å, while the newly formed H–ONO bond shortens from 1.08 Å to 0.97 Å.		Deleted
L441-L445 (3.1.2 Primary reactions of 2,4-DNP with O_3, •OH, and •NO_2)	Thus, the O–H bond is more readily cleaved than a C–H bond, making the hydroxyl hydrogen the preferred	In 2,4-DNP, the intramolecular hydrogen bond between the hydroxyl group and the ortho-nitro group	Changed

	abstraction site for $\bullet NO_2$.	significantly weakens the O–H bond, lowering its bond dissociation energy, which further favors hydroxyl hydrogen abstraction by $\bullet NO_2$.	
L446-L451 (3.1.2 Primary reactions of 2,4-DNP with O_3, •OH, and $\bullet NO_2$)	**Figure 3** Thermodynamics, kinetics, and temperature dependence of the reactions of 2,4-DNP with O_3, •OH, and $\bullet NO_2$. (a–c) reaction energy barriers ($\Delta E^{\neq}$) and reaction energies ($\Delta_r E$) for the key pathways (unit: kcal mol^{-1}). (d–e) Temperature-dependent	**Figure 3** Thermodynamics, kinetics, and temperature dependence of the reactions of 2,4-DNP with O_3, •OH, and $\bullet NO_2$. (a–c) reaction energy barriers ($\Delta E^{\neq}$) and reaction energies ($\Delta_r E$) for the key pathways (unit: kcal mol^{-1}). (d–e) intrinsic temperature-dependent	Changed

	reaction rate constants for the major channels.	reaction rate constants for the major channels.	
L476-L478 (3.1.2 Primary reactions of 2,4-DNP with O_3, •OH, and $•NO_2$)	strongly suggest that the direct transformation of 2,4-DNP initiated by $•NO_2$ is negligible under ambient atmospheric conditions	might suggest that the direct transformation of 2,4-DNP initiated by $•NO_2$ is negligible	Changed
L479-L494 (3.1.2 Primary reactions of 2,4-DNP with O_3, •OH, and $•NO_2$)	This multi-level distinction clarifies that while the direct reaction of $•NO_2$ with parent 2,4-DNP is negligible, the indirect pathways involving $•NO_2$ and oxidized intermediates or multiphase processes may still be	However, to provide a complete picture, it is useful to distinguish three distinct levels of $•NO_2$ involvement in the atmospheric chemistry of 2,4-DNP, a distinction that has been emphasized in recent multiphase	Changed

	environmentally relevant. Therefore, the atmospheric degradation of 2,4-DNP is expected to be dominated by oxidation processes initiated by •OH radicals and O_3.	studies(Rana et al., 2023). Level (i) is the direct reaction of •NO_2 with the parent compound 2,4-DNP, which we have shown to be kinetically negligible even under nighttime conditions (see pseudo-first-order analysis below). Level (ii) is the reaction of •NO2 with primary oxidation intermediates such as IM3' (Section 3.1.3), which exhibits a remarkably low barrier of 2.01 kcal mol^{-1} for HAA and represents a potentially important indirect nitration	

		pathway under high-NO_2 conditions. Level (iii) is the multiphase $•NO_2/O_3$ chemistry in aerosol water or microdroplets, where $•NO_2$ can participate through N_2O_4 uptake and hydrolysis, leading to nitration via NO_2+ or NO+ species(Rana et al., 2023).	
L495 (3.1.2 Primary reactions of 2,4-DNP with O_3, •OH, and $•NO_2$)		(Level ii)	Added
L495 (3.1.2 Primary reactions of 2,4-DNP with O_3, •OH, and		in Section 3.1.3	Added

•NO_2)			
L496 (3.1.2 Primary reactions of 2,4-DNP with O_3, •OH, and •NO_2)	of its environmental fate		Deleted
L536-L543 (3.1.2 Primary reactions of 2,4-DNP with O_3, •OH, and •NO_2)		**Table 1** Calculated energy barriers ($\Delta E^{\neq}$, kcal mol^{-1}), reaction energies ($\Delta_r E$, kcal mol^{-1}), and rate constants ($k$tot, cm^3 $molecule^{-1}$ s^{-1}) at 298.15 K for the representative reaction channels of 2,4-DNP with O_3, •OH, and •NO_2 in the gas and aqueous phases. "—" indicates that the rate constant was not calculated because the corresponding pathway	Added

		is kinetically insignificant (Complete rate constant data for all channels are provided in Table S3). *k*tot at 298.15 K for each oxidant is the sum of all contributing channels for that oxidant.	
L545-L548 (3.1.2 Primary reactions of 2,4-DNP with O_3, •OH, and •NO_2)	pathways are listed in Table S2. Specifically, the	pathways are compiled in Table 1, which summarizes the thermodynamic and kinetic data for O_3, •OH, and •NO_2 in both gas and aqueous phases. Several trends are evident from these data. The	Changed
L552-L553 (3.1.2 Primary reactions of	08	17	Changed

2,4-DNP with O_3, •OH, and $•NO_2$)			
L559-L562 (3.1.2 Primary reactions of 2,4-DNP with O_3, •OH, and $•NO_2$)	In summary, the atmospheric degradation of 2,4-DNP is kinetically dominated by •OH, with O_3 playing a significant role in the aqueous phase, while the direct trans-formation contribution of $•NO_2$ can be neglected in environmental assessments.		Deleted
L563-L607 (3.1.2 Primary reactions of 2,4-DNP with O_3, •OH, and $•NO_2$)		It should be emphasized that the trends described above, however, reflect only the intrinsic molecular reactivity of each	Added

		oxidant; their actual atmospheric importance depends on oxidant concentrations, phase partitioning, and aerosol liquid water content. To bridge this gap between intrinsic reactivity and atmospheric relevance, pseudo-first-order rate constants were estimated using literature-reported oxidant concentrations. These estimates are presented below, providing a more realistic assessment of the relative contributions of each	

		pathway under typical tropospheric conditions. The literature review indicates that •OH concentrations typically reach $1 \times 10^6 \sim 3 \times 10^6$ molecules cm^{-3}, while $\bullet NO_2$ levels are lower due to rapid photolysis under daytime conditions. During heavily polluted nighttime conditions, however, •OH concentrations drop substantially. Geyer et al.(Geyer et al., 2003) reported a nocturnal •OH concentration of $(1.85 \pm 0.82) \times 10^5$ cm^{-3} during the BERLIOZ	

		campaign, and in UK urban surface environments, night-time OH levels were determined to be in the range of 10^5 ~ 10^6 molecules cm^{-3}(Khan et al., 2011). Meanwhile, $•NO_2$ can accumulate significantly at night, with nocturnal maxima reaching 8.43 ± 0.4 ppb in Guangzhou(Qin et al., 2009). Using these literature-reported concentrations, the pseudo-first-order rate constants under nighttime conditions can be estimated. For	

		the •OH pathway, with kOH = 3.18 × 10^{-15} cm^3 $molecule^{-1}$ s^{-1} and [OH] ≈ 10^5 ~ 10^6 molecules cm^{-3}, k'OH ≈ 10^{-10} ~ 10^{-9} s^{-1}. For the direct •NO_2 pathway, with $k$$NO_2$ ≈ 10^{-28} cm^3 $molecule^{-1}$ s^{-1} and [NO_2] ≈ 10^{10} ~ 10^{11} molecules cm^{-3} (corresponding to 0.4 ~ 4 ppb at 298 K and 1 atm), k'NO_2 ≈ 10^{-18} ~ 10^{-17} s^{-1}. Even under the most favorable nighttime conditions (lowest •OH, highest •NO_2), the direct •NO_2 pathway remains more than 7 orders of	

		magnitude slower than the •OH pathway, corresponding to a lifetime of $>10^{10}$ s, which is negligible on atmospheric timescales. Therefore, while a full diurnal box model simulation would be required to quantify all pathways under varying pollution regimes, the quantitative analysis above confirms that the direct reaction of $•NO_2$ with parent 2,4-DNP is negligible even under nighttime conditions. The possible involvement of $•NO_2$ in subsequent reactions	

		with primary oxidation intermediates will be discussed separately to provide a complete mechanistic picture of its environmental fate. In summary, the atmospheric degradation of 2,4-DNP is kinetically dominated by •OH, with O_3 playing a significant role in the aqueous phase, while the direct transformation contribution of $•NO_2$ can be neglected in environmental assessments. The overall contribution of aqueous-phase	

		reactions to the atmospheric fate of 2,4-DNP depends critically on the fraction of the compound that partitions into the aqueous phase. For 2,4-DNP, the Henry's law constant has been determined as 5.70 × 10^{-8} atm·m^3/mol at 5 °C(Lüttke and Levsen, 1997), indicating a strong tendency to partition into the aqueous phase. The partitioning is further modulated by its acid dissociation constant (pKa ≈ 4.09 at 25 °C), as the	

		deprotonated phenolate form is substantially more water-soluble than the neutral phenol(Schwarzenbach et al., 1988). In addition, the aerosol liquid water content—which varies widely depending on relative humidity, particle composition, and atmospheric conditions—determines the available aqueous volume for multiphase reactions. Without quantitative information on these partitioning parameters under specific atmospheric	

		conditions, the aqueous-phase rate constants should be interpreted as intrinsic reactivity indicators rather than direct measures of atmospheric importance.	
L608 (3.1.2 Primary reactions of 2,4-DNP with O_3, •OH, and •NO_2)	1	2	Changed
L610-L615 (3.1.2 Primary reactions of 2,4-DNP with O_3, •OH, and •NO_2)	This study establishes the reliability of the theoretically derived rate constant for the reaction between 2,4-DNP and ozone through systematic	The calculated rate constants are further validated through systematic benchmarking against available experimental and computational data	Changed

	benchmarking against available experimental and computational data for structurally related aromatic compounds.	for structurally related aromatic compounds, as summarized in Table 2 and Table S4.	
L616-L617 (3.1.2 Primary reactions of 2,4-DNP with O_3, •OH, and •NO_2)	as summarized in Table 1		Deleted
L624-L630 (3.1.2 Primary reactions of 2,4-DNP with O_3, •OH, and •NO_2)	This result is consistent with established activity trends of nitro-substituted aromatic systems, thereby supporting the reasonableness of the calculated rate constant.	This trend is consistent with the established understanding of substituent effects in phenolic oxidation: electron-donating groups such as –CH_3 and –OCH_3 enhance reactivity(Pillar et al., 2014; Pillar et al., 2015; Pillar-Little and	Changed

		Guzman, 2017; Rana and Guzman, 2020), while electron-withdrawing nitro groups deactivate the aromatic ring toward electrophilic attack.	
L649 (3.1.3 The subsequent reactivity mechanism of the key intermediate IM3')	O_2 as well as	both O_2 and	Changed
L654 (3.1.3 The subsequent reactivity mechanism of the key intermediate IM3')	prime		Deleted
L656-L657		(hydrogen abstraction at	Added

(3.1.3 The subsequent reactivity mechanism of the key intermediate IM3’)		C3)	
L666 (3.1.3 The subsequent reactivity mechanism of the key intermediate IM3’)	to approximately 1.17 Å	significantly	Changed
L667-L668 (3.1.3 The subsequent reactivity mechanism of the key intermediate IM3’)	to about 1.30 Å.	accordingly, indicating synchronous bond breaking and bond forming	Changed
L673 (3.1.3 The subsequent reactivity mechanism of	relatively electron-rich		Deleted

the key intermediate IM3’)			
L680 (3.1.3 The subsequent reactivity mechanism of the key intermediate IM3’)	similar		Deleted
L683-L684 (3.1.3 The subsequent reactivity mechanism of the key intermediate IM3’)	which both involve the oxidant abstracting	, in which the oxidant abstracts	Changed
L686 (3.1.3 The subsequent reactivity mechanism of the key intermediate IM3’)	channel RI*	RI* channel	Changed
L688	relatively electron		Deleted

(3.1.3 The subsequent reactivity mechanism of the key intermediate IM3')	dense		
L690-L691 (3.1.3 The subsequent reactivity mechanism of the key intermediate IM3')		, within the $\bullet NO_2$ reaction system,	Added
L691 (3.1.3 The subsequent reactivity mechanism of the key intermediate IM3')	path	pathway	Changed
L692 (3.1.3 The subsequent reactivity mechanism of	the HAA mechanism	HAA	Changed

the key intermediate IM3')			
L694-L725 (3.1.3 The subsequent reactivity mechanism of the key intermediate IM3')	The above computational results elucidate, at the microscopic mechanistic level, the possible pathways of IM3' with O_2 and $\bullet NO_2$. However, to assess its ultimate fate in the real atmospheric, it is necessary to further consider the competition between these oxidants under realistic atmospheric concentrations. In particular, the large concentration difference between O_2	This corresponds to Level (ii) of $\bullet NO_2$ involvement as distinguished in Section 3.1.2: the reaction of $\bullet NO_2$ with a primary oxidation intermediate. While O_2 dominates the overall fate of IM3' due to its concentration advantage (see below), the low barrier for the $\bullet NO_2$ + IM3' HAA pathway (2.01 kcal mol^{-1}) suggests that nitration via this indirect route could be significant under elevated $\bullet NO_2$	Changed

	and •NO_2 must be taken into account when evaluating the dominant degradation channels and their environmental significance.	conditions, such as in polluted urban plumes at night. It should be emphasized that the competition between O_2 and •NO_2 for IM3' must be evaluated based on effective rates (k × [oxidant]) rather than second-order rate constants alone. The atmospheric concentration of O_2 is 5.4×10^{18} molecules cm^{-3} (0.21 atm). For the reaction of IM3' with O_2 via HAA (barrier = 2.86 kcal mol^{-1}), the barrier height indicates that the reaction is near	

		the gas-kinetic limit, with rate constants for alkyl radical + O_2 reactions typically in the range of 10^{-12} ~ 10^{-11} cm^3 $molecule^{-1}$ s^{-1}(Miyoshi et al., 1990; Morgan et al., 1982). Taking a conservative estimate of $kO_2 \approx 10^{-12}$ cm^3 $molecule^{-1}$ s^{-1}, the effective rate is $k'O_2 \approx 10^{-12} \times 5.4 \times 10^{18} \approx 5.4 \times 10^6$ s^{-1}, corresponding to a lifetime of 0.2 microseconds—consistent with the well-established behavior that alkyl radicals react with O_2 on timescales of 10 ~	

		100 nanoseconds(Vereecken and Francisco, 2012; Calvert et al., 2015). For the reaction of IM3' with $\bullet NO_2$ via HAA (barrier = 2.01 kcal mol^{-1}), even under the most favorable nighttime conditions with $[\bullet NO_2] \approx 10^{10} \sim 10^{11}$ molecules cm^{-3}, and taking $kNO_2 \approx 10^{-11}$ cm^3 $molecule^{-1}$ s^{-1}, the effective rate is $k'NO_2 \approx 10^{-1} \sim 1$ s^{-1}, corresponding to a lifetime of 1 ~ 10 seconds. Thus, $k'O_2$ is more than 6 orders of magnitude faster than	

		k'NO_2. The overwhelming concentration advantage of O_2—more than 10^7 times that of $•NO_2$—ensures that the reaction of IM3' with O_2 is the dominant atmospheric fate of this intermediate. This is fully consistent with the established behavior that addition of O_2 is essentially the sole atmospheric fate of organic radicals formed during the oxidation of organic compounds(Calvert et al., 2015).	

L732-L735 (3.2. Molecular dynamics)		The results obtained with this surrogate provide molecular-level insights into specific interaction mechanisms, but should not be directly extrapolated to real atmospheric aerosols without considering the additional complexity of real particle surfaces.	Added
L739-L740 (3.2. Molecular dynamics)	Figure 5	Figure 5	Changed
L745 (3.2. Molecular dynamics)	Independent Gradient Model	IGM	Changed
L759 (3.2. Molecular dynamics)	dominant	dominate	Changed
L763 (3.2. Molecular dynamics)	e		Deleted

L764 (3.2. Molecular dynamics)	C	O	Changed
L785-L786 (3.2. Molecular dynamics)		investigate	Added
L805-L806 (3.2. Molecular dynamics)	steric hindrance effects	competitive solvation	Changed
L816 (3.2. Molecular dynamics)		may	Added
L834-L849 (3.2. Molecular dynamics)		The MD simulations presented here are limited to molecular-scale adsorption behavior in the idealized C60/water/2,4-DNP system. The results provide insights into how hydration modulates specific non-covalent	Added

		interactions, but they do not account for key aerosol properties that control humidity effects in real atmospheric particles—including liquid water content, ionic strength, phase behavior, viscosity, and particle morphology. These properties can vary substantially with relative humidity, particle composition, and atmospheric conditions, and they collectively determine the physical state and water uptake of aerosol particles. Their absence in the current model	

		means that the simulated hydration effects represent a simplified scenario that may not fully capture the complexity of real aerosol surfaces. Consequently, the MD results should be interpreted as molecular-scale insights into adsorption behavior under idealized conditions, rather than as direct predictions of atmospheric persistence or humidity-dependent partitioning. Quantitative assessments of	

		atmospheric residence time, gas–particle partitioning, or long-range transport would require additional modeling that incorporates these aerosol properties and atmospheric transport processes, and are beyond the scope of the present study.	
L853 (3.3 Ecotoxicity assessment)		clear	Added
L854-L855 (3.3 Ecotoxicity assessment)	the oxidant with of high environmental relevance,	one of the key atmospheric oxidants	Changed
L857 (3.3 Ecotoxicity assessment)	Can provide a crucial	may serve a useful	Changed
L862-L871 (3.3 Ecotoxicity		A conceptual mass-fate	Added

assessment)		diagram integrating the DFT kinetics, MD adsorption, and QSAR toxicity predictions is provided in Figure S3 to illustrate the overall atmospheric transformation framework of 2,4-DNP. Parent 2,4-DNP undergoes gas-aqueous partitioning controlled by Henry's law and participates in three parallel transformation pathways: gas-phase oxidation, bulk aqueous-phase oxidation, and heterogeneous reactions at the gas-aqueous	

		interface revealed by MD simulations. Oxidation pathways calculated by DFT generate key intermediates IM3’ and IM17. These intermediates further transform into a series of products, and the Ames mutagenicity and developmental toxicity of transformation products are evaluated via yield-weighted QSAR prediction.	
L880 (3.3 Ecotoxicity assessment)	4	5	Changed
L900-L918 (3.3 Ecotoxicity assessment)		To further assess the reliability of the QSAR predictions, an	Added

		independent cross-validation was performed using Toxtree (version 3.1.0)(Patlewicz et al., 2008). For Ames mutagenicity, Toxtree's Benigni/Bossa rulebase was employed, which uses rule-based structural alerts that are algorithmically distinct from the statistical consensus method used in T.E.S.T(Benigni et al., 2007). The cross-validation results (Table S5) show consistent predictions for the majority of compounds, with	

		deviations observed only for compounds with probability scores close to the classification threshold. For developmental toxicity, Toxtree does not provide a dedicated prediction model. Instead, we employed its Cramer decision tree to perform a toxicological concern threshold (TTC)-based classification. The Cramer decision tree classifies compounds into three classes based on their chemical structure: Class I (low toxicity concern), Class	

		II (moderate toxicity concern), and Class III (high toxicity concern)(Cramer et al., 1976). Class III compounds are assigned the lowest TTC value (90 μg person^{-1} day^{-1})(Munro et al., 1996), indicating the highest potential for adverse health effects, including developmental toxicity. As shown in Table S5, all 2,4-DNP and its ozonolysis products were classified as Cramer Class III, consistent with the T.E.S.T. predictions	

		that all compounds exhibit developmental toxicity potential. This approach follows established practices in computational toxicology for the developmental toxicity screening of nitro-organic compounds(Yong-Di et al., 2022).	
L919-L727 (3.3 Ecotoxicity assessment)	The QSAR models utilized in this study provide valuable preliminary information for risk prioritization, the inherent uncertainties associated with in silico predictions must be	The toxicity predictions presented here are screening level assessments based on QSAR models. They are intended for hazard prioritization and hypothesis generation, not as definitive	Changed

	acknowledged. The predictive performance is fundamentally constrained by the chemical space of the training sets and the defined applicability domains.	toxicological conclusions. Several factors limit their predictive re-liability. First, QSAR model performance is constrained by the chemical space of training sets and the defined applicability domains.	
L928 (3.3 Ecotoxicity assessment)		predicted	Added
L928 (3.3 Ecotoxicity assessment)	are lower	of the predictions may be diminished	Changed
L929-L932 (3.3 Ecotoxicity assessment)		As highlighted by the Ames/QSAR International Challenge Projects, even the best performing models	Added

		achieve a balanced accuracy of approximately 76.9 % at 100 % coverage(Uesawa, 2024).	
L932 (3.3 Ecotoxicity assessment)	In addition	Second	Changed
L933 (3.3 Ecotoxicity assessment)		the classification	Added
L935-L937 (3.3 Ecotoxicity assessment)	These compounds should therefore be regarded as high-priority targets for experimental validation.		Deleted
L938-L941 (3.3 Ecotoxicity assessment)		While a quantitative weight of evidence (qWoE) approach has been shown to achieve accuracy comparable to	Added

		experimental Ames tests(Tintó-Moliner and Martin, 2020), such approaches are beyond the scope of this screening level study.	
L941 (3.3 Ecotoxicity assessment)	Therefore, the present	Overall, the	Changed
L942-L943 (3.3 Ecotoxicity assessment)	rather than definitive—Future studies are recommended to validate these predictions	(Vom Eyser et al., 2013). Experimental validation	Changed
L944-L946 (3.3 Ecotoxicity assessment)	experiments, and to develop targeted removal strategies for toxic nitrocarbonyl-type products.	toxicity assays—is recommended for the high-priority compounds identified here.	Changed
L947 (4 Conclusions)	Conclusion	Conclusions	Changed

L952-L954 (4 Conclusions)	•OH and O_3; oxidation pathways, while direct reaction with •NO_2	the •OH pathway in the gas phase, while O_3 plays a significant role in the aqueous phase; the direct reaction of •NO_2 with the parent compound	Changed
L955-L958 (4 Conclusions)		, although reactions of •NO_2 with oxidation intermediates (barrier as low as 2.01 kcal mol^{-1}) and multiphase •NO_2/O_3 chemistry represent distinct pathways that may be environmentally relevant under certain conditions	Added
L961 (4 Conclusions)	atmospheric particle	the idealized C60 aerosol	Changed

L963-L972 (4 Conclusions)	Under low-hydration conditions, solute-particle interactions are enhanced, while under high-hydration conditions, adsorption is weakened due to competitive binding and steric hindrance effects from water molecules; and ozonolysis of 2,4-DNP does not lead to harmless degradation but generates secondary products with significantly increased mutagenicity and developmental toxicity. Collectively, 2,4-DNP is a relatively persistent	with enhanced solute-particle interactions under low-hydration conditions and weakened adsorption under high-hydration and QSAR predictions indicate that certain ozonolysis products exhibit elevated Ames mutagenicity and developmental toxicity indicators relative to the parent compound.	Changed

	pollutant whose atmospheric lifetime depends strongly on humidity and whose oxidation does not detoxify but rather amplifies environmental risk.		
L975-L976 (4 Conclusions)	reveals that ozonolysis increases toxicity	predicts that ozonolysis products may exhibit increased toxicity indicators	Changed
L977-L981 (4 Conclusions)		that oxidative degradation necessarily leads to detoxification. While the quantitative conclusions apply specifically to 2,4-DNP, the qualitative framework established here—linking	Added

		substituent electronic effects to reaction kinetics, interfacial behavior, and toxicity indicators—may serve as a reference for understanding related nitroaromatic systems.	
L982-L1008 (4 Conclusions)	Several limitations should be noted: the aerosol surrogate (C60) and QSAR toxicity models do not fully capture real atmospheric particle complexity or definitive toxicological outcomes; experimental validation via in vitro and in vivo assays is needed. Despite these cave-ats,	Several limitations should be noted: the aerosol surrogate (C60), while useful for isolating specific non-covalent interactions, does not capture the full chemical complexity of real atmospheric particle—particularly the presence of oxygen-containing	Changed

	our findings have clear implications for atmospheric chemistry and climate. The humidity-dependent adsorption behavior implies that 2,4-DNP may have longer residence time and greater long-range transport under dry conditions, affecting its global distribution. Moreover, the production of toxic transformation products suggests that current air quality models may underestimate the health risks of nitrophenolic	functional groups, surface defects, heteroatoms, and transition metals that may influence reactivity and product formation. As a result, the C60 model may overestimate the contribution of π-π interactions and underestimate the role of polar interactions. The 1 ns MD timescale is sufficient for the rigid C60/small molecule system studied here, but longer simulations and polarizable force fields may be needed to capture slower	

	emissions. Regulatory attention to 2,4-DNP and its derivatives is therefore warranted.	dynamical processes on more complex surfaces. The QSAR toxicity predictions are screening-level estimates requiring experimental validation. A full diurnal box model simulation incorporating temporally resolved oxidant concentrations, Henry's law partitioning, and aerosol liquid water content would be needed to fully quantify the atmospheric importance of each pathway under realistic conditions.	

		Additionally, downstream multiphase aging processes such as oligomerization or metal-catalyzed reactions, which may influence the fate of phenolic compounds in real atmospheric particles, were not addressed in this study and would require complementary experimental and modeling approaches. Future complementary simulations using more realistic carbon models, such as amorphous carbon clusters or graphene with	

		functional groups, would be valuable to validate the trends identified here.	
L1009-L1026 (4 Conclusions)		Based on these findings, we recommend the following directions for future research: (i) Experimental validation of predicted kinetics: Advanced kinetic techniques such as laser-induced fluorescence or cavity ring-down spectroscopy should be employed to measure the rate constants for the reactions of 2,4-DNP with O_3 and •OH,	Added

		providing direct experimental confirmation of the theoretical trends. (ii) In vitro toxicity testing: The high-priority ozonolysis products identified in this study (IM54, P1, and P2) should be subjected to Ames mutagenicity assays and zebrafish embryo developmental toxicity tests to validate the QSAR predictions. (iii) Refined interfacial models: Complementary MD simulations using more realistic carbonaceous models, such as	

		functionalized graphene or amorphous carbon clusters, would help assess the influence of surface functional groups and defects on the adsorption behavior of 2,4-DNP. (iv) Diurnal box model simulations: Full diurnal chemical box models incorporating temporally resolved oxidant concentrations, Henry's law partitioning, and aerosol liquid water content are needed to fully quantify the atmospheric importance of each oxidation	

		pathway under different pollution regimes. Despite these caveats, the mechanistic insights into the molecular-level reactivity and interfacial behavior of 2,4-DNP provide a foundation for future experimental and modeling studies on the multiphase fate of nitrophenolic compounds.	
L1045–L1638 (References)		Al-Abadleh et al. (2022); Andreae and Gelencsér (2006); Bejan et al. (2007); Benigni et al. (2007); Calvert et al. (2015); Cornelissen et al.	Added

		(2005); Cramer et al. (1976); Decesari et al. (2018); Geyer et al. (2003); Guzman et al. (2022); Hems and Abbatt (2018); Khan et al. (2011); Lindorff-Larsen et al. (2010); Lüttke and Levsen (1997); Mayer (2011); Miyoshi et al. (1990); Morgan et al. (1982); Munro et al. (1996); Ng et al. (2017); Patlewicz et al. (2008); Pillar-Little and Guzman (2017); Pillar-Little and Guzman (2018); Pillar-Little et al. (2014); Poster et al.	

		(2007); Qin et al. (2009); Rana and Guzman (2020); Rana and Guzman (2022a); Rana and Guzman (2022b); Rana et al. (2023); Schwarzenbach et al. (1988); Tintó-Moliner and Martin (2020); Uesawa (2024); Vereecken and Francisco (2012); Wang et al. (2004); Witt et al. (2025); Yong-di et al. (2022)	
L2-L5 (Supplement)	Unveiling the multiphase fate of 2,4-dinitrophenol on aerosols: Interfacial hydration governs competing oxidation	Unveiling the multiphase fate of 2,4-dinitrophenol on aerosols: Interfacial hydration modulates competing oxidation	Changed

	pathways and unexpected toxicity amplification	pathways and predicted increase in toxicity	
L27-L28 (Supplement)		**Table S2** Optimized bond lengths (Å) of the stationary points along the O_3, •OH, •NO_2 and IM3' reaction pathways of 2,4-DNP.	Added
L30 (Supplement)	S2	S3	Changed
L35 (Supplement)	S3;116	S4;11	Changed
L38 (Supplement)	S2	S3	Changed
L39-L43 (Supplement)	**Table S4** The Ames mutagenicity, development toxicity for 2,4-DNP and the intermediates (IMs series) and final products (Ps series)	**Table S5** Cross-validation of Ames mutagenicity, development toxicity for 2,4-DNP and the intermediates (IMs series) and final products (Ps series) using T.E.S.T. and Toxtree. "ND" = not detected (negative), "D" = detected	Changed

		(positive), “NA” = not applicable/outside applicability domain. Cramer Class III indicates the highest priority for toxicity concern.	
L47-L52 (Supplement)		**Figure S3** Conceptual mass-fate diagram of 2,4-DNP in the atmosphere, integrating DFT kinetics, MD adsorption, and QSAR toxicity predictions. The diagram illustrates gas-aqueous partitioning, parallel transformation pathways (gas-phase oxidation, aqueous-phase oxidation, and heterogeneous	Added

		reactions), and the toxicity evaluation of transformation products.	

Ahmaruzzaman, M., Mishra, S. R., Gadore, V., Yadav, G., Roy, S., Bhattacharjee, B., Bhuyan, A., Hazarika, B., Darabdhara, J., and Kumari, K.: Phenolic compounds in water: From toxicity and source to sustainable solutions - An integrated review of removal methods, advanced technologies, cost analysis, and future prospects, Journal of Environmental Chemical Engineering, 12, 10.1016/j.jece.2024.112964, 2024.

Al-Abadleh, H. A., Motaghedi, F., Mohammed, W., Rana, M. S., Malek, K. A., Rastogi, D., Asa-Awuku, A. A., and Guzman, M. I.: Reactivity of aminophenols in forming nitrogen-containing brown carbon from iron-catalyzed reactions, Commun Chem, 5, 112, 10.1038/s42004-022-00732-1, 2022.

Albinet, A., Minero, C., and Vione, D.: Phototransformation processes of 2,4-dinitrophenol, relevant to atmospheric water droplets, Chemosphere, 80, 753-758, 10.1016/j.chemosphere.2010.05.016, 2010.

Andreae, M. O. and Gelencsér, A.: Black carbon or brown carbon? The nature of light-absorbing carbonaceous aerosols, Atmos. Chem. Phys., 6, 3131-3148, 10.5194/acp-6-3131-2006, 2006.

Athar, M. and Patnaik, A.: Through-Bond-Driven Through-Space Interactions in a Fullerene C60 Noncovalent Dyad: An Unusual Strong Binding between Spherical and Planar π Electron Clouds and Culmination of Dyadic Fractals, Journal of Physical Chemistry A, 126, 3629-3641, 10.1021/acs.jpca.1c10828, 2022.

Atkinson, R., Tuazon, E. C., Wallington, T. J., Aschmann, S. M., Arey, J., Winer, A. M., and Pitts, J. N.: Atmospheric chemistry of aniline, N, N-dimethylaniline, pyridine, 1,3,5-triazine, and nitrobenzene, Environmental Science & Technology, 21, 64-72, 10.1021/es00155a007, 1987.

Barton, D. H. R. and Cookson, R. C.: The Principles of Conformational Analysis, Quarterly Reviews, 10, 44-82, 10.1039/qr9561000044, 1956.

Bejan, I., Barnes, I., Olariu, R., Zhou, S., Wiesen, P., and Benter, T.: Investigations on the gas-phase photolysis and OH radical kinetics of methyl-2-nitrophenols, Physical Chemistry Chemical Physics, 9, 5686-5692, 10.1039/b709464g, 2007.

Benfenati, E., Benigni, R., DeMarini, D. M., Helma, C., Kirkland, D., Martin, T. M., Mazzatorta, P., Ouédraogo-Arras, G., Richard, A. M., Schilter, B., Schoonen, W., Snyder, R., and Yang, C.: Predictive Models for Carcinogenicity and Mutagenicity: Frameworks, State-of-the-Art, and Perspectives, Journal of Environmental Science and Health Part C-Environmental Carcinogenesis & Ecotoxicology Reviews, 27, 57-90, 10.1080/10590500902885593, 2009.

Benigni, R., Bossa, C., Netzeva, T., Rodomonte, A., and Tsakovska, I.: Mechanistic QSAR of aromatic amines: new models for discriminating between homocyclic mutagens and nonmutagens, and validation of models for carcinogens, Environ Mol Mutagen, 48, 754-771, 10.1002/em.20355, 2007.

Calvert, J. G., Orlando, J. J., Stockwell, W. R., and Wallington, T. J.: The Mecha-nisms of Reactions Influencing Atmospheric Ozone, Oxford University Press, 10.1093/oso/9780190233020.001.0001, 2015.

Canneaux, S., Bohr, F., and Henon, E.: KiSThelP: A Program to Predict Thermodynamic Properties and Rate Constants from Quantum Chemistry Results, Journal of Computational Chemistry, 35, 82-93, 10.1002/jcc.23470, 2014.

Cassano, A., Manganaro, A., Martin, T., Young, D., Piclin, N., Pintore, M., Bigoni, D., and Benfenati, E.: CAESAR models for developmental toxicity, Chemistry Central Journal, 4, 10.1186/1752-153x-4-s1-s4, 2010.

Chapleski, R. C., Zhang, Y. F., Troya, D., and Morris, J. R.: Heterogeneous chemistry and reaction dynamics of the atmospheric oxidants, O3, NO3, and OH, on organic surfaces, Chemical Society Reviews, 45, 3731-3746, 10.1039/c5cs00375j, 2016.

Cornelissen, G., Gustafsson, O., Bucheli, T. D., Jonker, M. T. O., Koelmans, A. A., and M van Noort, P. C.: Extensive sorption of organic compounds to black carbon, coal, and kerogen in sediments and soils: mechanisms and consequences for distribution, bioaccumulation, and biodegradation, Environmental Science and Technology, 39, 10.1021/es050191b, 2005.

Cramer, G. M., Ford, R. A., and Hall, R. L.: Estimation of toxic hazard—A decision tree approach, Food and Cosmetics Toxicology, 16, 255-276, https://doi.org/10.1016/S0015-6264(76)80522-6, 1976.

Decesari, S., Kovarich, S., Pavan, M., Bassan, A., Ciacci, A., and Topping, D.: Evaluating the mutagenic potential of aerosol organic compounds using informatics-based screening, Atmos. Chem. Phys., 18, 2329-2340, 10.5194/acp-18-2329-2018, 2018.

Delaria, E. R. and Cohen, R. C.: Measurements of Atmosphere-Biosphere Exchange of Oxidized Nitrogen and Implications for the Chemistry of Atmospheric NOx, Accounts of Chemical Research, 56, 1720-1730, 10.1021/acs.accounts.3c00090, 2023.

EPA, U. S.: User's Guide for T.E.S.T. (version 5.1) (Toxicity Estimation Software Tool): A Program to Estimate Toxicity from Molecular Structure., U.S. Environmental Protection Agency, 2020.

Fan, W. L., Chen, T., Zhu, Z. L., Zhang, H., Qiu, Y. L., and Yin, D. Q.: A review of secondary organic aerosols formation focusing on organosulfates and organic nitrates, Journal of Hazardous Materials, 430, 10.1016/j.jhazmat.2022.128406, 2022.

Frisch, M. J., Trucks, G. W., Schlegel, H. B., Scuseria, G. E., Robb, M. A., Cheeseman, J. R., Scalmani, G., Barone, V., Petersson, G. A., Nakatsuji, H., Li, X., Caricato, M., Marenich, A. V., Bloino, J., Janesko, B. G., Gomperts, R., Mennucci, B., Hratchian, H. P., Ortiz, J. V., Izmaylov, A. F., Sonnenberg, J. L., Williams, Ding, F., Lipparini, F., Egidi, F., Goings, J., Peng, B., Petrone, A., Henderson, T., Ranasinghe, D., Zakrzewski, V. G., Gao, J., Rega, N., Zheng, G., Liang, W., Hada, M., Ehara, M., Toyota, K., Fukuda, R., Hasegawa, J., Ishida, M., Nakajima, T., Honda, Y., Kitao, O., Nakai, H., Vreven, T., Throssell, K., Montgomery Jr., J. A., Peralta, J. E., Ogliaro, F., Bearpark, M. J., Heyd, J. J., Brothers, E. N., Kudin, K. N., Staroverov, V. N., Keith, T. A., Kobayashi, R., Normand, J., Raghavachari, K., Rendell, A. P., Burant, J. C., Iyengar, S. S., Tomasi, J., Cossi, M., Millam, J. M., Klene, M., Adamo, C., Cammi,

R., Ochterski, J. W., Martin, R. L., Morokuma, K., Farkas, O., Foresman, J. B., and Fox, D. J.: Gaussian 16 Rev. C.01, 2016.

Geyer, A., Bächmann, K., Hofzumahaus, A., Holland, F., Stefan, Konrad, Klüpfel, T., Pätz, H. W., Perner, D., Mihelcic, D., Schäfer, H. J., Volz-Thomas, A., and Platt, U.: Nighttime formation of peroxy and hydroxyl radicals during the BERLIOZ campaign: Observations and modeling studies, Journal of Geophysical Research, 108, 8249, 2003.

Grundlingh, J., Dargan, P. I., El-Zanfaly, M., and Wood, D. M.: 2,4-dinitrophenol (DNP): a weight loss agent with significant acute toxicity and risk of death, J Med Toxicol, 7, 205-212, 10.1007/s13181-011-0162-6, 2011.

Guzman, M. I., Pillar-Little, E. A., and Eugene, A. J.: Interfacial Oxidative Oligomerization of Catechol, ACS Omega, 7, 36009-36016, 10.1021/acsomega.2c05290, 2022.

Hems, R. F. and Abbatt, J. P. D.: Aqueous Phase Photo-oxidation of Brown Carbon Nitrophenols: Reaction Kinetics, Mechanism, and Evolution of Light Absorption, ACS Earth and Space Chemistry, 2, 225-234, 10.1021/acsearthspacechem.7b00123, 2018.

Hu, W., Liu, D. D., Su, S. H., Ren, L. J., Ren, H., Wei, L. F., Yue, S. Y., Xie, Q. R., Zhang, Z. M., Wang, Z. H., Yang, N., Wu, L. B., Deng, J. J., Qi, Y. L., and Fu, P. Q.: Photochemical Degradation of Organic Matter in the Atmosphere, Advanced Sustainable Systems, 5, 10.1002/adsu.202100027, 2021.

Humphrey, W., Dalke, A., and Schulten, K.: VMD: Visual molecular dynamics, Journal of Molecular Graphics, 14, 33-38, https://doi.org/10.1016/0263-7855(96)00018-5, 1996.

Khan, M. A. H., Hoque, M. M. N., Alam, S. S., Ashfold, M. J., Nickless, G., and Shallcross, D. E.: Estimation and comparison of night-time OH levels in the UK urban atmosphere using two different analysis methods, Journal of Environmental Sciences, 23, 60-64, https://doi.org/10.1016/S1001-0742(10)60373-7, 2011.

Kroll, J. H. and Seinfeld, J. H.: Chemistry of secondary organic aerosol: Formation and evolution of low-volatility organics in the atmosphere, Atmospheric Environment, 42, 3593-3624, 10.1016/j.atmosenv.2008.01.003, 2008.

Kromann, J. C., Steinmann, C., and Jensen, J. H.: Improving solvation energy predictions using the SMD solvation method and semiempirical electronic structure methods, Journal of Chemical Physics, 149, 10.1063/1.5047273, 2018.

Lee, D., Schwegler, E., and Kanai, Y.: Dependence of Water Dynamics on Molecular Adsorbates near Hydrophobic Surfaces: First-Principles Molecular Dynamics Study, Journal of Physical Chemistry C, 118, 8508-8513, 10.1021/jp502850k, 2014.

Lefebvre, C., Rubez, G., Khartabil, H., Boisson, J. C., Contreras-García, J., and Hénon, E.: Accurately extracting the signature of intermolecular interactions present in the NCI plot of the reduced density gradient versus electron density, Physical Chemistry Chemical Physics, 19, 17928-17936, 10.1039/c7cp02110k, 2017.

Li, J., Han, Z. W., Sun, Y. L., Li, J. W., and Liang, L.: Chemical formation pathways of secondary organic aerosols in the Beijing-Tianjin-Hebei region in wintertime, Atmospheric Environment, 244, 10.1016/j.atmosenv.2020.117996, 2021.

Li, J., Han, Z. W., Wu, J., Tao, J., Li, J. W., Sun, Y. L., Liang, L., Liang, M. J., and Wang, Q. G.: Secondary organic aerosol formation and source contributions over east China in summertime, Environmental Pollution, 306, 10.1016/j.envpol.2022.119383, 2022a.

Li, M., Wang, X. F., Lu, C. Y., Li, R., Zhang, J., Dong, S. W., Yang, L. X., Xue, L. K., Chen, J. M., and Wang, W. X.: Nitrated phenols and the phenolic precursors in the atmosphere in urban Jinan, China, Science of the Total Environment, 714, 10.1016/j.scitotenv.2020.136760, 2020.

Li, M., Wang, X. F., Zhao, Y. N., Du, P., Li, H. Y., Li, J. R., Shen, H. Q., Liu, Z. Y., Jiang, Y. R., Chen, J., Bi, Y. J., Zhao, Y., Xue, L. K., Wang, Y., Chen, J. M., and Wang, W. X.: Atmospheric Nitrated Phenolic Compounds in Particle, Gaseous, and Aqueous Phases During Cloud Events at a Mountain Site in North China: Distribution

Char-acteristics and Aqueous-Phase Formation, Journal of Geophysical Re-search-Atmospheres, 127, 10.1029/2022jd037130, 2022b.

Li, P. Y., Feng, L., Li, G. Y., and Bai, F. Q.: Effects of Electron Donating Ability of Substituents and Molecular Conjugation on the Electronic Structures of Organic Radicals, Chemical Research in Chinese Universities, 39, 202-207, 10.1007/s40242-023-2364-2, 2023.

Lindorff-Larsen, K., Piana, S., Palmo, K., Maragakis, P., Klepeis, J. L., Dror, R. O., and Shaw, D. E.: Improved side-chain torsion potentials for the Amber ff99SB protein force field, Proteins, 78, 1950-1958, 10.1002/prot.22711, 2010.

Liu, X. H., Meng, T. T., Bai, F. Y., Ni, S., and Zhao, Z.: Theoretical investigation on the atmospheric degradation mechanism, kinetics, and fate of hydroxymethyl nitrate initiated by OH radicals, New Journal of Chemistry, 47, 11414-11424, 10.1039/d3nj01628e, 2023.

Liu, Z. Y. and Lu, T.: Theoretical Insight into Complexation Between Cyclocarbons and C60 Fullerene, Chemistry-a European Journal, 30, 10.1002/chem.202402227, 2024.

Lu, T., TST calculator, http://sobereva.com/310 (accessed 12 11, 2025).

Lu, T., Sobtop, Version [1.0], http://sobereva.com/soft/Sobtop (accessed on 17 01 2026).

Lu, T. and Chen, F. W.: Multiwfn: A multifunctional wavefunction analyzer, Journal of Computational Chemistry, 33, 580-592, 10.1002/jcc.22885, 2012.

Lu, T. and Chen, Q. X.: Independent gradient model based on Hirshfeld partition: A new method for visual study of interactions in chemical systems, Journal of Computational Chemistry, 43, 539-555, 10.1002/jcc.26812, 2022.

Lüttke, J. and Levsen, K.: Phase partitioning of phenol and nitrophenols in clouds, Atmospheric Environment, 31, 2649-2655, https://doi.org/10.1016/S1352-2310(96)00228-2, 1997.

Lyu, Y., Xu, H., Yuan, H. X., Cui, Y. L., Zhang, C. Z., and Meng, Q. T.: Intermolecular interaction mechanisms between dinitrophenol and water: a molecular

dynamics and DFT study, European Physical Journal Plus, 140, 10.1140/epjp/s13360-025-06478-8, 2025.

Maeda, S., Harabuchi, Y., Ono, Y., Taketsugu, T., and Morokuma, K.: Intrinsic Reaction Coordinate: Calculation, Bifurcation, and Automated Search, International Journal of Quantum Chemistry, 115, 258-269, 10.1002/qua.24757, 2015.

Mahilang, M., Deb, M. K., and Pervez, S.: Biogenic secondary organic aerosols: A review on formation mechanism, analytical challenges and environmental impacts, Chemosphere, 262, 10.1016/j.chemosphere.2020.127771, 2021.

Mangotra, A. and Singh, S. K.: Volatile organic compounds: A threat to the environment and health hazards to living organisms - A review, Journal of Biotechnology, 382, 51-69, 10.1016/j.jbiotec.2023.12.013, 2024.

Mao, Y. F., Qin, H., Huang, W. X., Lei, Y. S., Gao, X. J., Zhou, T. H., Wu, D. L., and Xu, L. Q.: Toward an atomic-scale understanding of competitive adsorption between ions and molecules near aqueous interfaces, Chemical Engineering Journal, 495, 10.1016/j.cej.2024.153699, 2024.

Mayer, J. M.: Understanding hydrogen atom transfer: from bond strengths to Marcus theory, Accounts of chemical research, 44, 36-46, 10.1021/ar100093z, 2011.

McNeill, V. F.: Atmospheric Aerosols: Clouds, Chemistry, and Climate, Annual Re-view of Chemical and Biomolecular Engineering, 8, 10.1146/annurev-chembioeng-060816-101538, 2017.

Miyoshi, A., Matsui, H., and Washida, N.: Rates of reaction of hydroxyalkyl radicals with molecular oxygen, The Journal of Physical Chemistry, 94, 3016-3019, 1990.

Morgan, C. A., Pilling, M. J., Tulloch, J. M., Ruiz, R. P., and Bayes, K. D.: Direct de-termination of the equilibrium constant and thermodynamic parameters for the reaction allyl radical + oxygen ⇌ allylperoxy radical, ChemInform, 13, 1982.

Munro, I. C., Ford, R. A., Kennepohl, E., and Sprenger, J. G.: Correlation of structural class with no-observed-effect levels: A proposal for establishing a threshold of concern, Food and Chemical Toxicology, 34, 829-867, https://doi.org/10.1016/S0278-6915(96)00049-X, 1996.

Nagy, P. R.: State-of-the-art local correlation methods enable affordable gold standard quantum chemistry for up to hundreds of atoms, Chem Sci, 15, 14556-14584, 10.1039/d4sc04755a, 2024.

Ng, N. L., Brown, S. S., Archibald, A. T., Atlas, E., Cohen, R. C., Crowley, J. N., Day, D. A., Donahue, N. M., Fry, J. L., Fuchs, H., Griffin, R. J., Guzman, M. I., Herrmann, H., Hodzic, A., Iinuma, Y., Jimenez, J. L., Kiendler-Scharr, A., Lee, B. H., Luecken, D. J., Mao, J., McLaren, R., Mutzel, A., Osthoff, H. D., Ouyang, B., Picquet-Varrault, B., Platt, U., Pye, H. O. T., Rudich, Y., Schwantes, R. H., Shiraiwa, M., Stutz, J., Thornton, J. A., Tilgner, A., Williams, B. J., and Zaveri, R. A.: Nitrate radicals and biogenic volatile organic compounds: oxidation, mechanisms, and organic aerosol, Atmos. Chem. Phys., 17, 2103–2162, 17, 10.5194/acp-17-2103-2017, 2017.

Ohto, T., Dodia, M., Imoto, S., and Nagata, Y.: Structure and Dynamics of Water at the Water-Air Interface Using First-Principles Molecular Dynamics Simulations within Generalized Gradient Approximation, Journal of Chemical Theory and Computation, 15, 595-602, 10.1021/acs.jctc.8b00567, 2019.

Patlewicz, G., Jeliazkova, N., Safford, R. J., Worth, A. P., and Aleksiev, B.: An evaluation of the implementation of the Cramer classification scheme in the Toxtree soft-ware, SAR QSAR Environ Res, 19, 495-524, 10.1080/10629360802083871, 2008.

Perumpully, S. J. and Gautam, S.: Impact of aerosols on atmospheric processes and climate variability: A synthesis of recent research findings, Geosystems and Geoenvironment, 4, 100317, https://doi.org/10.1016/j.geogeo.2024.100317, 2025.

Pillar-Little, E. A. and Guzman, M. I.: Oxidation of Substituted Catechols at the Air–Water Interface: Production of Carboxylic Acids, Quinones, and Polyphenols, Environmental Science & Technology, 51, 4951-4959, 10.1021/acs.est.7b00232, 2017.

Pillar-Little, E. A. and Guzman, M. I.: An Overview of Dynamic Heterogeneous Oxidations in the Troposphere, Environments, 5, 104, 2018.

Pillar-Little, E. A., Camm, R. C., and Guzman, M. I.: Catechol oxidation by ozone and hydroxyl radicals at the air-water interface, Environ Sci Technol, 48, 14352-14360, 10.1021/es504094x, 2014.

Pillar, E. A., Camm, R. C., and Guzman, M. I.: Catechol Oxidation by Ozone and Hydroxyl Radicals at the Air-Water Interface, Environmental Science & Technology, 48, 14352-14360, 10.1021/es504094x, 2014.

Pillar, E. A., Zhou, R., and Guzman, M. I.: Heterogeneous Oxidation of Catechol, Journal of Physical Chemistry A, 119, 10349-10359, 10.1021/acs.jpca.5b07914, 2015.

Pino-Rios, R., Inostroza, D., Cárdenas-Jirón, G., and Tiznado, W.: Orbital-Weighted Dual Descriptor for the Study of Local Reactivity of Systems with (Quasi-) Degenerate States, Journal of Physical Chemistry A, 123, 10556-10562, 10.1021/acs.jpca.9b07516, 2019.

Poster, D., Nguyen, T., Brown, R., and Ball, W.: Evidence for a pore-filling mechanism in the adsorption of aromatic hydrocarbons to a natural wood char, https://doi.org/10.1021/es0617845, 2007.

Qin, M., Xie, P., Su, H., Gu, J., Peng, F., Li, S., Zeng, L., Liu, J., Liu, W., and Zhang, Y.: An observational study of the HONO–NO_2 coupling at an urban site in Guangzhou City, South China, Atmospheric Environment, 43, 5731-5742, https://doi.org/10.1016/j.atmosenv.2009.08.017, 2009.

Rana, M. S. and Guzman, M. I.: Oxidation of Phenolic Aldehydes by Ozone and Hydroxyl Radicals at the Air–Water Interface, The Journal of Physical Chemistry A, 124, 8822-8833, 10.1021/acs.jpca.0c05944, 2020.

Rana, M. S. and Guzman, M. I.: Oxidation of Phenolic Aldehydes by Ozone and Hydroxyl Radicals at the Air-Solid Interface, ACS Earth Space Chem, 6, 2900-2909, 10.1021/acsearthspacechem.2c00206, 2022a.

Rana, M. S. and Guzman, M. I.: Oxidation of Catechols at the Air-Water Interface by Nitrate Radicals, Environ Sci Technol, 56, 15437-15448, 10.1021/acs.est.2c05640, 2022b.

Rana, M. S., Bradley, S. T., and Guzman, M. I.: Conversion of Catechol to 4-Nitrocatechol in Aqueous Microdroplets Exposed to O3 and NO2, ACS ES&T Air, 1, 80-91, 10.1021/acsestair.3c00001, 2023.

Salvador, C. M. G., Tang, R. Z., Priestley, M., Li, L. J., Tsiligiannis, E., Le Breton, M., Zhu, W. F., Zeng, L. M., Wang, H., Yu, Y., Hu, M., Guo, S., and Hallquist, M.: Ambient nitro-aromatic compounds - biomass burning versus secondary formation in rural China, Atmospheric Chemistry and Physics, 21, 1389-1406, 10.5194/acp-21-1389-2021, 2021.

Schaefer, T. and Herrmann, H.: Competition kinetics of OH radical reactions with oxygenated organic compounds in aqueous solution: rate constants and internal optical absorption effects, Physical Chemistry Chemical Physics, 20, 10939-10948, 10.1039/c7cp08571k, 2018.

Schwarzenbach, R. P., Stierli, R., Folsom, B. R., and Zeyer, J.: Compound properties relevant for assessing the environmental partitioning of nitrophenols, 22:1, 10.1021/es00166a009

Journal Name: Environ. Sci. Technol.; (United States) Journal Volume: 22:1, 1988.

Shenghur, A., Weber, K. H., Nguyen, N. D., Sontising, W., and Tao, F. M.: Theoretical Study of the Hydrogen Abstraction of Substituted Phenols by Nitrogen Dioxide as a Source of HONO, Journal of Physical Chemistry A, 118, 11002-11014, 10.1021/jp508516c, 2014.

Shi, K., Mei, X. L., Chen, C. R., and Liu, C. Q.: Impact of atmospheric O3 and NO2 on the secondary sulfates in real atmosphere, Journal of Environmental Sciences, 150, 277-287, 10.1016/j.jes.2024.02.019, 2025.

Shirts, M. R., Pitera, J. W., Swope, W. C., and Pande, V. S.: Extremely precise free energy calculations of amino acid side chain analogs: Comparison of common molecular mechanics force fields for proteins, Journal of Chemical Physics, 119, 5740-5761, 10.1063/1.1587119, 2003.

Shukla, S. S., Dorris, K. L., and Chikkaveeraiah, B. V.: Photocatalytic degradation of 2,4-dinitrophenol, Journal of Hazardous Materials, 164, 310-314, 10.1016/j.jhazmat.2008.08.047, 2009.

Spiegel, M., Semidalas, E., Martin, J. M. L., Bentley, M. R., and Stanton, J. F.: Post-CCSD(T) corrections to bond distances and vibrational frequencies: the power of Λ, Molecular Physics, 122, 10.1080/00268976.2023.2252114, 2024.

Steiner, T.: The Hydrogen Bond in the Solid State, Angewandte Chemie International Edition, 41, 48-76, https://doi.org/10.1002/1521-3773(20020104)41:1<48: AID-ANIE48>3.0.CO;2-U, 2002.

Sun, J., Mu, Q., Kimura, H., Murugadoss, V., He, M., Du, W., and Hou, C.: Oxidative degradation of phenols and substituted phenols in the water and atmosphere: a review, Advanced Composites and Hybrid Materials, 5, 627-640, 2022.

Sun, Y. N., Yao, J. F., Tang, Y. Z., Zhang, Y. J., Wu, W. Z., and Sun, J. Y.: Theoretical study on the atmospheric degradation mechanism and subsequent products of E,E-2,4-hexadienal with hydroxyl radical, International Journal of Quantum Chemistry, 121, 10.1002/qua.26563, 2021.

Sushko, I., Novotarskyi, S., Körner, R., Pandey, A. K., Cherkasov, A., Li, J., Gramatica, P., Hansen, K., Schroeter, T., Müller, K. R., Xi, L., Liu, H., Yao, X., Öberg, T., Hormozdiari, F., Dao, P., Sahinalp, C., Todeschini, R., Polishchuk, P., Artemenko, A., Kuz'min, V., Martin, T. M., Young, D. M., Fourches, D., Muratov, E., Tropsha, A., Baskin, I., Horvath, D., Marcou, G., Muller, C., Varnek, A., Prokopenko, V. V., and Tetko, I. V.: Applicability domains for classification problems: Benchmarking of distance to models for Ames mutagenicity set, J Chem Inf Model, 50, 2094-2111, 10.1021/ci100253r, 2010.

Szatylowicz, H., Jezuita, A., Ejsmont, K., and Krygowski, T. M.: Substituent Effect on the σ- and π-Electron Structure of the Nitro Group and the Ring in Meta- and Para-Substituted Nitrobenzenes, Journal of Physical Chemistry A, 121, 5196-5203, 10.1021/acs.jpca.7b03418, 2017.

Tam, J. Y. C., Lorsbach, T., Schmidt, S., and Wicker, J. S.: Holistic evaluation of biodegradation pathway prediction: assessing multi-step reactions and intermediate products, Journal of Cheminformatics, 13, 63, 10.1186/s13321-021-00543-x, 2021.

Thangamani, D., Shankar, R., Vijayakumar, S., and Kolandaivel, P.: Mechanism and kinetics of the atmospheric degradation of 2-formylcinnamaldehyde with O3 and hydroxyl OH radicals - a theoretical study, Molecular Physics, 114, 3055-3075, 10.1080/00268976.2016.1214293, 2016.

Tintó-Moliner, A. and Martin, M.: Quantitative weight of evidence method for combining predictions of quantitative structure-activity relationship models, SAR QSAR Environ Res, 31, 261-279, 10.1080/1062936X.2020.1725116, 2020.

Tiwari, J., Tarale, P., Sivanesan, S., and Bafana, A.: Environmental persistence, hazard, and mitigation challenges of nitroaromatic compounds, Environmental Science and Pollution Research, 26, 28650-28667, 10.1007/s11356-019-06043-8, 2019.

Tomas, A., Olariu, R. I., Barnes, I., and Becker, K. H.: Kinetics of the reaction of O_3 with selected benzenediols, International Journal of Chemical Kinetics, 35, 223-230, https://doi.org/10.1002/kin.10121, 2003.

Tuñón, I. and Williams, I. H.: Chapter Two - The transition state and cognate concepts, in: Advances in Physical Organic Chemistry, edited by: Williams, I. H., and Williams, N. H., Academic Press, 29-68, https://doi.org/10.1016/bs.apoc.2019.09.001, 2019.

Tyburski, R., Liu, T. F., Glover, S. D., and Hammarström, L.: Proton-Coupled Electron Transfer Guidelines, Fair and Square, Journal of the American Chemical Society, 143, 560-576, 10.1021/jacs.0c09106, 2021.

Uesawa, Y.: Progress in Predicting Ames Test Outcomes from Chemical Structures: An In-Depth Re-Evaluation of Models from the 1st and 2nd Ames/QSAR International Challenge Projects, International Journal of Molecular Sciences, 25, 1373, 2024.

Van Der Spoel, D., Lindahl, E., Hess, B., Groenhof, G., Mark, A. E., and Berendsen, H. J. C.: GROMACS: Fast, flexible, and free, Journal of Computational Chemistry, 26, 1701-1718, https://doi.org/10.1002/jcc.20291, 2005.

Vereecken, L. and Francisco, J. S.: Theoretical studies of atmospheric reaction mechanisms in the troposphere, Chemical Society Reviews, 41, 6259-6293, 10.1039/c2cs35070j, 2012.

vom Eyser, C., Börgers, A., Richard, J., Dopp, E., Janzen, N., Bester, K., and Tuerk, J.: Chemical and toxicological evaluation of transformation products during advanced oxidation processes, Water Science and Technology, 68, 1976-1983, 10.2166/wst.2013.452, 2013.

Wang, C. L., Zhao, N., Ma, Z. J., He, M. X., Hou, C. X., and Sun, J. F.: Unraveling the heterogeneous reaction of 4-nitrocatechol with ozone in the atmosphere: A combined DFT, molecular dynamics, and environmental risk assessment, Atmospheric Research, 331, 10.1016/j.atmosres.2025.108632, 2026.

Wang, J., Wolf, R. M., Caldwell, J. W., Kollman, P. A., and Case, D. A.: Development and testing of a general amber force field, J Comput Chem, 25, 1157-1174, 10.1002/jcc.20035, 2004.

Witt, R. P., Todd, M. B., Oladele, M. E., and Guzman, M. I.: Ozonolysis of phenolic aldehydes from industrial-based lignin wastewaters, Sci Total Environ, 998, 180190, 10.1016/j.scitotenv.2025.180190, 2025.

Xing, L., Wu, J., Elser, M., Tong, S., Liu, S., Li, X., Liu, L., Cao, J., Zhou, J., El-Haddad, I., Huang, R., Ge, M., Tie, X., Prévôt, A. S. H., and Li, G.: Wintertime secondary organic aerosol formation in Beijing–Tianjin–Hebei (BTH): contributions of HONO sources and heterogeneous reactions, Atmos. Chem. Phys., 19, 2343-2359, 10.5194/acp-19-2343-2019, 2019.

Yan, J. P., Wang, X. P., Gong, P., and Wang, C. F.: Nitrated polycyclic aromatic compounds in the atmospheric environment: A review, Critical Reviews in Environ-mental Science and Technology, 51, 1159-1185, 10.1080/10643389.2020.1748486, 2021.

Yang, B., Ren, P. P., Xing, L., Wang, S. H., and Sun, C. L.: Roles of hydrogen bonding interactions and hydrophobic effects on enhanced water structure in aqueous solutions of amphiphilic organic molecules, Spectrochimica Acta Part a-Molecular and Biomolecular Spectroscopy, 296, 10.1016/j.saa.2023.122605, 2023a.

Yang, B. R., Liang, A. B., and Wang, L. M.: The atmospheric oxidation mechanism of acetophenone initiated by the hydroxyl radicals, Atmospheric Environment, 309, 10.1016/j.atmosenv.2023.119905, 2023b.

Yong-di, H. E., Jin-ou, S., Bin, W. U., Xiao-wen, W., Ji-biao, X. I. E., and Bin, W.: Prediction of toxicity of nitro-organic compounds by Toxicity Estimation Software Tool and Toxtree software, Chinese Journal of Pharmacology and Toxicology, 36, 509-520, 10.3867/j.issn.1000-3002.2022.07.005, 2022.

Young, D., Martin, T., Venkatapathy, R., and Harten, P.: Are the Chemical Structures in Your QSAR Correct?, Qsar & Combinatorial Science, 27, 1337-1345, 10.1002/qsar.200810084, 2008.

Zhao, Y. and Truhlar, D. G.: The M06 suite of density functionals for main group thermochemistry, thermochemical kinetics, noncovalent interactions, excited states, and transition elements: two new functionals and systematic testing of four M06-class functionals and 12 other functionals, Theoretical Chemistry Accounts, 120, 215-241, 10.1007/s00214-007-0310-x, 2008.